

May 2020

Understanding the Role of Protein Kinases Kin1 and Kin2 in the Protein Folding Pathways in the Yeast *Saccharomyces Cerevisiae*

Chandrima Ghosh
University of Wisconsin-Milwaukee

Follow this and additional works at: <https://dc.uwm.edu/etd>



Part of the [Biochemistry Commons](#), [Microbiology Commons](#), and the [Molecular Biology Commons](#)

Recommended Citation

Ghosh, Chandrima, "Understanding the Role of Protein Kinases Kin1 and Kin2 in the Protein Folding Pathways in the Yeast *Saccharomyces Cerevisiae*" (2020). *Theses and Dissertations*. 2378.
<https://dc.uwm.edu/etd/2378>

This Dissertation is brought to you for free and open access by UWM Digital Commons. It has been accepted for inclusion in Theses and Dissertations by an authorized administrator of UWM Digital Commons. For more information, please contact open-access@uwm.edu.

UNDERSTANDING THE ROLE OF PROTEIN KINASES KIN1 AND
KIN2 IN THE PROTEIN FOLDING PATHWAYS IN THE YEAST
SACCHAROMYCES CEREVISIAE

by

Chandrima Ghosh

A Dissertation Submitted in

Partial Fulfillment of the

Requirements for the Degree of

Doctor of Philosophy

in Biological Sciences

at

The University of Wisconsin-Milwaukee

May 2020

ABSTRACT

UNDERSTANDING THE ROLE OF PROTEIN KINASES KIN1 AND KIN2 IN PROTEIN FOLDING PATHWAYS IN THE YEAST *SACCHAROMYCES CEREVISIAE*

by

Chandrima Ghosh

The University of Wisconsin-Milwaukee, 2020
Under the Supervision of Dr. Madhusudan Dey

Eukaryotic protein kinases catalyze the transfer of the γ -phosphate of an ATP to a serine/threonine/tyrosine residue present in a protein substrate. The phosphorylation of proteins has profound effects on their activity and protein-protein interactions, thus regulating a plethora of cellular processes, including cell growth, differentiation and protein homeostasis (or proteostasis). Our lab is the first to demonstrate that protein kinases Kin1 and its paralog Kin2 in the budding yeast *Saccharomyces cerevisiae*, orthologs of human microtubule affinity-regulating kinase (MARK), contribute to protein-folding homeostasis inside the endoplasmic reticulum (ER), in addition to their canonical roles in cellular exocytosis. The main aim of my studies is to fully understand the Kin kinase signaling pathway and how it contributes to the ER protein-folding homeostasis in the yeast *Saccharomyces cerevisiae*. Specifically, I study how Kin kinases are activated and what their upstream and downstream effectors are.

My studies have revealed that the N-terminal half of Kin1 or Kin2 protein containing the kinase domain (KD) with a short kinase extension region (KER) was sufficient to complement the function of full-length Kin1 or Kin2. I have also found that phosphorylation of a single residue in Kin1 (Thr-302) or Kin2 (Thr-281) was important for their kinase domain function. Furthermore, I have found that phosphorylation of Thr-302 or Thr-281 occurred *in trans* by an upstream kinase.

These results are published in *Molecular and Cellular Biology*. Further studies are directed towards identifying the Thr-302 or Thr-281 upstream kinase.

One third of total cellular proteins fold and mature inside the ER. Due to abiotic or biotic stresses, unfolded proteins may accumulate inside the ER lumen, causing ER stress. During ER stress, a dual kinase RNase Ire1 is activated and it restores the ER protein-folding homeostasis in *Saccharomyces cerevisiae* as follows. The active Ire1 initiates a signaling pathway by removing an intervening sequence from the *HAC1* mRNA by an unconventional splicing mechanism. Matured *HAC1* mRNA then translates an active transcription factor Hac1, which enhances the expression of protein folding enzymes and chaperones that help mitigate ER stress. We and others have shown that *HAC1* splicing requires co-localization of the *HAC1* mRNA with the Ire1 protein, which is mediated by a bipartite element (BE) present in the 3'-UTR of the *HAC1* mRNA. I have shown that the Kin kinases and a BE-RNA-protein complex (RNP) significantly contribute to *HAC1* mRNA splicing. Here I have characterized and determined the role of a component of the proposed RNP, an uncharacterized protein Pal2.

Our collaborator Dr. Benjamin Turk at Yale University identified a list of putative substrates of Kin kinases, using a phospho-proteomics based approach¹. We have shown that Kin2 specifically phosphorylates the Ser-222 residue of Pal2. Further, molecular genetic studies showed that the yeast strain lacking Pal2 and its paralog Pal1 was deficient in maintaining ER protein homeostasis, which could be restored by expressing a wild-type Pal2 protein, but not by its unphosphorylated form. These data suggest that both Kin kinases and its substrate Pal2 significantly contribute to ER protein homeostasis. Overall, my finding of Pal2 phosphorylation by Kin kinases provides a novel mechanistic insight into the physiological signaling pathways mediated by the Kin kinases.

© Copyright by Chandrima Ghosh, 2020
All Rights Reserved

To the loving memory of my mother

Dr. Purnima Ghosh,

to whom I owe my existence.

TABLE OF CONTENTS

List of Figures	ix
List of Tables	xiii
List of Abbreviations	xiv
Acknowledgements	xvi
1. Chapter 1: Literature Review	1
Protein Kinases.....	1
Endoplasmic Reticulum Protein Homeostasis	14
The Kin/Par-1/MARK family of Protein Kinases.....	26
Proteostasis in Health and Disease.....	30
Protein Kinases in Health and Disease.....	32
2. Chapter 2: Adaptation to Endoplasmic Reticulum Stress Requires Trans-phosphorylation within the Activation Loop of Protein Kinases Kin1 and Kin2, Orthologs of Human Microtubule Affinity-regulating Kinase	36
Introduction	36
Results	38
Bioinformatics analysis on yeast proteins Kin1 and Kin2 and comparison with related kinases in higher eukaryotes.....	38

In vivo assay to study Kin2 function	39
Kin1 and Kin2 proteins require a kinase domain followed by an extra set of residues to activate the UPR	40
Understanding the importance of the Kin2 KER.....	44
Kin2 _{mini} is tethered to a membrane bound organelle	51
Computer modeling to predict the structure of Kin2 kinase domain	55
Mass spectrometric approach to identify phosphorylation sites on Kin2 _{mini}	57
Activation loop phosphorylation is important for kinase activity of Kin2 _{mini}	59
Activation loop phosphorylation is important for activity of full length Kin2	61
Activation loop phosphorylation is important for Kin1 _{mini} kinase activity	66
Phosphorylation of the residue T302 in Kin1 or T281 in Kin2 occurs in trans	67
The glutamate substitution of T281 restores the defective ER-stress response associated with a mutation at the HAC1-3'-UTR.....	71
3. Chapter 3: Phosphorylation of Pal2 by the Kinases Kin1 and Kin2 Modulates HAC1 mRNA Splicing in the <i>Saccharomyces cerevisiae</i> Unfolded Protein Response	74
Introduction	74
Results	76
Identification of the Ribonucleoprotein (RNP) complex	76
Analysis of the 3'-BE specific proteomes identified Pal2 as a putative HAC1 mRNA binding protein.....	77
Yeast genome encodes two paralogs of the Pal protein-Pal1 and Pal2	79
Role of Pal1 and Pal2 proteins in yeast UPR	80
Comparison of protein sequences of Pal protein from related fungal species.....	85

Physiological role of truncated Pal proteins in the ER stress response	86
Association of Pal1 and Pal2 proteins with HAC1 mRNA	88
Kin1 and Kin2 substrate identification	90
Identification of specific Pal2 residues phosphorylated by Kin2	93
In vitro and in vivo phosphorylation of Pal2 by Kin2	95
Importance of phosphorylation of Kin2 Thr-281 for its activation	96
Effect of Pal2 Phosphorylation on ER stress response	98
Contribution of the Pal proteins in targeting HAC1 mRNA to the ER stress site.....	101
4. Chapter 4: Discussion and future prospects	104
5. Chapter 5: Materials and methods	114
Appendix I	153
Appendix II	160
Bibliography	161
Curriculum Vitae	174

LIST OF FIGURES

Chapter 1

Figure 1.1 Schematic of the kinase domain structure.....	4
Figure 1.2 Inactive to active transition for activation of the kinase domain.	5
Figure 1.3 Schematic representation of ATP and important catalytic motifs and residues in the active site of PKA.....	7
Figure 1.4 Schematic representation of activation of AGC kinases.....	9
Figure 1.5 Schematic representation of activation of CaM kinases.....	10
Figure 1.6 Schematic representation of activation of CMGC kinases.....	11
Figure 1.7 Schematic representation of activation of a receptor tyrosine kinase.....	12
Figure 1.8 Schematic representation of activation of a non-receptor tyrosine kinase.....	13
Figure 1.9 Schematic representation of targeting secretory proteins to the ER by SRP.....	16
Figure 1.10 Protein synthesis, folding and targeting.....	18
Figure 1.11 Schematic representation of Ire1-mediated UPR pathway.....	22
Figure 1.12 Schematic representation of the PERK-mediated UPR pathway.....	24
Figure 1.13 Schematic representation of the Atf6-mediated UPR pathway.....	25
Figure 1.14 Domain organization of the MARK/Par-1/Kin kinase family of proteins.....	28

Chapter 2

Figure 2.1 Schematic representation of Kin kinases and its counterparts.....	38
Figure 2.2 Schematic representation of Kin kinase constructs and scheme to study the kinase function...40	
Figure 2.3 <i>In vivo</i> assay to study Kin2 protein kinase function.....	42
Figure 2.4 <i>In vivo</i> assay to study Kin1 protein kinase function.....	43
Figure 2.5 Pairwise sequence alignment of the KER of Kin1 and Kin2.....	44

Figure 2.6 Two distinct regions within the KER control the Kin2 kinase function.	46
Figure 2.7 Replacement of KER-I by the Mark3 UBA domain	48
Figure 2.8 L436A point mutation in the UBA-like domain in Kin2	49
Figure 2.9 Replacement of KER-III by the GST	50
Figure 2.10 Expression and localization of GFP-Kin2 _{mini} fusion protein.....	52
Figure 2.11 Membrane fractionation of cells harboring Kin2 _{mini}	54
Figure 2.12 Localization of GFP-KA1 _{Kin2}	55
Figure 2.13 Ribbon representation of the predicted structure of Kin2 kinase domain.....	56
Figure 2.14 Mutational analysis of reported phosphorylation sites of Kin2	59
Figure 2.15 Activation loop phosphorylation is important for Kin2 _{mini} kinase activity	61
Figure 2.16 Activation loop mutations affect the protein function of full length Kin2.....	63
Figure 2.17 Activation loop phosphorylation is required for full Kin2 kinase function.	65
Figure 2.18 Activation loop phosphorylation is important for Kin1 _{mini} kinase activity.	67
Figure 2.19 Mechanism of Kin2 _{mini} phosphorylation on T281	68
Figure 2.20 Growth test to ensure functionality of the Kin2 mutant used for kinase assays	69
Figure 2.21 Phosphorylation of Kin2-T281 or Kin1-T302 occurs <i>in trans</i>	71
Figure 2.22 <i>HAC1</i> nucleotides GG (1143-44) play an important role in UPR.....	72
Figure 2.23 Thr-281 phosphorylation is required to suppress the defective alleles of <i>HAC1</i> mRNA.	73

Chapter 3

Figure 3.1 Working hypothesis: An RNA-Protein (RNP) Complex Assembles on the 3'-BE and Controls the <i>HAC1</i> mRNA Targeting	75
Figure 3.2 Construct designs for identification of RNP components	76
Figure 3.3 Analysis of 3'-BE specific proteomes of <i>HAC1</i> mRNA.....	77
Figure 3.4 Pal1 and Pal2 protein sequence alignment.	79

Figure 3.5 Pal1 and Pal2 double deletion strains is sensitive to Tunicamycin.....	80
Figure 3.6 Pal2 deletion strain shows a severe UPR defect compared to Pal1 deletion.....	81
Figure 3.7 Pal1 and Pal2 double null strain displays slow growth phenotype	81
Figure 3.8 Splicing of <i>HAC1</i> mRNA is reduced in the Pal1 and Pal2 double deletion strain.....	82
Figure 3.9 Hac1 protein production is reduced in the Pal1 and Pal2 double deletion strain.....	83
Figure 3.10 <i>UPRE</i> -driven LacZ reporter gene expression is reduced in the Pal1 and Pal2 double deletion strain	84
Figure 3.11 Analysis of Hac1 protein expression from the intron-less <i>HAC1</i> mRNA.....	85
Figure 3.12 Alignment of protein sequences of Pal2 homologs.....	86
Figure 3.13 Truncation analysis of Pal2	87
Figure 3.14 Truncation analysis of Pal1	88
Figure 3.15 Truncated Pal proteins bind to the 3'-BE of <i>HAC1</i> mRNA <i>in vitro</i>	89
Figure 3.16 Kin1 phosphorylates Pal2 <i>in vitro</i>	91
Figure 3.17 Circular dichroism spectroscopy of recombinant Pal2 protein	92
Figure 3.18 Kin2 specifically phosphorylates Pal2 <i>in vitro</i>	92
Figure 3.19 Pal2 is phosphorylated at multiple sites.	93
Figure 3.20 Kin2 phosphorylates Ser-222 of Pal2 <i>in vitro</i>	94
Figure 3.21 Pal1 is not a substrate of Kin2.....	95
Figure 3.22 Kin1 or Kin2 phosphorylates Pal2 <i>in vivo</i>	96
Figure 3.23 T281 phosphorylation of Kin2 is important for Pal2 phosphorylation	97
Figure 3.24 Phosphorylation of Pal2 is important for ER stress response	99
Figure 3.25 Hac1 protein expression is reduced in Pal2-4ala cells	100
Figure 3.26 Schematic representation of Pal1 and Pal2 proteins	100
Figure 3.27 <i>HAC1</i> foci formation is reduced in Pal1 and Pal2 double deletion strain.....	102
Figure 3.28 Analysis of Ire1-YFP and Pal2-GFP colocalization	103

Chapter 4

Figure 4.1 Sak1, Tos3 and Elm1 deletion strains are not deficient in ER stress response	106
Figure 4.2 LKB1 complex does not phosphorylate Kin2	106
Figure 4.3 T281 phosphorylation status in non-essential kinase null strains	107
Figure 4.4 Snf1 does not contribute to the ER stress response	111
Figure 4.5 Model for Kin2-Pal2 pathway in promoting the UPR	113

LIST OF TABLES

Table 1 Phosphorylation sites on Kin1 and Kin2 proteins	57
Table 2 A list of putative 3'-BE and 5'-RD binding proteins.....	78
Table 3 List of yeast strains used in this study	153
Table 4 List of plasmids used in this study.....	155

LIST OF ABBREVIATIONS

AD	Alzheimer's disease
ATF4	Activated transcription factor 4
ATF6	Activated transcription factor 6
ATP	Adenosine 5' triphosphate
BiP	Immunoglobulin heavy chain binding protein
BSA	Bovine serum albumin
bZIP	Basic leucine zipper
CHOP	C/EBP-homologous protein
DMF	Dimethylformamide
DTT	Dithiothreitol
eIF2 α	Alpha-subunit of eukaryotic initiation factor 2
ERAD	ER associated degradation
ERO	ER oxidase
GADD-34	Growth arrest and DNA damage inducible protein 34
GST	Glutathione-S- transferase
HM	Hydrophobic motif
HSP	Heat shock protein
IRE1	Inositol requiring enzyme 1
KD	Kinase domain
kDa	Kilodalton
KER	Kinase extension region

TOR	Target of rapamycin
ORF	Open reading frame
PAGE	Polyacrylamide gel electrophoresis
PD	Parkinson's disease
PERK	PKR like endoplasmic reticulum (ER)-resident eIF2 α kinase
PIF	PDK1 interacting fragment
PKA	cAMP dependent protein kinase
PKR	Double stranded RNA dependent protein kinase
PMSF	Phenylmethylsulfonyl fluoride
RIDD	Regulated IRE1-dependent decay
S1P	Site- 1 protease
S2P	Site- 2 protease
SDS	Sodium dodecyl sulphate
TCA	Trichloroacetic acid
TEMED	N'N'N'N'-tetra ethyl methyl ethyl diamine
uORF	Untranslated open reading frame
UPR	Unfolded protein response
UTR	Untranslated region

ACKNOWLEDGEMENTS

I would like to start by expressing my deepest gratitude to my advisor, Dr. Madhusudan Dey, for giving me the opportunity to pursue doctoral studies in his laboratory. I wish to sincerely thank him for his mentorship through all these years. His enthusiastic approach towards research, and his guidance made my time at UW-Milwaukee thoroughly enjoyable. During this time in Dr. Dey's lab, I have had the privilege to learn several advanced tools in microbiology, molecular biology and biochemistry directly from Dr. Dey. His constant encouragement on several interesting projects that I was working on has motivated me, taught me how to multitask, approach a problem critically from different aspects and rapidly take decisions. These accomplishments would not have been possible without his constant assistance and dedicated involvement through every step of this process. Thank you for your understanding and unwavering support through all the ups and downs during these years.

I would like to take this opportunity to thank my graduate advisory committee, including Dr. Charles Wimpee, Dr. Douglas Steeber, Dr. Heather Owen, Dr. Sergei Kuchin and Dr. David Frick. I have had the privilege to work with Dr. Wimpee as a teaching assistant for several years. His lectures, teaching style and enthusiasm for biology has left a strong impression on me. His valuable suggestions during committee meetings have helped me immensely. Dr. Steeber's guidance on research has helped me to think critically and approach problems from different perspectives. His valuable suggestions, support and compassion has kept me motivated all throughout. I am grateful that I have had the privilege to work with Dr. Owen who helped me with different aspects of research, especially confocal microscopy, to attain beautiful images for my dissertation. I sincerely thank Dr. Kuchin for his attention to details and creative ideas which have immensely helped me to take a project in a new direction. I have also had the privilege to work in

Dr. Frick's laboratory where I learned the technique of size exclusion chromatography. I am thankful for his mentorship and several constructive recommendations. I have been lucky to have such an amazing group of scientists in my graduate advisory committee.

I am grateful to have had the opportunity to work with some amazing postdoctoral fellows, dedicated graduate students and enthusiastic undergraduate trainees in Dr. Dey's laboratory. Working with them has taught me how to be more collaborative, compassionate and patient when it comes to research. Their passionate participation and critical suggestions have steered me in the right direction. Stimulating discussions with them have guided me to analyze problems from a different aspect and helped me to evolve as a researcher.

I would like to thank the Biological Sciences Department for providing the infrastructure for research. I am grateful to Dr. Dey, our department as well as UWM for supporting me by providing assistantships, fellowships, and giving me several platforms to present my research.

Most importantly I would like to express my profound gratitude to my father, Dr. Somnath Ghosh and my late mother, Dr. Purnima Ghosh for their unconditional love and unwavering support. I am grateful to them for inspiring me and encouraging me to realize my dream of pursuing a career in research. I will forever be indebted to them for their sacrifices. I would like to thank my brother, Sourav Ghosh, who has been my pillar of strength through all the ups and downs that we faced as a family during these last few years. Without all their support, I would not have been able to complete my doctoral work. Lastly, I would like to acknowledge the kindness, compassion and love that I received from my extended family and friends in India and here in the US. This accomplishment would not have been possible without them. Thank you.

Chandrima Ghosh

1. Chapter 1: Literature Review

Protein Kinases

Protein phosphorylation is a post-translational modification and a critical event in cells of eukaryotic organisms^{2,3}. The process of phosphorylation is coordinated by enzymes called protein kinases which catalyze the transfer of a terminal phosphoryl group of an ATP molecule to a serine (Ser), threonine (Thr) or tyrosine (Tyr) residue on a substrate protein^{4,5}. By doing so, kinases orchestrate several signal transduction pathways and complex functions in the cell⁶. Kinase activity was first observed by Eugene Kennedy who saw phosphorylation of casein by a liver enzyme way back in the 1950s⁷. Since then, extensive progress has been made in the field of kinases. Researchers have been able to determine the structure and mode of activation of kinases. The pursuit to gain mechanistic insights into the functioning of kinases eventually led to the discovery of many kinase signaling cascades.

This large superfamily of eukaryotic protein kinases account for nearly 2.5% of the proteomes^{8,9}. Most of these kinases are related to one another through homology of their kinase domain (catalytic cores)¹⁰. Most protein kinases remain in a basal inactive state and are activated in the presence of regulatory stimuli by intricate mechanisms like dimerization and autophosphorylation^{11,12}. The human kinome is comprised of 568 kinases⁶ whereas the yeast kinome is comprised of 129 kinases¹³. Based on sequence homology each kinase contains a conserved kinase domain (KD).

Structure of a classical protein kinase:

The crystal structure of the catalytic domain of cyclic-AMP-dependent protein kinase

(PKA) is the first deciphered structure of a protein kinase domain. This kinase has been co-crystallized with a pseudo-substrate peptide inhibitor (PKI)^{14,15}. The KD of PKA contains two lobes: the N-terminal lobe (N-lobe) and the C-terminal lobe (C-lobe) (**Fig. 1.1A**)¹⁵. The two lobes are connected by a flexible hinge region. The active site is in the deep cleft between the two lobes. ATP binds at this cleft and the γ -phosphate of ATP is projected out towards the opening of the cleft (**Fig. 1.1A**)¹⁴.

The N-lobe is comprised of 5 anti-parallel β -strands (β 1- β 5) and one α -helix also known as the helix α C₁₄. The main function of the N-lobe is to bind ATP¹⁶. Between strands β 1 and β 2 there is a glycine rich motif (GXGX Φ G, where X is any amino acid, and Φ is an aromatic amino acid) called the P-loop that helps coordinate the phosphates of the ATP. In this motif, Φ is mostly a conserved aromatic amino acid (phenylalanine or tyrosine) which helps to cap the region of phosphotransfer reaction¹⁷. On the strand β 3 there is a conserved Lys residue (e.g. Lys₇₂ in PKA), that interacts with the α and β -phosphates of ATP.

The C-lobe is comprised of four β -strands (β 6, β 7, β 8 and β 9) and several α -helices (**Fig. 1.1A**). The major function of the C-lobe is substrate recognition and catalysis of the phosphotransfer reaction¹⁸.

In PKA, the catalytic loop is between β 6 and β 7, and the metal (Mg^{2+}) binding region is between β 8 and β 9. The catalytic loop has a conserved RD-motif that harbors the catalytic base, Asp₁₆₆ which is directly involved in phosphotransfer reaction¹⁸. The metal binding loop consists of a highly conserved DFG motif (aspartate, phenylalanine, glycine; e.g. Asp₁₈₄ Phe₁₈₅ Gly₁₈₆ in PKA). It is important to note that there are two Mg^{2+} ions that coordinate with ATP. The aspartate (Asp₁₈₄ in PKA) and the asparagine (Asn₁₇₁ in PKA) in this loop interacts with the two

Mg²⁺¹⁹.

The activation loop spans from the DFG motif to the APE motif and contains one/two phospho-acceptor residues (e.g. Thr¹⁹⁷ in PKA)²⁰. In many kinases, activation loop phosphorylation is important to activate the kinase domain¹⁷. As mentioned before, phosphorylation of the activation loop is a key event to activate the kinase. The activation loop is a highly flexible structure that has the capacity to undergo large conformational changes when the kinase switches from its inactive to active state.

Mechanism of kinase activation:

During kinase activation, there are several important events that prime the kinase: conformational change in the activation loop, rotation of the helix α C and correct positioning of the conserved residues¹⁷.

When the kinase is inactive, the activation loop collapses into the active site and blocks the binding of ATP and substrate²¹. Once phosphorylated, the activation loop shifts away from the active site, allowing binding of ATP and substrate for catalysis. This involves a crankshaft-like movement at the N-terminal side of the loop, which correctly orients the DFG motif. In this process, the DFG motif flips by 180 degrees and attains a “DFG-in” conformation that initiates catalysis. In the “DFG-in” conformation, Asp of DFG is projected towards the active site, whereas, Phe of DFG is flipped out of the active site^{22–25}. In PKA, the activation loop Thr¹⁹⁷ is phosphorylated and it forms ionic interactions with Arg¹⁶⁵ (of the RD motif) in the catalytic loop. This ion pair is important for flipping the DFG motif in the correct orientation for catalysis¹⁷.

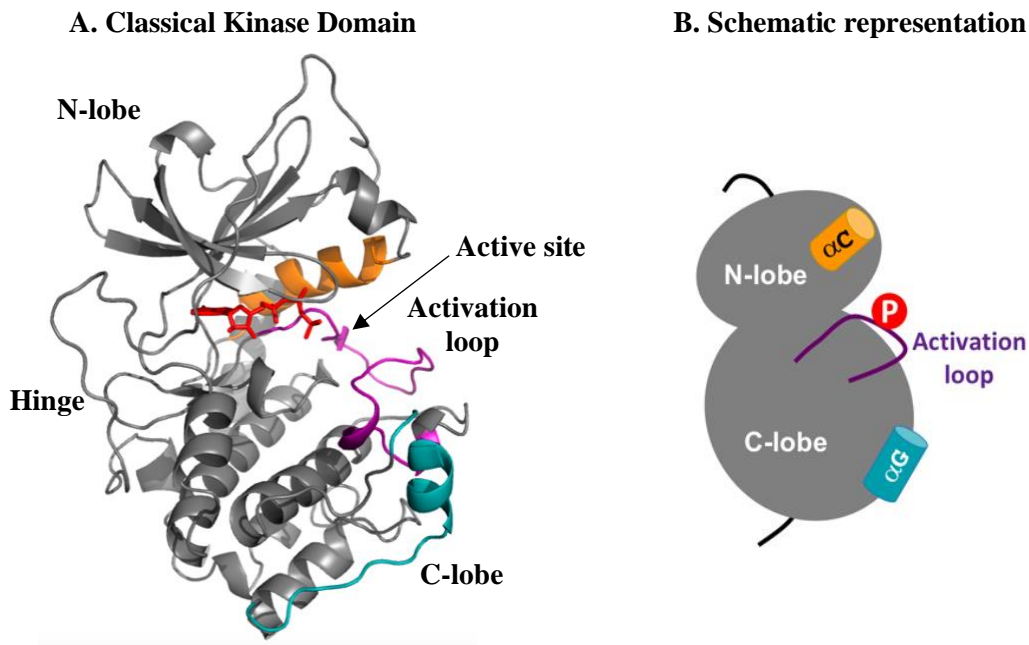


Figure 1.1 Schematic of the kinase domain structure

(A) Ribbon representation of the crystal structure of the cyclic AMP-dependent protein kinase domain. Some of the secondary structural elements are colored: helix αC in orange, helix αG in cyan and activation loop in purple. The N-lobe, C-lobe, hinge region and activation loop are labeled. The active site is in the deep cleft between the two lobes. The ATP (colored red) fits in the hydrophobic core at the active site. PDB ID- 1ATP. (B) Cartoon representation of the catalytic core of the PKA kinase domain. The N-lobe C-lobe are colored grey, helix αC is colored orange, helix αG is colored cyan, and the activation loop is colored purple. Phosphorylation on activation loop is denoted by a red circle with an inscribed “P”.

The rotational movement of the helix αC is required to bridge the gap between the N-terminal region of the helix αC and the activation loop¹⁷. This bridging favors the closed conformation of the kinase. This closed conformation, in turn, favors substrate binding near the helix αG_{26} (Fig. 1.2).

The correct positioning of conserved residues and correct orientation of ATP is essential for the phosphotransfer reaction. The adenine ring of the ATP is positioned in a hydrophobic pocket and the ribose is stabilized via hydrogen bonding. The phosphates of the ATP remain anchored by the main chain nitrogen atoms of the P-loop and by the metal ions (Mg^{2+}).

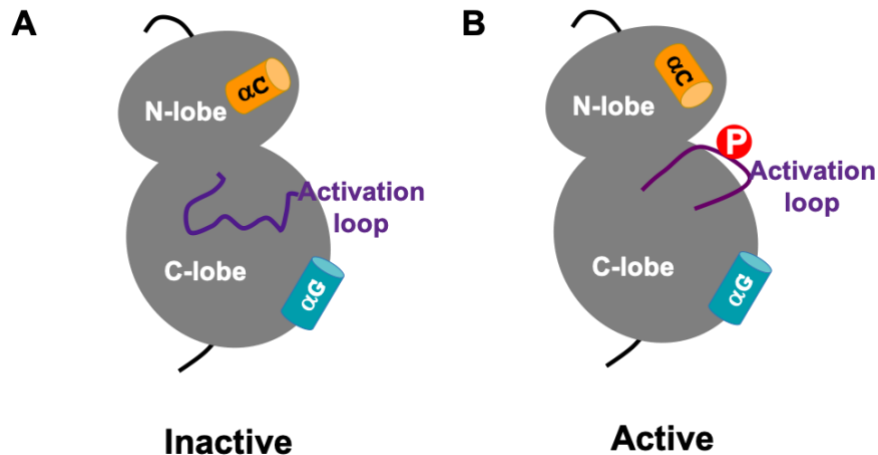


Figure 1.2 Inactive to active transition for activation of the kinase domain.

Cartoon representation of the catalytic core of a kinase domain. The N-lobe and C-lobe are colored grey, helix αC is colored orange, helix αG is colored cyan, and the activation loop is colored purple. Phosphorylation on activation loop is denoted by a red circle with an inscribed “P”. Schematic representation of the orientation of the helix αC and the conformation of the activation loop are shown in the inactive state (A) and active state (B).

Predicted mechanism of phosphotransfer reaction:

Once the kinase is active, it is primed for phosphotransfer which takes place in two steps²⁷:

Step 1: Binding and orientation of nucleotide and substrate, and conformational changes in the kinase.

The correct positioning of conserved residues is important for the phosphotransfer reaction. A proper orientation of ATP is also essential. The adenine ring of the ATP is positioned in a hydrophobic pocket and stabilized via hydrogen bonds with the N1, N6 or N7 of the adenine ring²⁸ (**Fig 1.3**). The oxygens of the phosphates of the ATP are anchored by the metal ions (Mg^{2+}). The Mg^{2+} neutralizes the electrostatic negative charge of the phosphoryl groups. The Mg^{2+} also activates the ATP for phosphotransfer. The positive charge on the Mg^{2+} polarizes the P-O bond of

the terminal phosphoryl group and thereby makes the terminal phosphorus atom more electrophilic and susceptible to a nucleophilic attack^{29,30}. Another structural feature that anchors the ATP is the glycine-rich phosphate binding P-loop. The glycines anchor the ATP by making mainchain contacts with the phosphoryl groups³¹. A conserved lysine residue also anchors the α - and β -phosphoryl groups of the ATP^{31,32}. The lysine is stabilized by an ionic interaction with a glutamate from the helix αC_{17} . Rotation of this helix αC couples it with the N-terminal region of the activation loop and modulates the activity of the kinase.

The phosphorylated activation loop of the kinase extends out in an open conformation and acts as a platform for substrate binding near the γ -phosphoryl group of the ATP. The conserved catalytic residue aspartate projects out from the catalytic loop (**Fig 1.3**). A conserved asparagine makes hydrogen bonds with the catalytic aspartate to orient it¹⁷.

Step 2: Nucleophilic attack by substrate hydroxyl group and acid-base catalysis.

Following proper positioning of the ATP, and orientation of the substrate the kinase attains an active conformation. The catalytic aspartate in the C-lobe acts like a catalytic base and extracts a proton from the -OH group of the substrate serine or threonine. This results in the formation of an alcoholate ion on the substrate. Next, the lone pair of electrons on the alcoholate ion initiates a nucleophilic attack on the phosphorus of the terminal phosphate for an “in-line” phosphotransfer³³. Consequently, the phospho-anhydrous bond bridging the oxygen and γ -phosphorus is broken, followed by subsequent release of the phosphoryl group²⁷ (**Fig 1.3**).

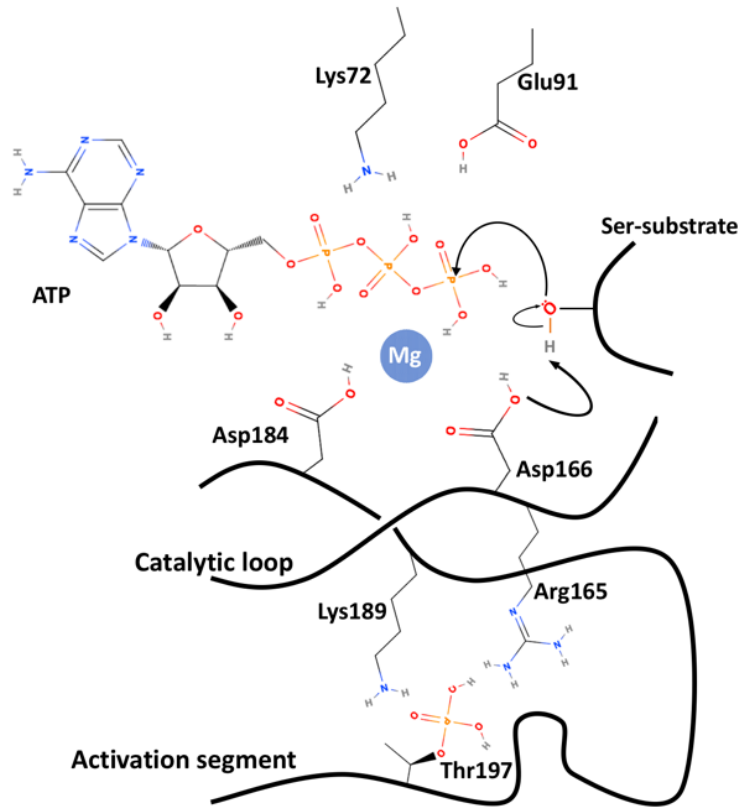


Figure 1.3 Schematic representation of ATP and important catalytic motifs and residues in the active site of PKA

In the predicted mechanism of phosphotransfer, the catalytic Asp166 attacks the –OH of the substrate Ser. This results in an alcoholate ion that attacks the phosphorus of the γ -phosphate of the ATP. (Adapted from Johnson *et al*, Cell, 1996)

In addition to the KD, protein kinases may contain additional regulatory domains, subunits or both. Depending on sequence homology and mode of activation of these eukaryotic protein kinases, they can be classified into 4 large groups, each of which may comprise kinases of multiple related families. These groups are i) AGC group, ii) CaMK group, iii) CMGC group and iv) PTK group¹⁶.

i) AGC group kinases

This group of protein kinases mainly comprises the cyclic-nucleotide-dependent kinase family (PKA and PKG), the protein kinase C (PKC) family, β -adrenergic receptor kinase (β ARK) and ribosomal S6 kinase family amongst others. AGC kinases comprise 12% of the human kinome³⁴. These are Ser/Thr kinases, and they tend to phosphorylate substrates on a Ser/Thr which is located close to an arginine (Arg) or lysine (Lys) residue within the consensus phosphorylation motif R-X-R/K-X-X-S/T³⁵. PKC family kinases prefer to phosphorylate a Ser/Thr which has basic residues on both the N- and C-terminal flanks¹⁶.

One of the widely studied AGC kinase is PDK1 in humans. It phosphorylates and activates several other AGC kinases and considered as a master regulator³⁶. Like any other kinase, the AGC kinases contain an activation loop which requires phosphorylation for kinase activation. AGC kinases also contain two unique features: a hydrophobic motif (HM, Φ -X-X- Φ , where Φ is a hydrophobic amino acid and X is any amino acid), and a Zipper/turn motif that folds back into the catalytic core³⁴. Phosphorylation of both of these motifs is also important for activation³⁷. Another regulatory motif on AGC kinases that are substrates of PDK1 is the PDK1 interacting fragment (PIF)³⁸. The PIF-pocket on PDK1 which binds the PIF acts as a regulatory feature³⁹. The HM phosphorylation initiates the docking of the AGC kinase to the PIF-pocket of PDK1 which activates PDK1. PDK1 then phosphorylates the activation loop of the AGC kinase. The

phosphorylated HM intramolecularly interacts with the PIF pocket of the AGC kinase and stabilizes its active conformation^{34,40} (**Fig 1.4**).

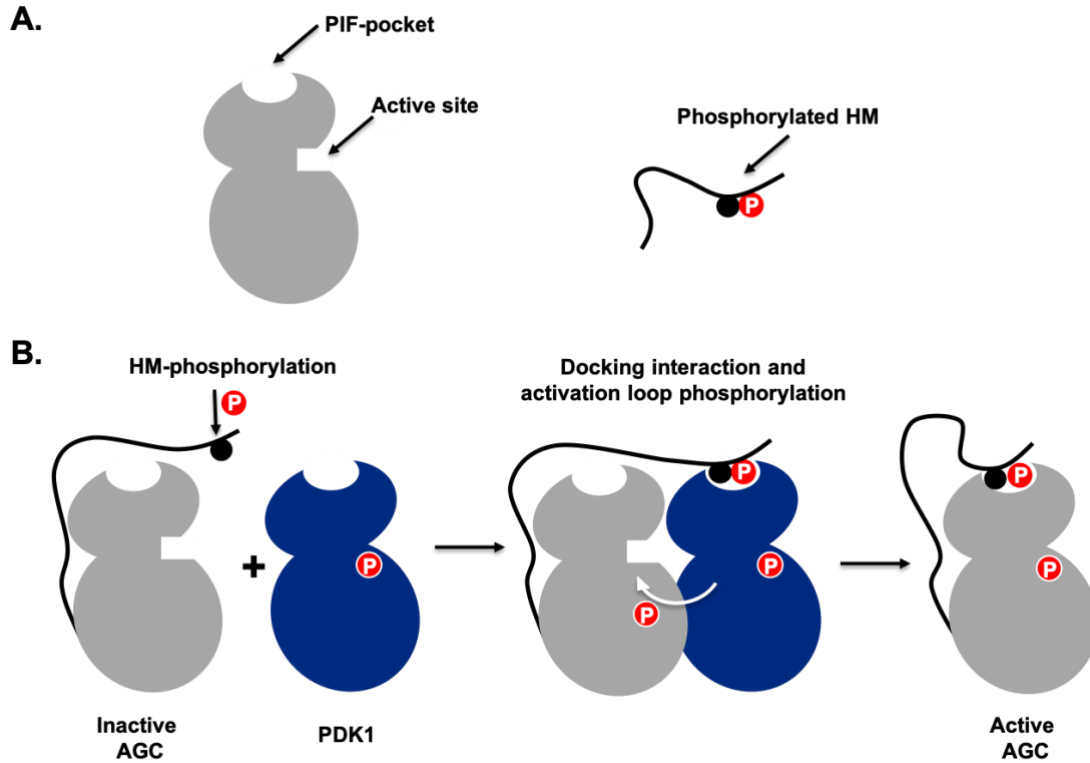


Figure 1.4 Schematic representation of activation of AGC kinases

(A) Schematic representation of the AGC kinase. The AGC kinase is colored gray with the PDK1 interacting fragment (PIF)-pocket and active site indicated. The hydrophobic motif (HM) is indicated as a black circle and phosphorylation is indicated in a red circle with a “P” inscribed. (B) PDK1 kinase is indicated in blue. The HM phosphorylation initiates the docking of the AGC kinase to the PIF-pocket of PDK1 which activates PDK1. PDK1 then phosphorylates the activation loop of the AGC kinase. The phosphorylated HM intramolecularly interacts with the PIF pocket of the AGC kinase and stabilizes its active conformation. (Adapted from Arencibia *et al*, *Biochimica et Biophysica Acta - Proteins and Proteomics*, 2013)

ii) CaMK group kinases

CaMK stands for Ca²⁺/ Calmodulin-activated protein kinase. These are a large group of Ser/Thr kinases that require calcium and calmodulin for activation but become independent of Ca²⁺/ Calmodulin after activation⁴¹. CaM-kinases have a bilobal catalytic domain which is

followed by a regulatory domain that comprises an auto-inhibitory and a calmodulin (CaM) binding domain. At low levels of Ca^{2+} , the auto-inhibitory domain keeps the CaM-kinase inactive. As the concentration of intracellular Ca^{2+} increases, CaM becomes saturated with four Ca^{2+} ions and it binds to the CaM-binding domain. This interaction releases the kinase from auto-inhibition and the kinase can catalyze a phosphorylation reaction^{41,42} (**Fig 1.5**). CaM-kinases can be further classified into smaller groups depending on the number of substrates. CaMK-I, CaMK-II and CaMK IV, all have multiple downstream effectors, but CaMK-III has only one. Some of these CaM-kinases prefer a substrate that has a basic residue in the N-terminal flank of the acceptor Ser/Thr. Some CaM-kinases prefer to have the basic residue on both N- and C-terminal flanks of the acceptor¹⁶.

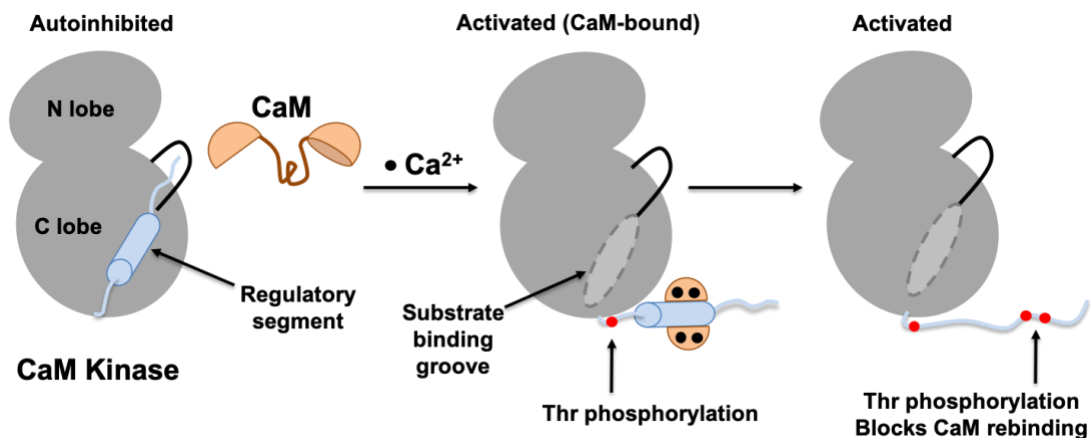


Figure 1.5 Schematic representation of activation of CaM kinases

The autoinhibited, activated (CaM-bound) and activated forms of the CaM kinase are shown. The bilobal kinase domain is colored grey, the regulatory segment is colored light blue, the Calmodulin is colored light orange, calcium ions are represented as black dots, substrate binding groove is the light grey oval with dotted border and phosphorylated threonine residues are represented as red dots. The regulatory segment of the CaMK, which contains three phosphorylatable threonine residues, remains bound to the substrate docking groove and keeps the CaMK autoinhibited. Interaction of the regulatory segment with Ca^{2+} /CaM initiates threonine phosphorylation and renders the kinase CaMK Ca^{2+} /CaM-independent. Subsequently the remaining two threonine residues are phosphorylated which inhibits the Ca^{2+} /CaM binding and keeps the kinase active. (Adapted from Bhattacharya *et al*, CSH Perspectives in Biology, 2019)

iii) CMGC group kinases

The CMGC group of kinases mostly comprise the cyclin-dependent kinases (CDKs), mitogen activated protein kinases (MAPKs), glycogen synthase kinases (GSKs) and CDK-like kinases⁴³. Most commonly studied CMGC kinases are CDKs and MAPKs because of their roles in human tumor suppression and cell-fate decisions respectively⁴³. CDKs are proline –dependent Ser/Thr kinases⁴⁴. Some CDKs prefer the sequence S/T-P-X-K/R which allows the proline to fit into the hydrophobic pocket. CDK activation occurs in two steps. First, cyclin binding to CDKs trigger a change in the CDK conformation, making it partially active⁴⁵. Second, the CDK activating kinase (CAK) phosphorylates a threonine residue on the activation loop of the CDK of the CDK-cyclin complex and fully activates the CDK (**Fig 1.6**). This allows ATP binding and catalysis of phosphorylation^{16,44,46}.

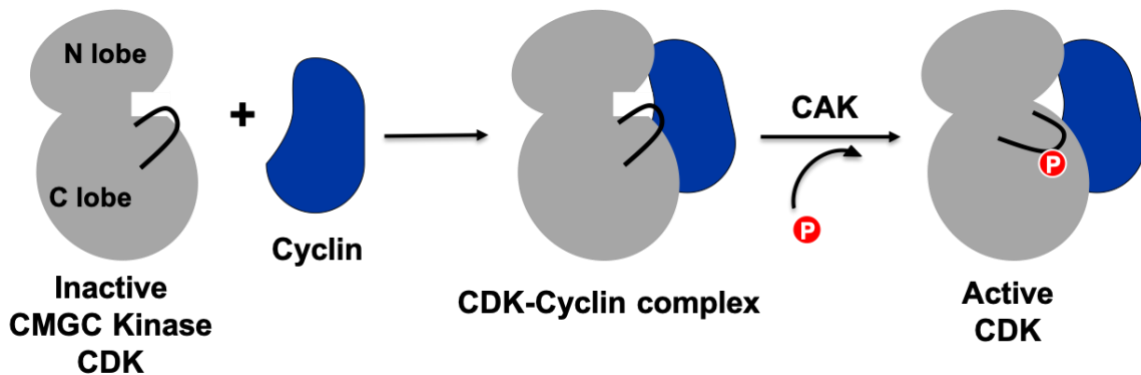


Figure 1.6 Schematic representation of activation of CMGC kinases

The CMGC kinase CDK is shown in grey color with the activation loop as a black curved line. Cyclin is colored blue. During activation of CDKs, cyclin first binds to the CDK for its partial activation and then the CAK (CDK activating kinase) phosphorylates the activation loop threonine of the cycline-bound CDK to fully activate it. (Adapted from Morgan, Nature, 1995)

iv) PTK group

The protein tyrosine kinase group comprises a large number of protein kinases and they specifically phosphorylate tyrosine residues of substrate proteins. PTKs are found mostly in metazoans and they have important roles in growth and differentiation. These kinases prefer a glutamic acid (Glu) residue on both N- and C-terminal flanks of the acceptor Tyr residue¹⁶. There are two classes in the PTK group- receptor tyrosine kinases (RTKs) and non-receptor tyrosine kinases (NRTKs)^{47,48}.

In RTKs, ligand binding to the extracellular ligand binding domain results in trans-autophosphorylation (**Fig 1.7**). Activation loop phosphorylation renders the kinase active and facilitates correct positioning of the residues involved in binding of Mg²⁺ and ATP for substrate phosphorylation. Additional tyrosine residues are phosphorylated, which serve as binding sites for downstream effectors²².

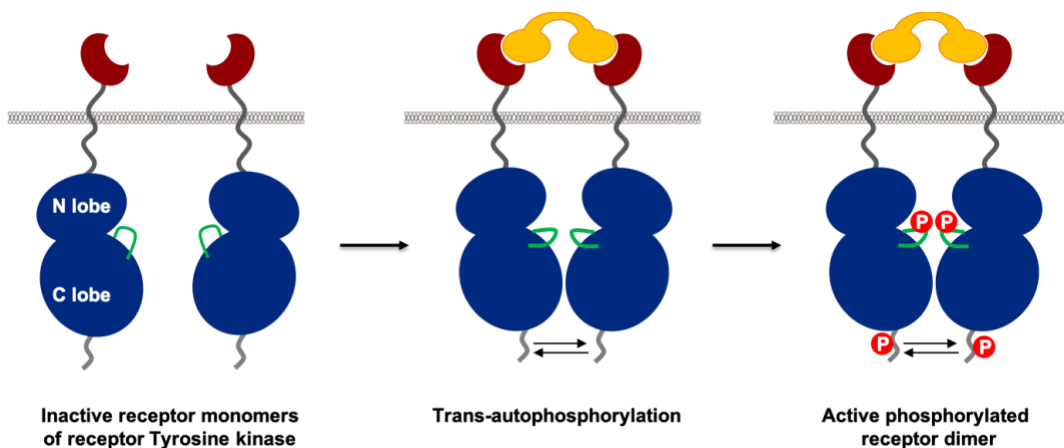


Figure 1.7 Schematic representation of activation of a receptor tyrosine kinase

Inactive receptor tyrosine kinase monomer kinase domains are indicated in blue, the transmembrane region is indicated as a grey curved line, the activation loop is colored green, and the ligand binding domain is colored maroon. The ligand is indicated as a yellow dumbbell shape. The ligand binding to the extracellular ligand binding domain results in trans-autophosphorylation. Activation loop phosphorylation renders the kinase active. Additional tyrosine residues are phosphorylated, which serve as binding sites for downstream effectors. (Adapted from Hubbard *et al*, JBC, 1998)

NRTKs (for example, Src) mostly contain protein-protein or protein-ligand interaction modules called the SH2 and SH3 domains⁴⁸. Src, an oncoprotein, remains autoinhibited through binding of the SH2 with a phospho-tyrosine at the C-terminal end of the KD^{49,50} (**Fig 1.8**). The SH3 remains bound to the linker joining the KD and the SH2 domain¹⁷ (**Fig 1.8**). The SH3 domain and the linker interact with the N lobe and stabilize the helix αC of the KD in an inactive state¹⁷. Ligands binding to the SH2 and SH3 domains releases the autoinhibition. The kinase undergoes trans-autophosphorylation on the activation loop which stabilizes the active conformation of the kinase for substrate phosphorylation^{51,52} (**Fig 1.8**).

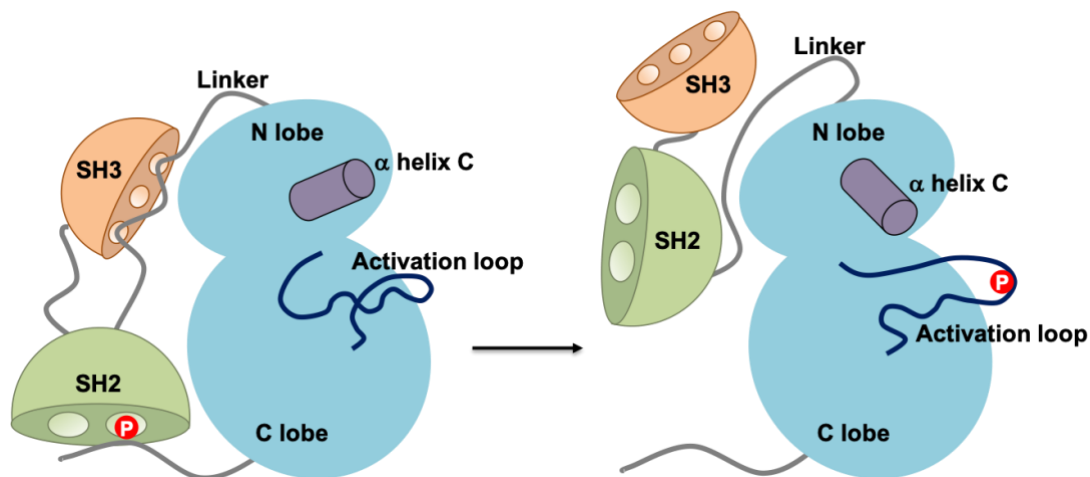


Figure 1.8 Schematic representation of activation of a non-receptor tyrosine kinase

The KD is indicated in blue, the SH2 domain in green, the SH3 domain in orange, the helix αC in purple, the activation loop is indicated with a dark blue curved line, the linkers are indicated as grey curved lines and phosphorylation is indicated as a red circle with a “P” inscribed. The SH2 and SH3 domains keep the kinase in an autoinhibited state by keeping the helix αC and activation loop in an inhibited conformation. Ligand binding to the SH2 and SH3 domains releases the autoinhibition and initiates activation loop phosphorylation. The kinase is activated for substrate binding and phosphorylation. (Adapted from Huse and Kuriyan, Cell, 2002)

Endoplasmic Reticulum Protein Homeostasis

The protein homeostasis or proteostasis network (PN) in eukaryotic cells (from yeast to human) is controlled by multiple signaling pathways that regulate the transcriptional and translational programs in the cell which govern protein synthesis, folding, distribution, localization and degradation. By doing so, these pathways control the development, cell differentiation and stress response that guide cells to change their physiology.

To date, many signaling pathways have been discovered which act to maintain homeostasis in the cell. Some examples are the phosphoinositide 3-kinase (**PI3K**) pathway, initiated by the PI3-kinase, which governs cell growth and differentiation, the MAP Kinase (**MAPK**) pathway initiated by Raf, MEKK1, which governs cell proliferation and cell migration, and the unfolded protein response (**UPR**) pathway, initiated by endoplasmic reticulum (ER)-resident proteins Ire1/PERK/Atf6, which alleviates the ER stress caused by the accumulation of unfolded or misfolded protein in the ER, and the ER-associated degradation (**ERAD**) pathway, which governs the degradation of unfolded proteins. Overall the proteostasis network comprising protein synthesis, folding, targeting and degradation is controlled and supported by more than 2000 proteins and sophisticated machineries in the cell through several signaling pathways.

Protein synthesis, folding and targeting

About one third of all the nascent polypeptide chains, either co-translationally or post-translationally enter the ER for correct folding to become biologically active⁵³. The endoplasmic reticulum (ER), the largest organelle in the cell, is a complex structure with an intricate network of interconnected tubules⁵⁴. The ER membrane is a bilayered structure that is continuous with the

nuclear membrane and encloses an internal compartment in the cell called the lumen. The ER plays a crucial role in protein targeting, protein folding, lipid biogenesis, calcium regulation and carbohydrate metabolism^{53,55,56}. The ER has different compartments each of which has unique functions. One of the primary functions of the ER is acting as the site for protein folding.

The transportation of the polypeptide chains towards the ER is mediated by a signal recognition particle (SRP)^{57,58}. The SRP interacts with the SRP receptor (SR), which is bound to the ER membrane, and transfers the polypeptide to the pre-inserted protein complex, called the translocon, in the ER membrane^{59,60}. This mechanism of targeting starts right after the signal sequence of the nascent polypeptide emerges out of the exit channel of the ribosome. The SRP recognizes and binds to a stretch of hydrophobic amino acid signal sequence (Tyr-Val-Thr-Phe-Ile-Ser-Leu-Leu-Phe in human serum albumin⁶¹) and consequently, leads to a momentary pause in translation. The mRNA-ribosome-elongating polypeptide chain-SRP complex is driven towards a free translocon on the ER membrane^{62,63}. The SRP-SR interaction leads to structural changes in the SRP that facilitate the transfer of the mRNA-ribosome-nascent polypeptide chain complex to the nearest translocon. Subsequently the SRP-SR interaction is dissolved and the SRP becomes free for another round of ER transport⁶⁴ (**Fig 1.9**).

In addition to targeting the nascent polypeptide chain to the ER, the signal peptide also acts to open the translocon channel. The signal peptide remains attached to the translocon channel while the polypeptide chain is threaded through the translocon like a large loop. Once the polypeptide chain has completely entered the ER lumen, the signal peptide is cleaved off by signal peptidase complex. The signal peptide is then released from the translocon and rapidly degraded⁶⁵.

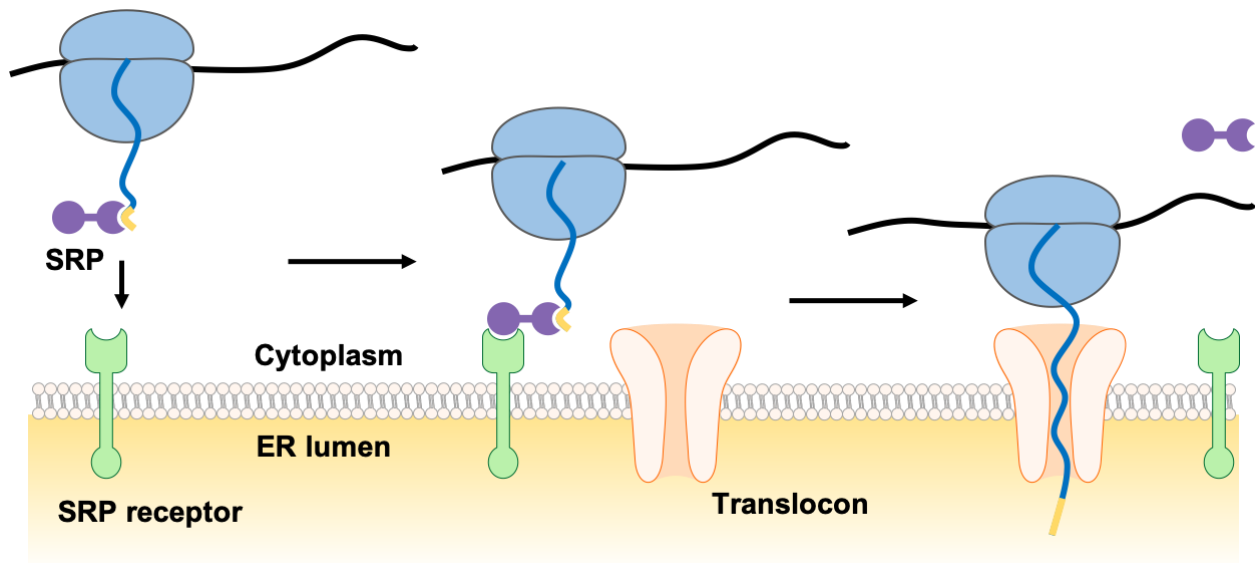


Figure 1.9 Schematic representation of targeting secretory proteins to the ER by SRP

The nascent polypeptide (blue curved lines) emerging from the ribosome (indicated in light blue) exit channel contains a signal peptide (yellow curved line) which is recognized by the SRP (purple dumbbell shape). The polypeptide chain is transported towards the ER by the SRP. The SRP interacts with the SRP receptor (SR, indicated in green), which is bound to the ER membrane, and transfers the polypeptide to the translocon (indicated in orange) in the ER membrane. Subsequently the SRP-SR interaction is dissolved and the SRP becomes free for another round of ER transport. (Adapted from Walter *et al*, Phil. Trans. R. Soc. Lond. B, 1982)

If a protein is destined for a secretory pathway or it is a luminal protein, it is released into the ER lumen, and then it keeps folding until it reaches its native stable conformation. On the contrary, trans-membrane proteins are not released into the ER lumen. In the simplest situation, where a transmembrane protein spans the membrane just once (i.e. single pass transmembrane protein), the signal sequence initiates translocation just like in the case of a soluble protein. However, a stretch of hydrophobic residues in the polypeptide chain called the stop transfer membrane anchor sequence results in translocation pause. In this situation, the protein is shifted laterally so that it remains anchored to the ER membrane. In the case of complex multi-pass proteins, there are additional pairs of start and stop hydrophobic sequences to reinitiate and stop

the translocation. These multi-pass transmembrane proteins, thus, get stitched in the ER membrane as they are being made⁶⁶.

Proteins can fold co-translationally as well as post-translationally⁶⁷. Although the exit channel of the ribosome can accommodate an α helix, there is more space for folding once the protein enters the ER lumen⁶⁸. With high concentrations of calcium ions and oxidizing conditions, the ER lumen provides the optimum environment for protein folding. In addition to protein folding, there are other events that lead to protein maturation like disulfide bond formation, N-linked glycosylation and glycosylphosphatidylinositol (GPI) anchor addition⁶⁹.

The ER lumen contains a high concentration of molecular chaperones that assist in protein folding and prevents the aggregation of mis-folded/unfolded proteins. The ER lumen houses the members of the Hsp70 and Hsp90 chaperone family⁷⁰. In metazoans, the glucose-regulated protein (GRP78/ BiP) is a member of the Hsp70 family⁷¹. The counterpart of BiP in yeast is Kar2. BiP is also called the master regulator of the ER. BiP facilitates protein folding and aggregation, regulates the translocation of nascent polypeptide chains to the ER, acts as an ER barrier by blocking the luminal side of the translocon, regulates the levels of calcium and prepares misfolded proteins for degradation^{72–77}. With the help of these protein-folding chaperones, the polypeptides are folded to their native quaternary structures and then transported via the Golgi body to designated locations in the cell where they can perform their biological activity (**Fig 1.10**).

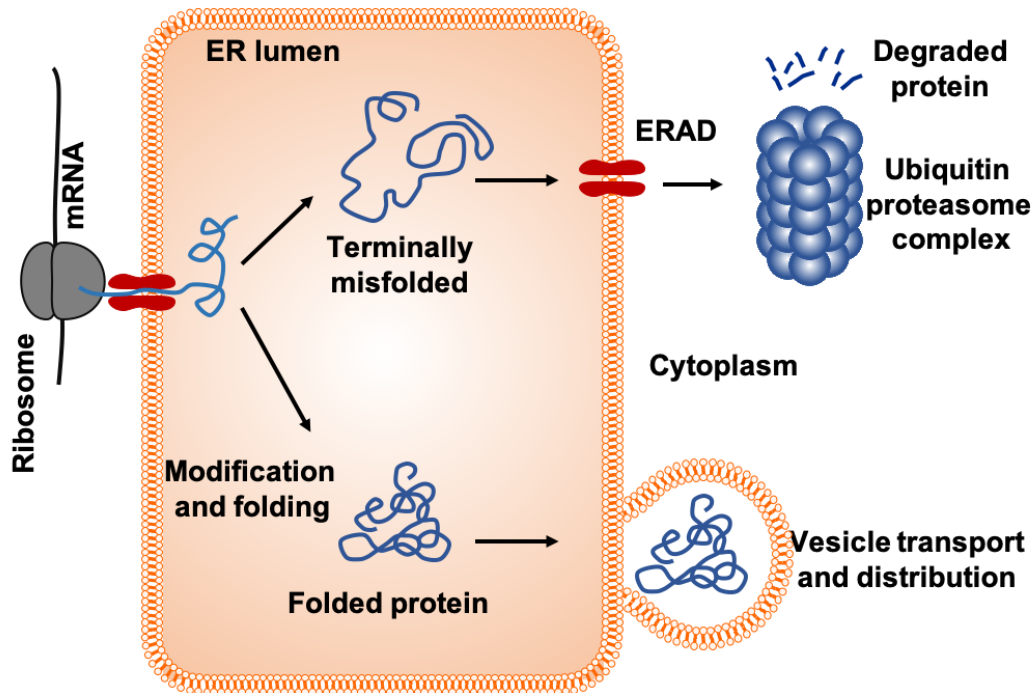


Figure 1.10 Protein synthesis, folding and targeting

The nascent polypeptide chain (blue scribbled line) is translocated to the ER through the translocon complex (indicated as red dumbbell). In the ER lumen (light orange gradient area), the polypeptide chain undergoes correct folding with the help of chaperones and modifications by glycosylation, palmitoylation, myristoylation and isoprenylation. Once proteins reach their native stable state, they are transported through vesicles to designated parts of the cell via Golgi complex. The misfolded proteins undergo degradation via the ERAD (ER associated degradation) pathway through the ubiquitin proteasome complex (indicated with clusters of blue circles). However, accumulation of misfolded proteins in the ER cause ER stress which in turn activates the UPR. (Adapted from Sitia and Braakman, Nature, 2003)

Protein degradation by ER associated protein degradation (ERAD)

Errors in modifications such as N-linked glycosylation or disulfide bond formation, can generate misfolded/unfolded proteins. These aberrant proteins in the ER are subjected to degradation via the ER-associated protein degradation (ERAD) pathway^{78,79}. ERAD is a multistep process that involves the retrotranslocation of the aberrant protein from the ER to the cytoplasm, followed by tagging the protein (ubiquitination) and finally, transport of the ubiquitinated protein to the proteasome complex for degradation⁸⁰.

There are three known ERAD pathways in the yeast *Saccharomyces cerevisiae*⁸¹. Misfolded proteins in the ER lumen trigger the ERAD-L pathway, misfolded proteins in the ER membrane trigger the ERAD-M pathway, and misfolded proteins in the cytoplasm trigger the ERAD-C pathway. Each of these ERAD pathways triggers a unique component to initiate protein degradation. For example, ERAD-L and ERAD-M substrate are directed to the Hrd1/Der2 ubiquitin ligase system and ERAD-C substrates are directed to the Doa10 ubiquitin ligase system^{82,83}.

Ubiquitination itself requires three enzymatic steps each of which is catalyzed by a specific enzyme. First, the enzyme E1 (ubiquitin activating enzyme) bonds with the ubiquitin molecule, which is a 76 amino acid-long conserved protein. Second, the enzyme E2 (ubiquitin conjugating enzyme) binds with the ubiquitin. Subsequently the enzyme E3 (ubiquitin ligase) catalyzes the bond formation between the ubiquitin and the protein substrate. This cycle is repeated until there are at least four ubiquitin molecules attached to the substrate protein. This tagging leads to the transfer of the protein to the proteasome complex and eventual degradation⁸⁴.

ER stress and the Unfolded Protein Response (UPR)

The secretory proteins fold and mature inside the ER. Perturbations to ER protein homeostasis due to biotic or abiotic factors lead to accumulation of unfolded protein inside the ER, a condition known as ER stress^{85,86}. ER stress activates a series of signaling pathways that alter the transcriptional and translational machinery in the cell. These pathways are collectively called the Unfolded Protein Response (UPR)^{87–90}.

The fundamental goal of the UPR is to help alleviate ER stress by four different ways. First, the UPR increases the capacity of the ER to handle the huge amount of unfolded proteins. Second, the UPR reduces overall translation in the cell to reduce the amount of nascent protein load in the ER. Third, the UPR induces the expression of certain genes that make chaperones to assist with the protein folding^{90,91}. Fourth, the UPR initiates apoptosis when the ER stress is prolonged⁹².

UPR in humans is initiated by three major ER-resident stress sensors, namely, Ire1, PERK and Atf6. These sensors initiate three parallel signaling pathways. Among these three pathways, the Ire1 pathway is conserved from yeast to humans (**Fig. 1.11**)⁸⁹.

i) The Ire1-mediated UPR pathway

The Ire1-mediated UPR pathway is the most conserved UPR pathway. *Saccharomyces cerevisiae* is known to have only the Ire1-mediated UPR pathway. During ER stress, this pathway is mediated by the trans-membrane ER resident protein, Ire1.

Ire1 contains an ER lumenal domain (Ire1-LD), a transmembrane region and a cytoplasmic kinase and RNase domain (Ire1_{cyto}). Under normal conditions, Ire1 exists as a monomer and the chaperone BiP (in human) or Kar2 (in yeast) remains associated with Ire1-LD⁹³. During ER stress, BiP/Kar2 is released⁹³. Ire1-LD senses the unfolded proteins in the ER lumen and it is activated⁹⁴. Activation of Ire1 requires its dimerization, oligomerization and trans-autophosphorylation^{95–98}. Active Ire1 in different organisms has different substrates. Ire1 cleaves the *HAC1* pre-mRNA in yeast, *XBPI* pre-mRNA in humans, *xbp-1* pre-mRNA in worm, and *bZIP74* pre-mRNA in rice plant^{99,100}. The active RNase domain of Ire1 cleaves the pre-mRNA at conserved regions in two stem-loop structures¹⁰¹. Ire1 cleaves the *HAC1* pre-mRNA in yeast^{102,103}. Subsequently, two exons

are joined by tRNA ligase¹⁰⁴. The mature *HAC1* mRNA translates the Hac1 protein, a transcription factor. Hac1 is translocated to the nucleus where it binds to the UPR elements (UPRE) and drives the expression of nearly 400 UPR genes which encode various proteins such as protein folding enzymes, ERAD components and lipid biosynthesis enzymes (**Fig 1.11**).

In mammals, there are two isoforms of Ire1: IRE1 α and IRE1 β encoded by the *ERN1* and *ERN2* genes respectively. IRE1 α is more ubiquitously expressed as compared to IRE1 β , which is expressed only in lung and intestinal epithelial cells. Hence, IRE1 α pathway is the most extensively studied UPR pathway^{105,106}. During ER stress, Ire1 cleaves the *XBPI* pre-mRNA¹⁰⁷. The exons are ligated by RtcB ligase that makes a frame-shifted mRNA¹⁰⁸, resulting in the production of Xbp1 (X-box binding protein-1) protein. Xbp1 is a B-ZIP (basic leucine zipper) transcription factor. Xbp1 is translocated to the nucleus where it binds to the UPRE and drives the expression of the UPR genes. Xbp1 induces expression of genes required for protein folding and genes necessary for the secretory pathway¹⁰⁷. Interestingly, in metazoans, both forms of *XBPI* mRNA (spliced and unspliced) are translated¹⁰⁹. However, the spliced version activates the UPR genes but the precursor version represses UPR signaling¹¹⁰. During ER stress response, the level of *XBPI* mRNA is increased but even when UPR is deactivated the *XBPI* levels keeps increasing. At this point, since Ire1 is also deactivated, the *XBPI* mRNA remains in its unspliced form. This unspliced *XBPI* mRNA translates into a protein that is a negative regulator of XBPI signaling¹¹⁰.

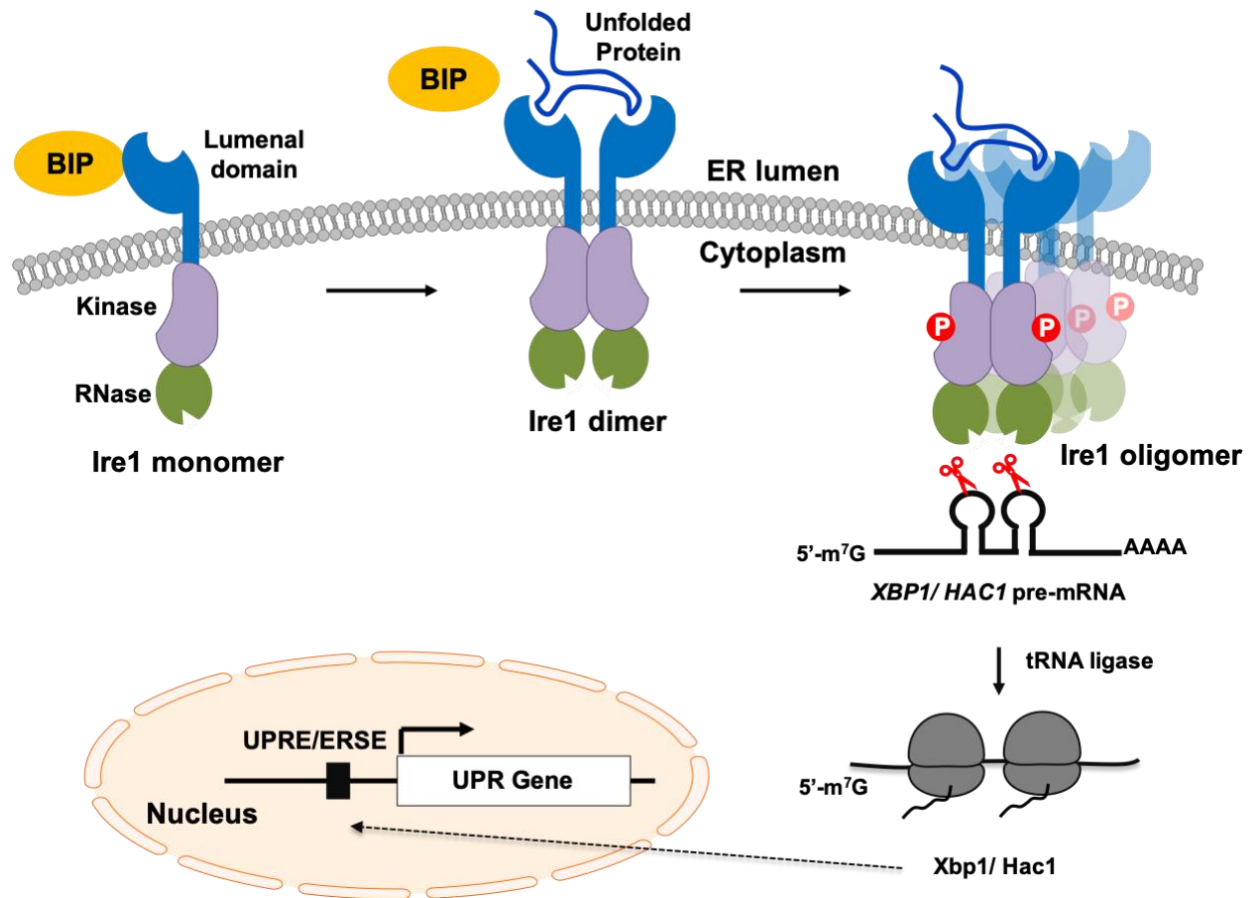


Figure 1.11 Schematic representation of Ire1-mediated UPR pathway

Ire1 contains a luminal domain (blue), cytoplasmic kinase domain (purple) and cytoplasmic RNase domain (green). Under normal conditions Ire1-LD remains associated with chaperone BiP (yellow) and remains inactive. During ER stress, BiP is released, and Ire1 is activated by dimerization, oligomerizes and autophosphorylation. Active Ire1 cleaves the XBP1/ *HAC1* mRNA in humans/ yeast. Mature mRNA translates into the protein Xbp1/ Hac1. These are active transcription factors that enter the nucleus, bind to the UPR element (UPRE) and activate the expressions of the UPR genes to alleviate ER stress. (Adapted from Walter and Ron, Science 2011)

ii) The PERK-mediated UPR pathway

The second ER stress sensor is PERK¹¹¹. Under conditions of ER stress, PERK is activated by dimerization in a back-to-back manner and autophosphorylation¹². The active PERK phosphorylates the alpha subunit of the eukaryotic initiation factor 2 (eIF2 α) at Ser-51. The phosphorylated eIF2 α inhibits the function of eIF2B that catalyzes the formation of an active eIF2-GTP-Met-tRNA_{iMet} ternary complex (TC) from its inactive GDP-bound form. The low TC reduces the overall rate of translation and the inflow of nascent proteins into the ER and helps to reduce the ER stress⁸⁸ (**Fig 1.12**).

PERK reduces the global translation; however, it paradoxically up-regulates the translation of Gcn4 in yeast cells or Atf4 in mammalian cells via the following unique mechanisms. The 5'-untranslated region (5'-UTR) of *GCN4/Atf4* mRNA contains four or two short inhibitory upstream open reading frames (uORFs)¹¹². Under physiological conditions, *GCN4* translation is repressed by these uORFs as they block the movement of the scanning ribosomes towards the start codon of *GCN4/Atf4*. During stress conditions, PERK phosphorylates eIF2 α , thereby reducing the formation of active eIF2-GTP-Met-tRNA_{iMet} ternary complex levels (TC). The low TC can allow the scanning ribosome to bypass the start codon of uORF1, uORF2, uORF3 and uORF4. Finally, ribosomes reach the authentic start codon of *GCN4* mRNA and translate protein¹¹³.

In metazoans, PERK induces the expression of Atf4, which is a transcription factor. Atf4 has two important target genes: CHOP (C/EBP homolog protein) and GADD34 (growth arrest and DNA damage-inducible 34). CHOP is a transcription factor and it regulates the expression of components involved in apoptosis. GADD34 is involved in dephosphorylating eIF2 α to counteract PERK to resume protein synthesis^{114,115}.

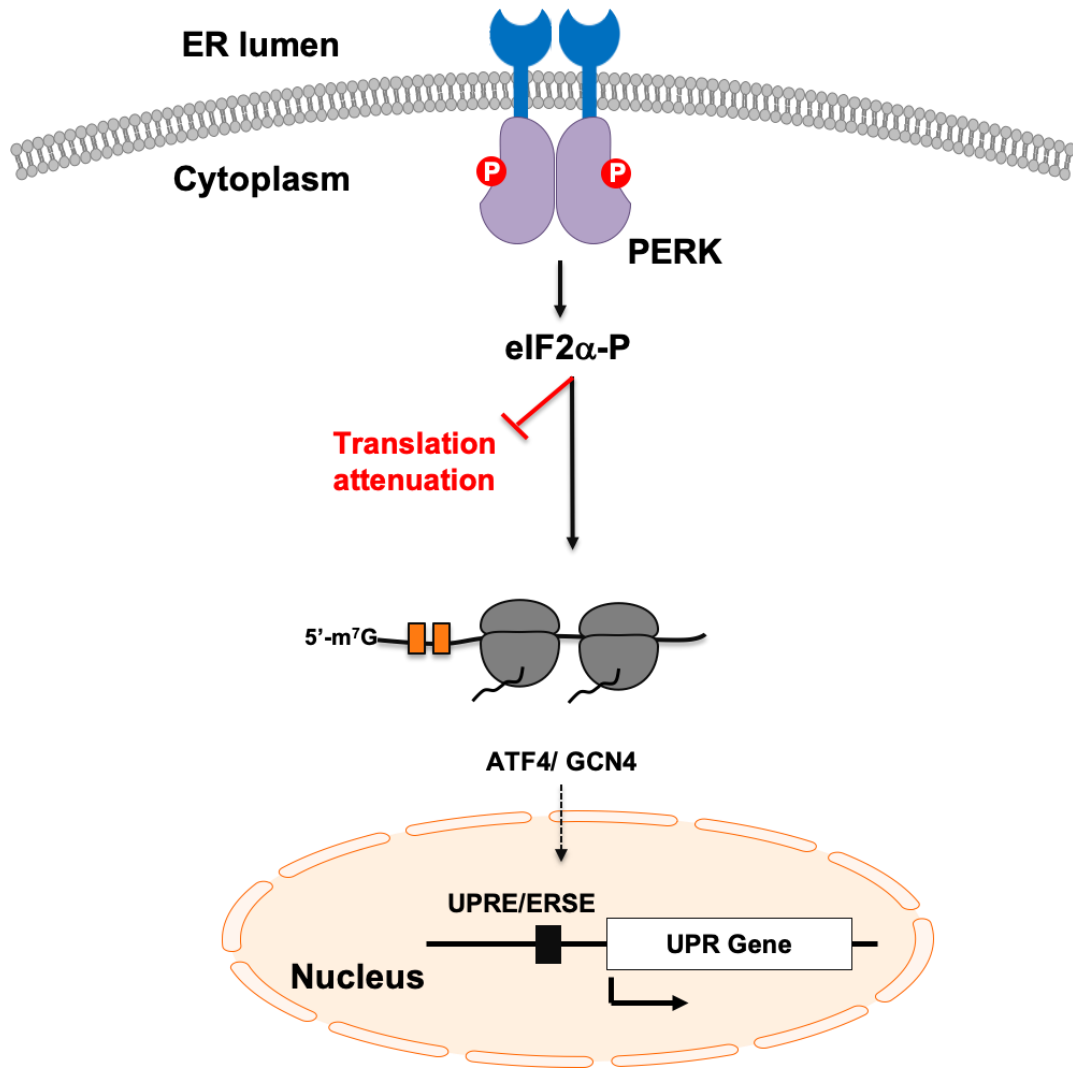


Figure 1.12 Schematic representation of the PERK-mediated UPR pathway

During ER stress, PERK (lumenal domain in blue and kinase domain in purple) is activated by dimerization and autophosphorylation. The active PERK phosphorylates the alpha subunit of the eukaryotic initiation factor 2 (eIF2 α). The phosphorylated eIF2 α inhibits the function of eIF2B that catalyzes the formation of an active ternary complex (TC). The low TC reduces the overall rate of translation and the inflow of nascent proteins into the ER and helps to reduce the ER stress. PERK reduces the global translation; however, it paradoxically up-regulates the translation of Gcn4 in yeast cells or Atf4 in mammalian cells via the following unique mechanisms. The 5'-untranslated region (5'-UTR) of *GCN4/Atf4* mRNA contains four or two short inhibitory upstream open reading frames (uORFs, represented as orange rectangles). Under normal conditions, *GCN4* translation is repressed. During stress conditions, low TC can allow the scanning ribosome to bypass the start codon of uORF1, uORF2, uORF3 and uORF4. Finally, ribosomes reach the authentic start codon of *GCN4* mRNA and translate protein. (Adapted from Walter and Ron, Science 2011)

iii) The Atf6-mediated UPR pathway

Atf6 contains a luminal domain that senses the ER stress. Under conditions of ER stress, Atf6 is translocated to the Golgi bodies via transport vesicles¹¹⁶. Then, the luminal domain and the transmembrane region of Atf6 are cleaved by 2 Golgi-resident proteases, S1P and S2P (site-1 and site-2 protease), respectively^{117,118}. As a result, the N-terminal cytosolic domain of Atf6 is released, which translocates to the nucleus and drives the expression of UPR genes (**Fig 1.13**). The cleavage of Atf6 shares some similarities with the cleavage of sterol response element binding protein (SREBP)¹¹⁸. In both cases, proteins are first translocated to the Golgi body and then the proteolytic cleavage takes place. The major difference in these two pathways is the initiation step: in the case of SREBP, it is the release from sterol repression, and in the case of Atf6, it is the accumulation of unfolded proteins. Amongst several targets of Atf6, major ones are protein folding chaperones like BiP and GRP94.

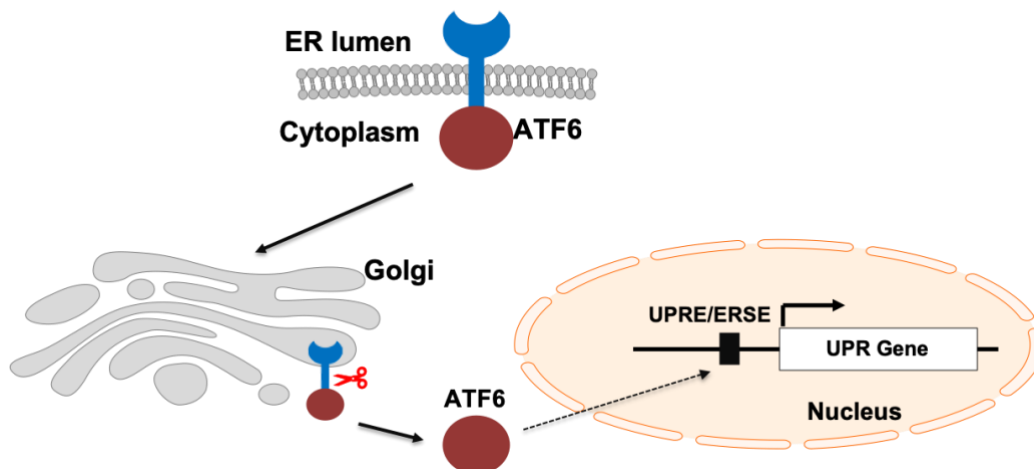


Figure 1.13 Schematic representation of the Atf6-mediated UPR pathway

During ER stress ATF6 (luminal domain in blue and cytoplasmic domain in maroon) is translocated to the Golgi body (light grey), where its cytoplasmic domain, which is an active transcription factor, is cleaved. The active transcription factor enters the nucleus, binds to the UPR element (UPRE) and activates the expressions of the UPR genes to alleviate ER stress. (Adapted from Walter and Ron, Science 2011)

In our lab, we study the inner workings of the UPR signaling pathways in budding yeast *Saccharomyces cerevisiae*. In yeast, UPR is known to be initiated by only Ire1 that has both kinase and endonuclease activities. Recently, our lab identified that kinases ‘Kin1’ and its isoform ‘Kin2’ significantly contribute to the UPR beyond their canonical role in cell polarity. These Kin kinases belong to the Kin/Par-1/MARK family of protein kinases and are known to have varied roles in the cells.

The Kin/Par-1/MARK family of Protein Kinases

Recent development in the field of kinases has brought into light the roles of two yeast protein kinases Kin1 and its isoform Kin2. The budding yeast Kin kinases are orthologs of worm PAR-1 (partitioning defective kinase) and the human MARK (microtubule affinity-regulating kinase) ¹¹⁹. The number of genes encoding the members of this family vary from lower to higher eukaryotes. *Schizosachharomyces pombe* contains only one whereas mammals contain more than four. Their roles include maintaining protein balance in the cell, establishing cell polarity, ensuring microtubule stability and cell cycle control.

The human MARK has a role in the progression of Alzheimer’s disease¹²⁰. During different cellular processes like cell polarity establishment, cell shape determination, cell differentiation, chromosome separation during mitosis and meiosis, and intracellular transport, microtubule reorganization is a key factor^{121,122}. Microtubule reorganization requires microtubule-associated proteins (MAPs) which bind to the microtubules¹²³. Phosphorylation status of MAPs determines their binding affinity to microtubules. MARK hyper-phosphorylates the MAP Tau at serine 262 in the KXGS motif and reduces the binding affinity of Tau to microtubules^{124,125}. The rapid phosphorylation of Tau results in its dissociation from the microtubule leading to microtubule

depolymerization. Microtubule depolymerization leads to the formation of paired helical fragments and neurofibrillary tangles, which are pathological hallmarks of neurodegenerative diseases¹²⁶.

PAR-1 in the worm *C. elegans* functions by providing anterior-posterior axis specification and determining asymmetry during cell division¹²⁷. Mutations in the Par genes in the worm can cause defects in early embryogenesis and embryonic lethality¹²⁸. Par-1 indirectly controls cell fate by determining the distribution of different regulators during development, and also by restricting degradation of germlasm proteins that are synthesized in the somatic cells^{129,130}.

PAR-1 homolog in *Drosophila* helps in the directional transport of biomolecules during the differentiation of the germline cell into the oocyte¹³¹. During the development of the fly embryo, a large amount of Oskar (*OSK*) mRNA is required in the posterior pole of the embryo. This transportation of the *OSK* mRNA to the posterior pole is essential for development and it is mediated by the Par-1 protein¹³². The Osk protein stability also depends on its phosphorylation by Par-1¹³³.

The Kin kinases (Kin1 and Kin2) in budding yeast have roles in establishing cell polarity and assisting in exocytosis¹³⁴. Kin1 in fission yeast assists in cell polarity establishment and initiates bipolar growth¹³⁵. However, detailed mechanisms of function of these kinases are yet unknown.

Members of this closely related family of Ser/Thr kinases share a similar domain architecture with an N-terminal conserved kinase domain, followed by an undefined spacer and a KA1 (kinase associated) domain at the C-terminal end (**Fig 1.14**). This KA1 domain remains associated with the catalytic kinase core and keeps the kinase in a dormant state. Detailed

mechanisms of release of the KA1 domain and activation of the kinases are yet to be determined. Some kinases in this family contain a UBA (ubiquitin associated) domain at the C-terminal end of the catalytic domain¹³⁶. Studies show that the UBA domain binds polyubiquitin and targets the protein for degradation through the Ubiquitin Proteasome System.

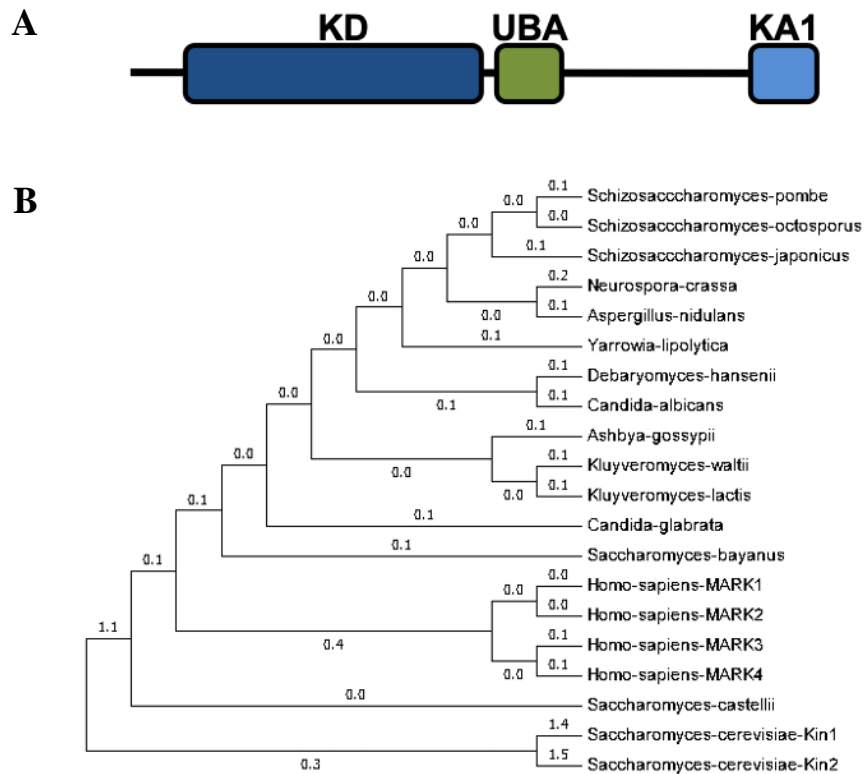


Figure 1.14 Domain organization of the MARK/Par-1/Kin kinase family of proteins

(A) The N-terminal kinase domain is colored dark blue, the UBA-associated domain green and the kinase associated domain 1 light blue. (B) Phylogenetic tree showing the relation between the different members of the MARK/Par-1/Kin family from diverse species (MEGA7).

Recent findings from our lab indicate that the yeast protein kinases, Kin1 and Kin2 have an added role in the UPR other than their ascribed role in cellular exocytosis. Kin1/Kin2 mediate the splicing, translocation and translation of the *HAC1* mRNA¹³⁷.

During ER stress, targeting of the *HAC1* pre-mRNA towards Ire1 for splicing requires a 3' bipartite element (3'BE), positioned at the 3'-UTR (untranslated region) of *HAC1*₁₃₈. Our lab provides evidence that two of the 3'BE nucleotides in *HAC1* (GG-1143-44) help to target the *HAC1* pre-mRNA towards Ire1 for splicing and improve the translation efficiency of the mature *HAC1* mRNA. This indicated that there is a 3'BE-ribonucleoprotein complex (3'BE-RNP) that drives the translocation, splicing and translation of *HAC1* mRNA. In order to identify the components of the 3'BE-RNP, our lab generated a 3'-BE crippled mutant of *HAC1* mRNA (*HAC1*-*GG1143-44CC*) that was not able to generate a wild type (WT) UPR response. Recently, we have shown that high-copy protein kinase gene *KIN1* or its paralog *KIN2* restores the defective ER-stress response associated with a mutation at the 3'-untranslated region (3'-UTR) of *HAC1* mRNA in the budding yeast *Saccharomyces cerevisiae*₁₃₇. Previously, Elbert and coworkers (2005) have shown that high-copy *KIN1* or *KIN2* suppresses the growth defect associated with mutations in several secretory proteins, including mutations in secretory/vacuolar pathway components *Sec1* and GTPase *Cdc42*₁₃₄. Thus, it appears that both *Kin1* and *Kin2* participate in the control of cellular protein homeostasis likely by engaging the UPR and by modulating the secretory pathways by yet unknown mechanisms. Indeed, a very limited number of studies have been done on how *Kin* kinases contribute independently or additively to either pathway.

This research is aimed at uncovering the mechanistic details to fully understand the *Kin* kinase signaling pathway in the budding yeast. I have been able to understand partially the mechanism of *Kin* kinase domain activation. In a collaborative project, we identified the downstream effector of the *Kin* kinase. These experiments and results are explained in detail in Chapters 2 and 3 followed by a summary and discussion on the future prospects of this research in Chapter 4.

Proteostasis in Health and Disease

Proteostasis is a tightly regulated process with many branches. Each branch of proteostasis is controlled by hundreds of factors. Based on large-scale genomic studies, it has been estimated that, in humans, there are about 280 factors that contribute to protein synthesis, 330 contribute to protein folding, 855 factors are involved in the Ubiquitin proteasome mediated degradation, and 533 factors in autophagy¹³⁹. Perturbance to any of these branches in proteostasis can lead to the onset of many diseases.

Diseases associated with protein synthesis

In eukaryotes, the process of translation is tightly regulated and mediated by several factors including the ribosomal subunits, the tRNAs that bring in the amino acids, the mRNA to be translated, and eukaryotic translation factors. Diseases associated with protein synthesis may arise from mutations in any of these factors¹⁴⁰.

An example of a disease caused by mutation in the mRNA is hereditary hyperferritinaemia or cataract syndrome which causes early onset of cataract in patients. The mutation in the 5'-untranslated region (5'-UTR) of the ferritin mRNA disturbs the mechanisms by which translation of ferritin (iron storage protein) is suppressed, causing excessive production of ferritin which aggregates in the lens and causes cataract¹⁴¹. A second example, the reduced expression of a cyclin-dependent kinase inhibitor (p16) which causes melanoma. In this case, there is a G to T mutation at the -34 position which creates an AUG codon in the 5'-UTR of the p16 mRNA. This lowers the levels of the wild type p16 tumor suppressor protein and dysregulation of the cell cycle leading to melanoma¹⁴². The Wolcott-Rallison syndrome, an autosomal recessive disorder is caused through impaired regulation of the translational initiation factor eIF2. A mutation in the gene encoding

PERK results in the reduced activity of PERK leading to increased production of insulin and causing diabetes mellitus in infants¹⁴³. Mutations in the ribosomal protein S19 encoded by RPS19 lead to onset of the Diamond-Blackfan anemia, a condition characterized by aregenerative anemia manifested during infancy¹⁴⁴. Other factors in translation, such as aberrant tRNAs and mutated charging enzymes, can cause neurological disorders. Evidence shows that mutations in the GARS gene encoding the glycyl tRNA synthetase result in muscular dystrophy¹⁴⁵.

Diseases associated with protein folding and aggregation

Biotic or abiotic factors such as heat stress, oxidative stress or stress from toxic components like cadmium, can result in protein unfolding. Unfolded proteins can form toxic aggregates leading to the onset of many diseases¹⁴⁶.

Some proteins contain unstructured disordered regions which are prone to misfolding and form aggregates. Other types of proteins undergo a partial unfolding step in order to form aggregates. An example of the latter is amyotrophic lateral sclerosis (ALS) caused by the unfolding and aggregation of the globular protein superoxide dismutase 1 (SOD1)¹⁴⁷. As protein folding is an error prone process, defects in the folding can lead to onset of diseases, for example, the cystic fibrosis transmembrane conductance regulator (CFTR) has a folding efficiency of ~25% and mutations can further lower that efficiency¹⁴⁸.

Toxic protein aggregates can disturb the overall cellular environment by engaging with and having deleterious effects on membranes and by interacting with macromolecules like RNA and membrane associated proteins. Overall, these can result in disturbing the cellular proteostasis network leading to an array of diseases.

Protein Kinases in Health and Disease

The human genome encodes more than 530 distinct kinases. Almost 30% of human proteins are modified by phosphorylation which regulates different cellular processes like growth, differentiation, proliferation and apoptosis. The process of phosphorylation is tightly regulated and any perturbation to kinase activity can lead to the onset of many diseases like metabolic disorders, neurodegenerative diseases and certain types of cancers¹⁰.

Kinases in neurological disorders

One of the most researched neurological disorders is Alzheimer's disease caused by hyperphosphorylation on Ser262 of tau protein by the kinase MARK2 (microtubule affinity-regulating kinase)¹⁵¹. A second example of an aberrant kinase associated neurodegenerative disorder is Parkinson's disease. The G2019S mutation in the gene of leucine-rich repeat kinase 2 (LRRK2) is a major cause of the development of Parkinson's disease¹⁵². In the progression of both Parkinson's disease and Huntington's disease, it has also been shown that the double stranded RNA-dependent protein kinase (PKR) has an important role. Evidence indicates that there is abnormal aggregation of phosphorylated PKR in tissue samples obtained from autopsies from patients suffering from these diseases. These aggregates have been predicted to play a role in the pathogenesis of Huntington's or Parkinson's disease¹⁵³.

Kinases in metabolic disorders

Cellular metabolism constitutes the essential chemical reactions which are responsible for various catabolic and anabolic cellular processes like ATP production, nucleic acid and protein synthesis, carbohydrate production, degradation and elimination of toxic wastes¹⁵⁴. Several protein

kinases are embedded in these metabolic pathways and hence abnormal protein kinase activity can impair these metabolic pathways causing an array of diseases.

In humans, *AKT2* which encodes a ubiquitous serine-threonine kinase plays a crucial role downstream of the insulin receptor in the phosphoinositide 3-kinase (PI3K) signaling pathway. It translates the physiological effects of insulin, and its malfunction has been implicated in glucose metabolism disorder and development of diabetes mellitus. Mutations in *AKT2* result in insulin resistance and onset of type 2 diabetes, hyperglycemia, dyslipidemia and hepatic steatosis¹⁵⁵. Another kinase implicated in the development of obesity and type 2 diabetes is the atypical Protein kinase C (aPKC). In insulin resistant states of obesity and diabetes, it has been observed that aPKC activation by insulin is defective in heart and skeletal muscles. This is a result of reduced activation of insulin receptor substrate (IRS)-dependent PI3K which works upstream of aPKC, and also reduced capability of the lipid product of PI3K to directly activate aPKC¹⁵⁶. Another group of kinases called the mammalian sterile twenty (MST) which comprise the germinal center kinase (GCK) II and III have been implicated in modulating the metabolism and in pathophysiology. MST1 is a key player in the progression of type 2 diabetes because of its role in the apoptosis of pancreatic β cells. Destruction of β cells leads to an increase in the blood glucose level thereby causing diabetes¹⁵⁷. In the cases of obesity and diabetes, another kinase that is affected is the AMP-activated protein kinase (AMPK). AMPK is known to be activated during cellular low energy states so that it can in turn activate energy generating processes like fatty acid oxidation and glucose transport. AMPK counteracts cellular processes like ER stress and oxidative stress that are activated during diabetes and obesity. Dysregulation in AMPK by its upstream kinase LKB1 leads to metabolic diseases and also certain types of cancers¹⁵⁸.

Kinases in cancer

Research progress in the field of kinase signaling pathways and cancer has advanced the understanding of the role of aberrant kinases in cancer progression. Protein kinases are embedded in most signaling cascades that guide cell differentiation and proliferation, and if these kinases are overexpressed or hyper active, it leads to oncogenesis¹⁵⁹.

One of the first extensively studied kinase mutations in cancer is in the Bcr-Abl fusion protein which causes chronic myeloid leukemia (CML) that accounts for up to 20% of all adult leukemias¹⁶⁰. The Abl tyrosine kinase has a role in oncogenesis associated with the reciprocal chromosome translocation that creates the Philadelphia chromosome²¹. Under normal conditions, the Abl kinase keeps shuttling between the nucleus and cytoplasm. However, the Bcr-Abl fusion protein remains in the cytoplasm where it is constitutively active and keeps interacting with its partners involved in the oncogenic pathway. For examples, Bcr-Abl interferes with the MAPK pathway causing increased proliferation of cells, the Janus-activated kinase (JAK)-STAT pathway leading to aberrant transcriptional activity, and the PI3K/AKT pathway causing enhanced apoptosis¹⁶². The first tyrosine kinase inhibitor designed to inhibit the Bcr-Abl kinase activity was Imatinib, which has now become the first line of treatment for CML. Imatinib binds close to the ATP binding site of Abl kinase in its inactive conformation and blocks its action semi competitively¹⁶³.

In multiple cases of lung cancer, particularly non-small cell lung carcinoma (NSCLC), it has been observed that the epidermal growth factor receptor (EGFR) tyrosine kinase contains mutations like in-frame deletions, nucleotide substitutions or in-frame duplications or insertions¹⁶⁴. Under normal conditions, EGFR tyrosine kinase adopts an autoinhibitory form. Following mutations in the kinase domain, it is destabilized, and the kinase hypersensitivity leads to inhibited

apoptosis, increased cell proliferation, angiogenesis and metastasis. So far, two inhibitors, namely erlotinib and gefitinib have been designed and approved to curb the EGFR activity by reversibly binding to its active site¹⁶⁵.

A kinase that has been implicated in the progression of breast cancer is the ErbB2 or Her2 belonging to the family of HER receptor tyrosine kinases. In breast cancer tumors, Her2 is overexpressed by up to 30%¹⁶⁶.

The slightest error or dysregulation in the proteostasis or mutations in the kinases that disrupt kinase signaling cascades can result in the onset of hundreds of diseases many of which could be life-threatening. Extensive research in drug target identification and drug development has led to discovery of small molecules which in the form of drugs can combat if not cure several diseases. Thus, it is important to gain mechanistic insights into these signaling pathways and understand the functioning of kinases so that it can lead to novel drug discovery and ensure better treatment of the diseases.

2. Chapter 2: Adaptation to Endoplasmic Reticulum Stress Requires Trans-phosphorylation within the Activation Loop of Protein Kinases Kin1 and Kin2, Orthologs of Human Microtubule Affinity-regulating Kinase

Introduction

Kin1 and Kin2 belong to the Kin1/Kin2/Mark/Par1 family of Ser/Thr protein kinases. Kin1 in fission yeast *Schizosaccharomyces pombe* has a role in cell polarity¹³⁵, Par-1 (partitioning-defective 1) in worm¹²⁷ *C. elegans* have been shown to be important for establishing cell polarity¹³², and MARK (microtubule affinity-regulating kinase)¹²⁰ in humans play a critical in the progression of Alzheimer's disease. Recently, the role of the two budding yeast Kin kinases, Kin1 and Kin2 has come to light. The Kin kinases were first described and partially characterized in the 90s. Both Kin1 and Kin2 were shown to be fairly large protein with 1064 and 1147 amino acids. Both these kinases contain an N-terminal catalytic kinase domain (KD) and they share about 85% amino acid identity in the KD^{167,168}. Recent studies show that Kin1 and Kin2 in budding yeast are involved in cellular exocytosis and cell polarity establishment¹³⁴ and the ER protein homeostasis pathway¹³⁷.

Cell polarity is a critical process that refers to the asymmetric distribution of biomolecules (RNAs, proteins and lipids) in the cells. Polarization is important for cell with growth, development, differentiation and cell division¹⁶⁹. Several essential yeast proteins that are important for establishing cell polarity and exocytosis are Cdc42, Rho3, Sec15, Sec4, Sec1 and Sec10. Genetic studies show that overexpression of the Kin kinases in the temperature sensitive secretory mutant strains can overcome the growth defect of the mutant strains¹³⁴. Furthermore, it was shown that the C-terminal end of the Kin kinases contain a KA1 (kinase associated 1) domain. The KD

and KA1 remain associated with each other and keep the kinases inactive¹³⁴. However, the detailed mechanism of release of the KA1 from KD and the mechanism of activation of the KD are as yet unknown.

Recent studies from our lab show that the Kin kinases are novel regulators of the Unfolded Protein Response pathway in the budding yeast¹³⁷. To date, the budding yeast UPR was known to be controlled by two key players, Ire1 and Hac1⁸⁷. During ER stress, targeting of the *HAC1* pre-mRNA towards the Ire1 for splicing requires a 3' bipartite element (3'BE), positioned at the 3'-UTR (untranslated region) of *HAC1*¹³⁸. Computer modelling predicts that the 3'-BE forms a helix-bulge-helix-bulge structure. Mutational, genetic and microscopy data provides evidence that there are two guanine nucleotides (GG1143,1144) on one of the bulges that play an important role in the translocation of the *HAC1* mRNA¹³⁷. In an attempt to identify the genes that can suppress the growth defect of the guanine mutations, our lab discovered that over expression of Kin2 can restore the optimum UPR response in the GG mutant strain. This evidence was backed by the increased splicing of *HAC1* mRNA in the GG mutant strain when Kin2 was overexpressed¹³⁷.

Here, we show that Kin1 and Kin2 proteins minimally require a kinase domain (KD) and an adjacent kinase extension region (KER) for their function both *in vivo* and *in vitro*. We also show that the functional mini Kin2 protein is predominantly localized within the cytoplasm and precipitated with the cellular membrane fraction, suggesting its association with the cellular endomembrane. Furthermore, we provide *in vivo* and *in vitro* evidence that the Kin2 residue Thr-281 and Kin1 residue Thr-302 within a flexible loop, also known as the activation loop, are phosphorylated *in trans* to activate the kinase domains.

Results

Bioinformatics analysis on yeast proteins Kin1 and Kin2 and comparison with related kinases in higher eukaryotes

Yeast Kin kinases contain an N-terminal kinase domain and a C-terminal KA1 domain separated by a long spacer of undefined function. As long as the KD and KA1 remain associated the kinase is inactive¹³⁴. Sequence analysis and bioinformatics show that these Kin kinases are closely related to the MARK in humans, PAR-1 in worm and share a similar domain architecture (Fig 2.1). Some kinases in the Kin1/Kin2/Mark/Par1 family contain a UBA (ubiquitin associated) domain at the C-terminal end of the catalytic domain¹³⁶. Studies show that the UBA domain binds polyubiquitin and targets the protein for degradation through the Ubiquitin Proteasome System.

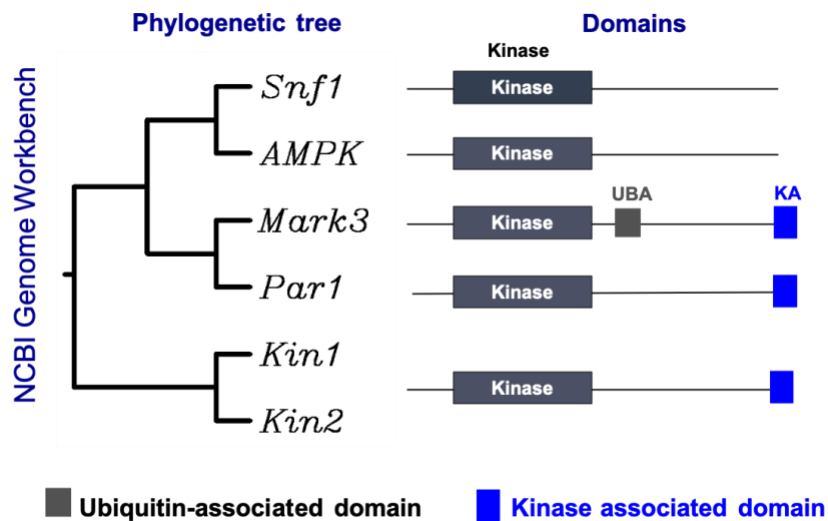


Figure 2.1 Schematic representation of Kin kinases and its counterparts

A phylogenetic tree was constructed using the protein sequences of Kin1, Kin2 and Snf1 from yeast, Par1 from worm, and AMPK and Mark3 from human. All the kinases share a similar domain architecture with an N-terminal KD (grey) and a C-terminal long region. Kin kinases, Par1 and Mark3 also contain a KA1 domain (blue) at the C-terminal end. Mark3 contains a UBA-like domain (dark green) after the KD.

***In vivo* assay to study Kin2 function**

In order to study the Kin kinase function in the yeast cells we developed an *in vivo* assay. We cloned the protein coding sequence with a Flag-tag (DYKDDDDK) under a *CYC1* promoter containing a galactose-inducible upstream activator sequence (*Gal-UAS*) (**Fig 2.2A**). The *CYC1* promoter is used to mimic the weak natural promoter of Kin1 and Kin2 and the *Gal-UAS* is used to induce the protein expression which is almost undetectable under the natural promoter (**Fig 2.2B**). In order to test the Kin2 function in UPR we use a functional complementation approach using a *kin1Δ kin2Δ* yeast strain. This *kin1Δ kin2Δ* yeast strain shows sensitivity to Tunicamycin. Tunicamycin blocks N-linked glycosylation of nascent protein and causes protein folding defects and ER stress¹⁷⁰. Hence, cells expressing a basal level of a functional Kin2 allele can grow on Tunicamycin. The Kin2 constructs were transformed in a *kin1Δ kin2Δ* yeast strain. The transformed cells were grown, serially diluted and spotted on synthetic minimal media with or without Tunicamycin. The transformed cells were also spotted and grown on synthetic media containing galactose. Galactose induces the expression of the kinase and this assay was used to test the kinase activity when the kinase was expressed at a higher level.

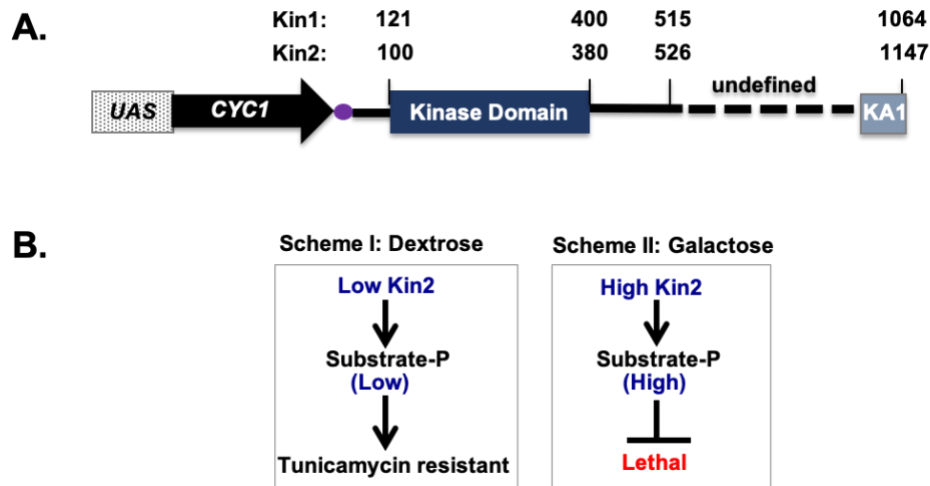


Figure 2.2 Schematic representation of Kin kinase constructs and scheme to study the kinase function

(A) The schematic representation of the tagged expression vectors. Both Kin1 and Kin2 are tagged with a Flag-epitope (close circle) at the N-terminus and expressed from a weak *CYC1* promoter containing a galactose inducible upstream activator sequence (*UAS*). The kinase domain (dark blue bar), long spacer (solid dashed line), newly defined kinase extension region (KER) and kinase-associated 1 (KA1) domain (light blue) are indicated. Numbers on the top indicate amino acid residues for Kin1 and Kin2. (B) Schemes for the proposed role of Kin2 and its substrate phosphorylation. On the dextrose medium (Scheme I), Kin2 expresses at a low level, leading to a low level of phosphorylation of its substrate and resistance to tunicamycin. On the galactose medium (Scheme II), Kin2 expresses at a high-level, which phosphorylates its own substrate as well as other unknown proteins promiscuously at a high-level, leading to a lethal phenotype.

Kin1 and Kin2 proteins require a kinase domain followed by an extra set of residues to activate the UPR

Previous reports show that protein kinase Kin2 or its N-terminal region (residues 1-526) are sufficient to suppress the growth defects of several secretory mutants¹³⁴. To determine the minimum length of Kin2 that can activate the UPR, we made several Kin2 constructs that lacked the DNA sequences encoding either N-terminal or C-terminal residues (**Fig 2.3**). Effects of truncations were then tested by a functional complementation approach. Each truncated Kin2 construct was introduced in a *kin1Δkin2Δ* strain. The resulting strains were then grown on the

medium containing dextrose, dextrose with tunicamycin or galactose. The *kin1 Δ kin2 Δ* strain containing the empty vector plasmid grew on the dextrose medium (**Fig 2.3A**, row 1) but did not grow on the medium containing Tunicamycin (**Fig 2.3A**, row 1). The same strain grew on the tunicamycin medium when the vector plasmid expressed a full-length Kin2 protein from its native promoter or from the weak *CYC1* promoter rows (**Fig 2.3A**, rows 2 and 3). The low level of Kin2 expression from either promoter was sufficient to promote growth on the medium containing tunicamycin likely by phosphorylating its substrate at a low level.

The minimum length of Kin2 that was able to complement the Kin1 and Kin2 double null strain, thus promoting growth on the tunicamycin medium was 94-510 (**Fig 2.3A**, row 4). Further deletion of 15-residues from the N-terminal end of Kin2-(94-526) or 10-residues from the C-terminal end of Kin2-(94-510) completely abolished yeast growth on the tunicamycin medium (**Fig 2.3A**, rows 5 and 6). Western blots from whole cell extract were probed with anti-Flag antibody to detect Flag-Kin2, and anti-Pgk1 antibody to determine loading control. The protein expression of Kin2-(94-500) was reduced to half that of Kin2-(94-510) (**Fig 2.3B**) possibly because the residues 500-510 likely play a role in maintaining the structural integrity of the protein.

To further confirm our results, we grew the *kin1 Δ kin2 Δ* yeast strain harboring the full-length Kin2 or its derivatives on the galactose medium (**Fig 2.3A**, Galactose). We observed that yeast cells expressing a full-length Kin2 grew on the galactose medium (**Fig 2.3A**, row 3), whereas cells expressing a truncated Kin2 protein did not grow on the galactose medium (**Fig 2.3**, row 4). The growth of the full length Kin2 on galactose was likely because the kinase domain (KD) of the full-length Kin2 is associated with its C-terminal KA1 domain as reported earlier¹³⁴, resulting in an inhibition of its KD function and a normal growth phenotype on the galactose medium. However, KD of the truncated Kin2-(94-510) protein is released from autoinhibition and results

in lack of cell growth on galactose medium. Cells expressing the truncated Kin2-(94-500) or Kin2-(110-526) protein grew on the galactose medium (**Fig 2.3**, rows 5 and 6) likely because of the lack of the kinase activity. These N-terminal or C-terminal residues are probably required for correct folding of the kinase domain in order to be functional inside the cell. Collectively, these data further confirm that Kin2 residues 94-510 are minimally required for its kinase function.

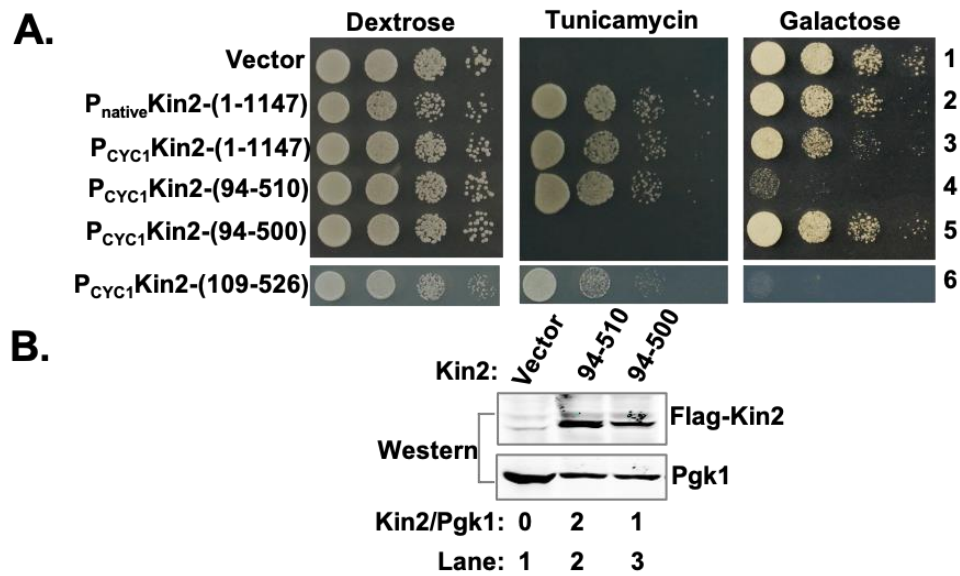


Figure 2.3 *In vivo* assay to study Kin2 protein kinase function

(A) Analysis of yeast cell growth. A *kin1Δkin2Δ* strain containing a vector plasmid (null) or expressing a wild type Kin2 from the native promoter [P_{native} Kin2-(1-1147)] or *CYC1* promoter [P_{CYC1} Kin2-(1-1147)] were grown, serially diluted, spotted and grown on a synthetic dextrose medium, dextrose plus tunicamycin (an ER stress inducer) medium, and galactose medium. A *kin1Δkin2Δ* strains expressing truncated Kin2 proteins from the *CYC1* promoter [P_{CYC1} Kin2-(94-510), P_{CYC1} Kin2-(94-500)] and P_{CYC1} Kin2-(109-526)] were also tested for their growth on the dextrose, tunicamycin and galactose media. (B) Analysis of Kin2 protein expression. Whole cell extracts were prepared from yeast cells containing a vector plasmid or indicated Kin2 derivatives (94-510 and 94-500) and subjected to SDS-PAGE followed by Western blot analyses using an anti-Flag (to detect Kin2) and anti Pgk1 (to determine the loading control) antibodies.

We observed a similar pattern with the paralog Kin1. We expressed the full length and truncated Kin1 constructs, introduced them in a *kin1Δkin2Δ* strain tested for their growth on dextrose and tunicamycin media. The full length Kin1 could complement the *kin1Δkin2Δ* strain

but the Kin1-(115-430) could not. The minimum length of Kin1 required to complement the *kin1Δkin2Δ* strain was Kin1-(115-515) suggesting that the growth defect was due to expression of a non-functional Kin1 kinase domain (**Fig 2.4A**). Western blots from whole cell extracts were probed with anti-Flag antibody to detect Flag-Kin1, and anti-Pgk1 antibody to determine loading control (**Fig 2.4B**).

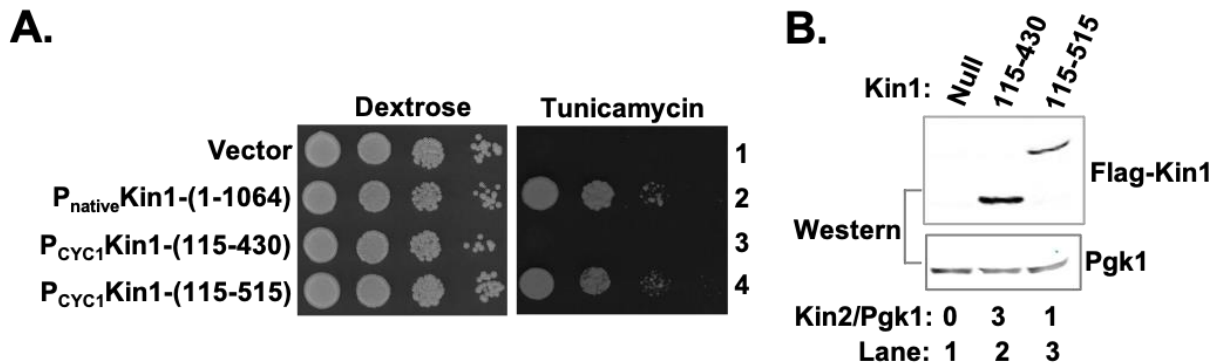


Figure 2.4 *In vivo* assay to study Kin1 protein kinase function

(A) Analysis of yeast cell growth. A *kin1Δkin2Δ* strain expressing a full-length Kin1 from its natural promoter [P_{native}Kin1-(1-1064)] and its indicated derivatives from the *CYC1* promoter [P_{CYC1}Kin1-(115-430) and P_{CYC1}Kin1-(115-515)] were grown, serially diluted, spotted and grown on dextrose and tunicamycin media. (B) Analysis of Kin1 protein expression. Whole cell extracts were prepared from yeast cells containing a vector plasmid or indicated Kin1 derivatives (115-430 and 115-515) and subjected to Western blot analyses using an anti-Flag (to detect Kin1) and anti Pgk1 (to determine the loading control) antibodies.

Collectively, we refer to the minimum functional Kin1 as Kin1_{mini} (i.e., Kin1 residues 115-515) and minimum functional Kin2 as Kin2_{mini} (i.e., Kin2 residues 94-526).

Using NCBI Blast we determined that the Kin1 residues 120-400 and Kin2 residues 94-510 showed sequence homology with the typical protein kinase PKA. However, residues 380-510 of Kin2 protein had no detectable homology to any conserved protein domain family other than with the residues 425-515 of Kin1 protein (**Fig 2.5**). We named this region as the kinase extension region (KER) and investigated the relative importance of KER in Kin2 protein.

Understanding the importance of the Kin2 KER

Pairwise sequence alignment of Kin1 and Kin2 protein sequences showed that Kin1 residues 463-482 had some homology with the Kin2 residues 442-462 (30% identities **Fig 2.5**). It also revealed that Kin1 lacked 23 residues corresponding to Kin2 residues 464-485 (**Fig 2.5**). Based on these findings, we proposed that KER of Kin2 was likely composed of three separate subdomains: KER-I (residues 386-440), KER-II (residues 440-480) and KER-III (residues 480-510). BLAST search with the small peptide sequences of each subdomain revealed that KER-I showed a partial protein sequence homology with the ubiquitin-associated (UBA) domain of several proteins, including a human autophagy protein Nbr1¹⁷¹ and a human Kin2 ortholog Mark3¹³⁶. This computational analysis suggested that the KER-I subdomain might adopt an UBA-like domain and KER-II & III subdomains might play an unknown role in the kinase domain function. To understand the role of each KER segment we deleted KER-I, II and III separately and studied the growth of the cells harboring these constructs on tunicamycin containing medium.

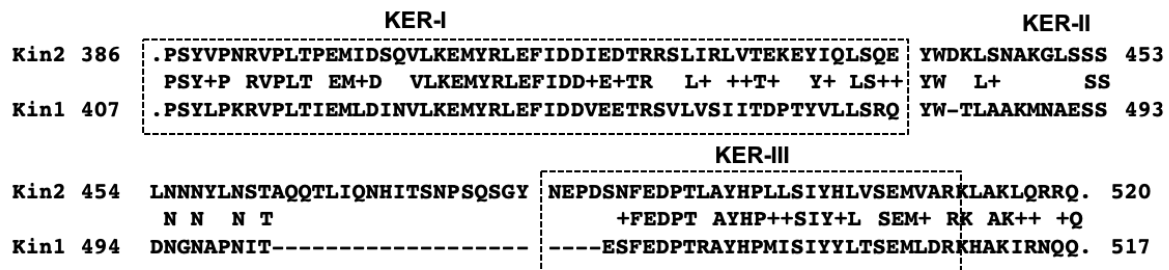


Figure 2.5 Pairwise sequence alignment of the KER of Kin1 and Kin2

Comparison of the KER sequences in Kin1 and Kin2 proteins. Protein sequences of Kin1 and Kin2 were pairwise aligned. From the sequence alignment, the KER residues of Kin1 (residues 407 to 517) and Kin2 (residues 386 to 520) are shown. In between two sequences, the conserved residues are shown by ‘letters’ and the identical residues are shown by “+” signs. The putative KER subdomains I and III are shown by boxes.

Three Kin2_{mini} constructs were generated by consecutively deleting DNA sequences encoding 40-residues from the C-terminal end [*e.g.*, Kin2-(94-480), Kin2-(94-440) and Kin2-(94-400)] and two Kin2_{mini} constructs by deleting DNA sequences encoding 40-residues from the internal region (*e.g.*, Kin2_{mini}-Δ(400-440) and Kin2_{mini}-Δ(440-480)] (**Fig 2.6B**). Each of these derivatives was then transformed into a *kin1* Δ*kin2*Δ strain and the resulting strains were tested for their growth on dextrose and dextrose plus tunicamycin media (**Fig 2.6A**). Yeast cells harboring Kin2_{mini}-Δ(440-480), like the Kin2_{mini}, grew on the tunicamycin medium (**Fig 2.6A**, rows 4 and 6), suggesting that Kin2_{mini}-Δ(440-480) expressed a functional protein. In contrast, yeast cells containing the Kin2-(94-480), Kin2-(94-440), Kin2-(94-400) and Kin2_{mini}-Δ(400-440) alleles were unable to grow on the tunicamycin medium (**Fig 2.6A**, rows 1, 2, 3 and 5). Western blot analysis was performed to show the expression of the truncated Kin2 proteins, (**Fig 2.6C**, lanes 1, 2 and 3). The protein expression was quantified (**Fig 2.6D**). These data suggested that growth defects were not due to major lack of protein expression, but due to expression of non-functional proteins. The Kin2_{mini}-Δ(400-440) protein expression was extremely low suggesting the residues 400-440 might play a role in conferring stability.

Taken together, it appears that Kin2 residues 440-480 (*i.e.*, KER-II) likely play a dispensable role, whereas residues 400-440 (*i.e.*, KER-I) and 480-526 (*i.e.*, KER-III) separately modulate the Kin2_{mini} function either by stabilizing the closed conformation of the KD as observed in typical kinases including the human Mark3₁₃₆, or by controlling the catalytic activity of the KD as observed in Ca₂₊/calmodulin-dependent protein kinase 1₁₇₂, or by dimerization like in Src family kinases₁₇₃.

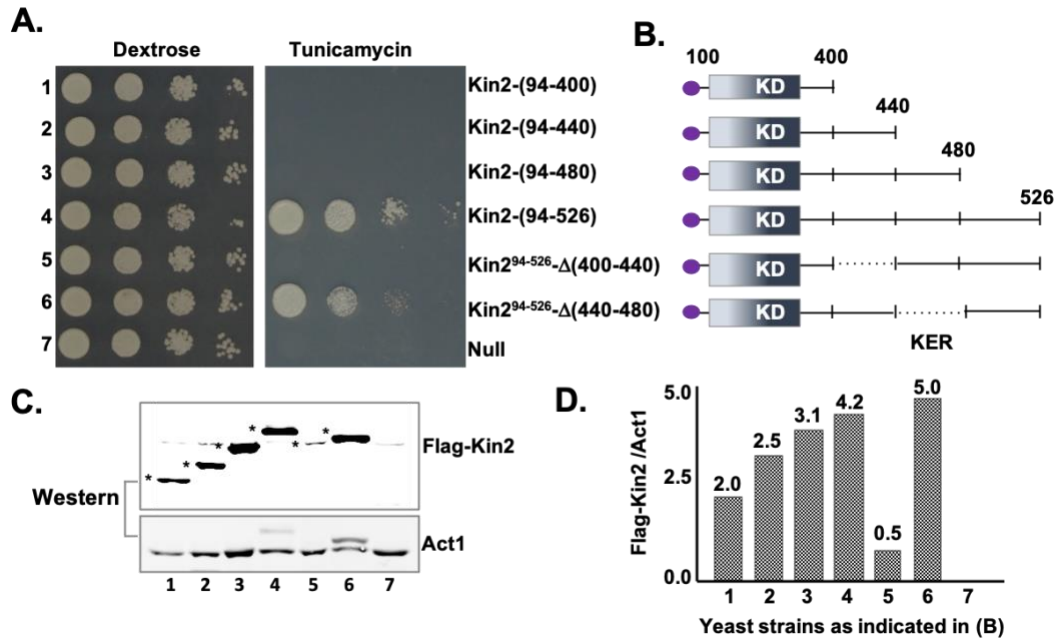


Figure 2.6 Two distinct regions within the KER control the Kin2 kinase function.

(A) Analysis of yeast cell growth. (Left panel) The *kin1*Δ*kin2*Δ deletion strains expressing the indicated Kin2 derivatives were tested for growth on dextrose and tunicamycin media. (Right panel) Schematic representation of Flag-epitope (violet circle)-tagged Kin2 deletion constructs. The kinase domain (solid bar) and the kinase extension region (KER, solid line) are shown. The dashed line indicates that the region is deleted. The number indicates residues number within the protein. (C) Analysis of Kin2 protein expression. Whole cell extracts from the indicated yeast cells (see panel B) were subjected to SDS-PAGE followed by Western blot analyses using anti-Flag and anti-actin (Act1) antibodies. The Flag-tagged Kin2 protein bands are indicated by “*” signs. (D) The relative expressions of Flag-Kin2 protein deletion mutants. The protein band intensities of Flag-tagged Kin2 and Act1 were measured using the ImageJ software. The ratios of Flag-Kin2 and Act1 are represented in a bar diagram.

KER-I sequences of Kin1 and Kin2 are partially similar to the UBA-like domain sequences of human Mark3 and Nbr1 proteins. However, the spatial arrangement of three constituent α -helices in the Mark3-UBA domain is different from the spatial arrangement of three constituent helices in Nbr1-UBA domain¹³⁶.

The UBA-like domain in Mark3 has 3 α helices oriented in three different directions and has been shown to bind the N-terminal lobe of kinase domain, implicating its potential role in integrating and stabilizing the kinase domain¹³⁶. We wanted to check if the KER-I of Kin2 which has certain sequence similarity to the UBA-like domain of MARK3 (**Fig 2.7A**) could be replaced by the latter. To address that, we made a chimeric protein where we replaced the Kin2-KER with MARK-UBA-like domain (Kin2-UBA_{Mark3}) (**Fig 2.7B**). We transformed this construct in the *kin1 Δ kin2 Δ* strain and the resulting strain was tested for their growth on dextrose and galactose to check kinase activity. The chimeric Kin2 grew on galactose media and the Western blot showed that the protein level was undetectable (**Fig 2.7C, D**). An explanation could be that deletion of the KER-I disrupted the protein folding and resulted in protein degradation or the UBA of Mark3 targeted the chimeric protein for degradation.

the binding of ubiquitin¹⁷¹. We wanted to check if mutation of the conserved leucine residue in Kin2 resulted in a stabilizing effect for Kin2 protein. We generated a Kin2 construct with a point mutation [(Kin2-(94-526)-L436A)]. We transformed this construct in the *kin1Δkin2Δ* strain and the resulting strain was tested for their growth on dextrose and dextrose with tunicamycin. The cells expressing the Kin2-(94-526)-L436A grew just like the cells expressing the wild type Kin protein (**Fig 2.8A**). To analyze if there was any difference in the levels of Kin2 protein the cells were grown and induced with galactose and collected at different time-points (4 hours and 8 hours) and subjected to a western blot analysis (**Fig 2.8B**). Cells collected at the 8th hour showed slightly more expression of Kin2-(94-526)-L436A as compared to wild type Kin2 protein. This could be likely because of the mutation that impaired ubiquitin binding and stabilized the protein.

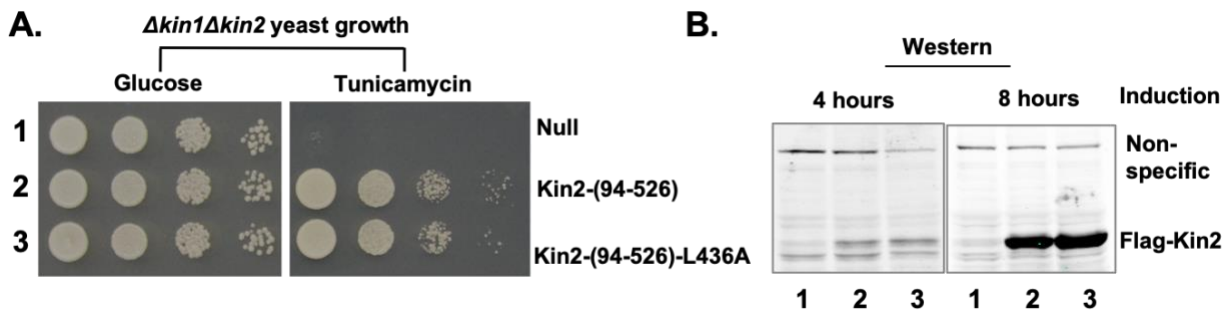


Figure 2.8 L436A point mutation in the UBA-like domain in Kin2

(A) *Δkin1Δkin2* strains expressing the indicated Kin2 alleles were grown on dextrose and dextrose with tunicamycin media. (B) Indicated strains were grown in galactose media for protein induction for 4 and 8 hours. Cell lysates were prepared and subjected to western blot analysis to detect the levels of Kin2 with anti-Flag antibody.

One of the mechanisms by which a kinase is activated is dimerization, and it is a common intermediate for many kinases including Src family kinase¹⁷³. To test if the KER-III has a function in dimerization, we took advantage of the ability of the protein glutathione S-transferase (GST) to dimerize. We replaced the Kin2 residues 480-526 with GST to construct a chimeric Kin2-(94-480)-GST. We transformed this construct in the *kin1Δkin2Δ* strain and the resulting strain was tested for their growth on dextrose and galactose to check kinase activity (Fig 2.9A). We predicted that, if the residues in KER-I had the ability to dimerize and activate Kin2, the cells expressing the Kin2-(94-480)-GST should not grow on galactose. However, we observed growth of the galactose containing media (Fig 2.9B) suggesting that KER-I likely does not dimerization to activate Kin2.

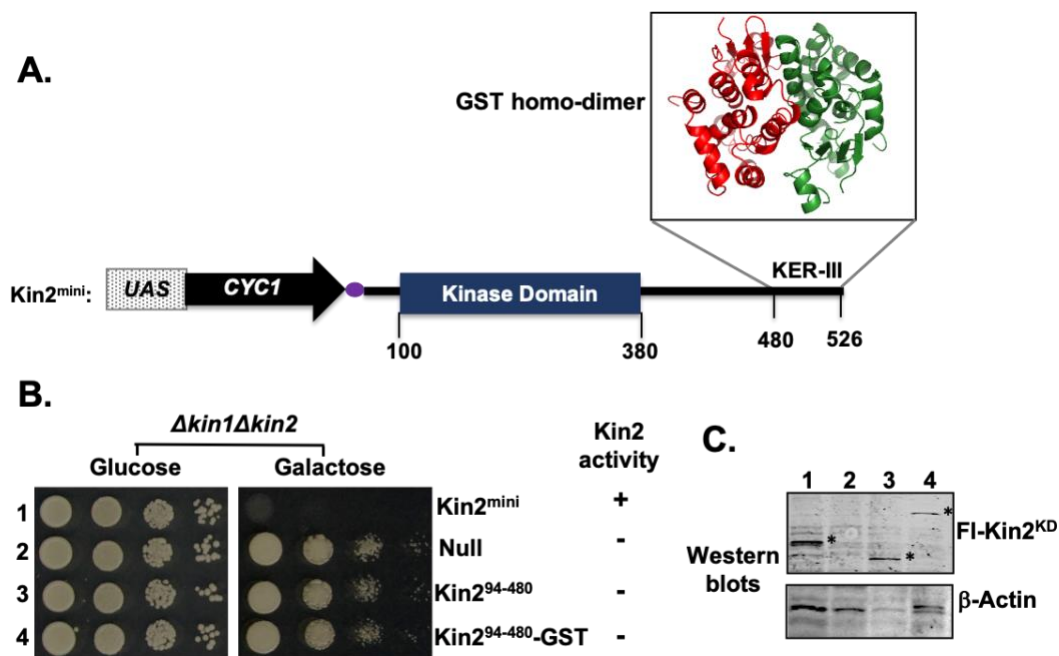


Figure 2.9 Replacement of KER-III by the GST

(A) Schematic of the Kin2 construct where KER-III was replaced by GST. Cartoon representations of crystal structure of two protomers of GST (PDB ID = 1BYE) are shown in red and green color. (B) The *kin1Δkin2Δ* yeast strains expressing indicated Kin2 proteins (were tested for growth on glucose and galactose media. No growth on the galactose medium indicates the positive (+) Kin kinase activity. (Lower panel) (C) Whole cell extracts from the indicated yeast strains were subjected to Western analysis using an anti-Flag antibody. Kin2 protein bands are indicated by the symbol “*”.

Kin2_{mini} is tethered to a membrane bound organelle

Previous studies have shown that Kin kinases precipitate with the membrane fraction¹⁷⁴, indicating that Kin kinases are likely to be associated with the plasma and/or organelle membranes. Previously we have shown that, under conditions of ER stress, both GFP-Kin2 and GFP-Kin2 Δ KA1 fusion proteins were predominantly visualized as discrete dots within the cytoplasm¹³⁷. Recently, Yuan et al. (2016) show that the GFP-fused full-length Kin2 protein is localized at the sites of polarized growth within the bud neck/tip¹⁷⁵. They also show that the GFP-Kin2-(1-526) fusion protein is localized at the bud tip¹⁷⁵. Collectively based on these observations, we hypothesized that the functional Kin2_{mini} might be a membrane-anchoring protein and we investigated the cellular localization of Kin2_{mini} protein.

We generated a GFP2-Kin2_{mini} fusion protein construct under the Kin2 native promoter in which the coding sequence of a monomeric A206K green fluorescence protein GFP2¹⁷⁶ was inserted at the N-terminal end of the Kin2_{mini} protein coding sequence (**Fig 2.10A**). The GFP2-Kin2_{mini} fusion protein, like the wild type Kin2_{mini} protein, complemented the *kin1 Δ kin2 Δ* strain and allowed yeast cells to grow on the tunicamycin medium (**Fig 2.10B**), suggesting that GFP2-Kin2_{mini} was a functional protein. Then, the GFP2-Kin2_{mini} fusion protein was transformed in a strain lacking a trans-membrane protein Ste2 (i.e., *ste2 Δ* strain). The *ste2 Δ* strain containing the GFP2-Kin2_{mini} was re-transformed with a plasmid expressing the Ste2-YFP (yellow fluorescent protein) fusion protein¹⁷⁶. The *ste2 Δ* strain co-expressing both GFP2-Kin2_{mini} and Ste2-YFP was then used for imaging studies by a two-photon microscope in the presence and absence of an ER stressor DTT. About 60-70% of cells showed the YFP signals at the edge of cells because of the membrane localization of Ste2 protein (**Fig 2.10C**). The same cells predominantly showed the GFP2 signals inside the cytoplasm (**Fig 2.10C**). Moreover, we observed that overall GFP2 signal

was 60% stronger in cells when treated with DTT (Fig 2.10D). Collectively, our data suggested that Kin2_{mini} localizes predominantly inside the cytoplasm.

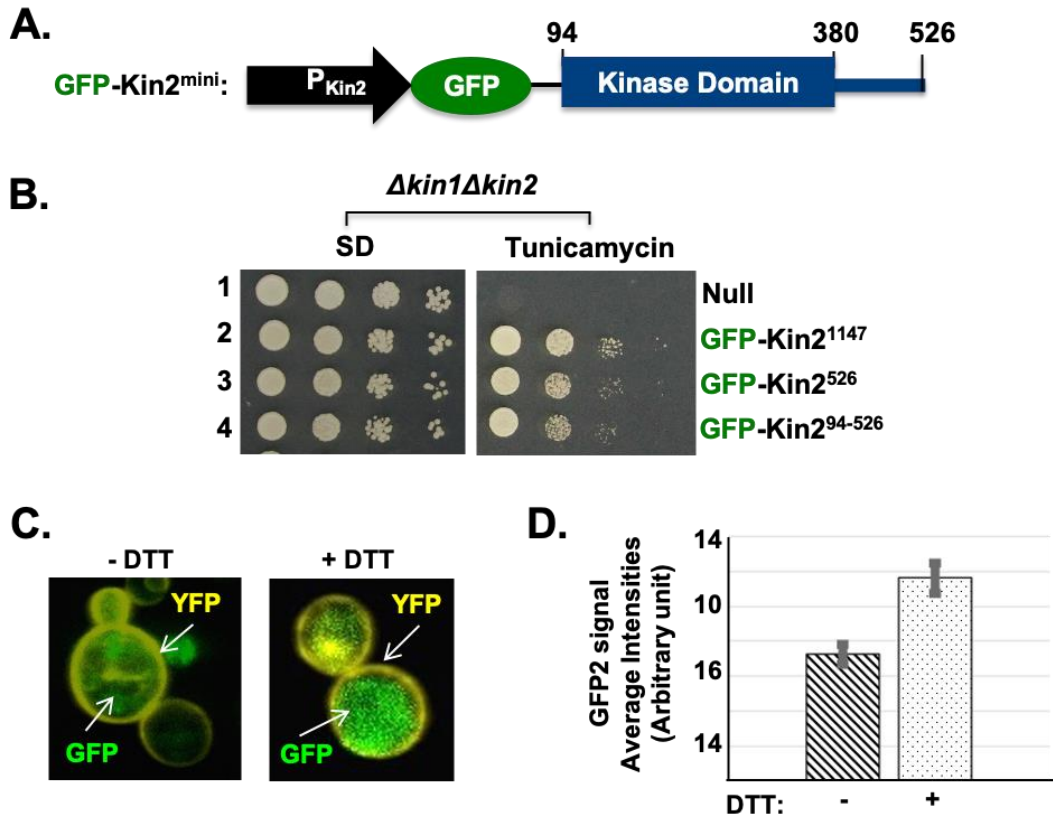


Figure 2.10 Expression and localization of GFP-Kin2_{mini} fusion protein

(A) Schematic representation of the GFP (green)-fused Kin2 (blue bar) expressed under the Kin2 native promoter (black arrow). (B) GFP-fused Kin2 constructs complemented the *kin1Δ kin2Δ* strain on tunicamycin medium suggesting these constructs encoded functional kinases. (C) The GFP2-fused Kin2_{mini} protein was expressed in a *ste2Δ* cell harboring a Ste2-YFP fusion protein. The GFP and YFP signals were detected by two-photon microscopy and shown by arrows. (D) Quantification of relative expression of GFP2 signals. The relative expression of GFP2 signal in the presence (+) and absence (-) of an ER stressor DTT were measured. The average intensities \pm weighted errors are represented as arbitrary units.

To determine whether or not Kin2_{mini} protein was associated with a membrane bound organelle, we prepared the whole cell extract from a *kin1Δkin2Δ* strain expressing the Flag-Kin2_{mini} and then separated soluble and insoluble fractions by centrifugation at 20,000g. Both soluble and insoluble fractions were subjected to SDS-PAGE and Western blot analysis using an anti-Flag antibody to detect Flag-Kin2 protein, an anti-Hac1 antibody to detect a soluble cytoplasmic protein and an anti-Kar2 antibody to detect an ER-resident and membrane-associated chaperone. As expected, majority of Hac1 protein was detected in the soluble fraction whereas Kar2 with the insoluble fraction (**Fig 2.11A**). A small fraction of Kar2 was also observed in the soluble fraction (**Fig 2.11A**), suggesting that a fraction of Kar2 protein might be released from the membranes and/or the speed 20,000g partially precipitated the cellular membranes. Interestingly, we observed that majority of Kin2_{mini} protein was separated with the insoluble fractions along with the Kar2 protein (**Fig 2.11A**, upper panel, lanes 2 and 3). These data suggest that Kin2_{mini} is a membrane-associated protein.

To rule out the possibility that the membrane-association was not a result of deposition of Kin2 inclusion bodies on the membrane, we treated the membrane fraction containing the Kin2_{mini} protein with 0.5 or 1% of Triton-X100 to break the lipid-lipid and lipid-protein interactions and to solubilize the membrane proteins. The soluble proteins were then separated from the pellet by centrifugation at 20,000g. Then, both soluble and pellet fractions were subjected to Western blot analysis. In the Western blot, we observed a significant amount of Kin2 protein in the 0.5% or 1% Triton-X100 solubilized fraction (**Fig 2.11B**, lanes 5 and 7) suggesting that Kin2_{mini} protein was associated with membrane, not precipitated as an inclusion body. Taken together, our data suggest that both Kin2_{mini}, like full-length Kin2, is an endomembrane kinase.

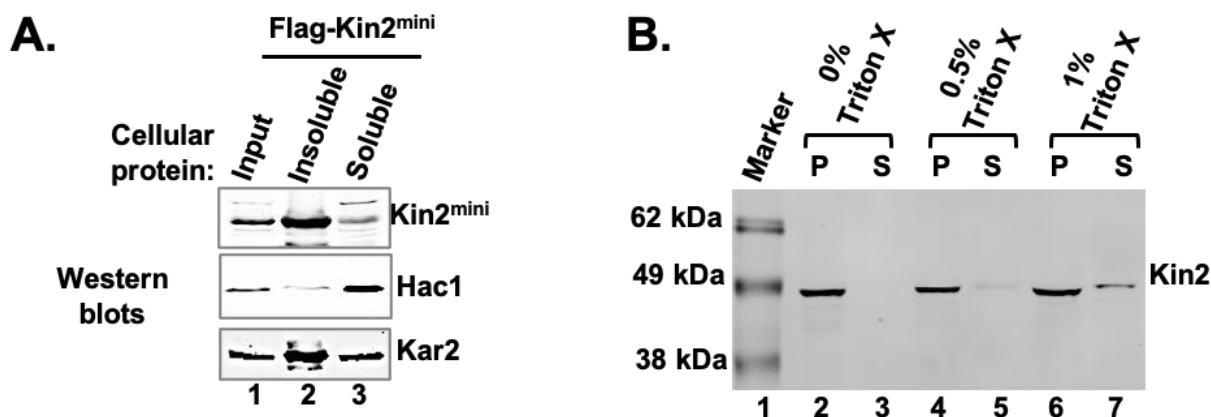


Figure 2.11 Membrane fractionation of cells harboring Kin2_{mini}

(A) Yeast cell extract containing the Flag-tagged Kin2_{mini} protein was separated by centrifugation as soluble and insoluble membrane fractions (see Materials and Method). Both fractions were subjected to SDS-PAGE and Western blot analysis using an anti-Flag antibody to detect Kin2, anti Hac1 antibody to detect soluble protein and anti-Kar2 antibody to detect an insoluble ER membrane-resident protein. (B) Triton X-100 partially solubilizes Kin2_{mini} protein from the membrane fraction. Yeast cell extract containing the Flag-tagged Kin2_{mini} protein was separated as soluble and insoluble membrane fractions. The insoluble fraction was mixed with 0.5 or 1% of TritonX-100 to solubilize the membrane bound proteins. The pellet (P) and supernatant (S) fractions were separated by centrifugation, subjected to SDS-PAGE and Western blot analysis using an anti-Flag antibody to detect Kin2 protein.

The C-terminal end of human Mark3 (ortholog of yeast Kin2) contains a KA1 domain that can drive the GFP-Mark3 protein to the cellular membrane¹⁷⁷, suggesting that KA1 motif plays a role in targeting the protein to the membrane. The bioinformatics analysis (using Clustal Omega) showed that the KA1 of Mark3 has extensive sequence similarity with the C-terminal 90 residues of Kin1 or Kin2 protein, which includes the KA1 motif (Kin2 residues 1048-1147) (**Fig 2.12A**).

We wanted check if KA1 of Kin2 had the ability to drive the protein to the cell membrane. To address that we constructed a GFP-KA1_{Kin2} fusion protein and expressed it from the Kin2 promoter (**Fig 2.12B**). We expressed this construct in a *kin1Δkin2Δ* strain, using confocal microscopy checked the localization of the KA1. GFP signals were observed majorly from near the cell membrane suggesting that the KA1 of Kin2 acts similar to that of Mark3 (**Fig 2.12C**).

domain activation, we searched the literature and the Protein Data Bank (PDB) for the crystal structure of Kin2. Because of the unavailability of the structure we used a homology modeling online tool, Swiss Model, to predict the crystal structure of Kin2 residues 94-526. From the generated results on Swiss Model, we used Pymol to analyze the predicted structure of Kin2.

The predicted Kin2 KD structure has a typical bilobal structure like the classical protein kinase PKA (**Fig 2.13**). It has an N-lobe, a C-lobe and the active site is embedded in between the two lobes. The activation loop ranges from the conserved APE to the DFG motif. Just like any typical kinase Kin2 also has landmark regions like the helix α C, helix α G, a conserved Lys-128 (K128) in the VAIK motif and a catalytic Asp-248 (D248) in the HRD motif¹⁵. To determine if these landmark regions or the conserved residues are phosphorylated to activate Kin2, we searched the database along with a mass spectrometric approach.

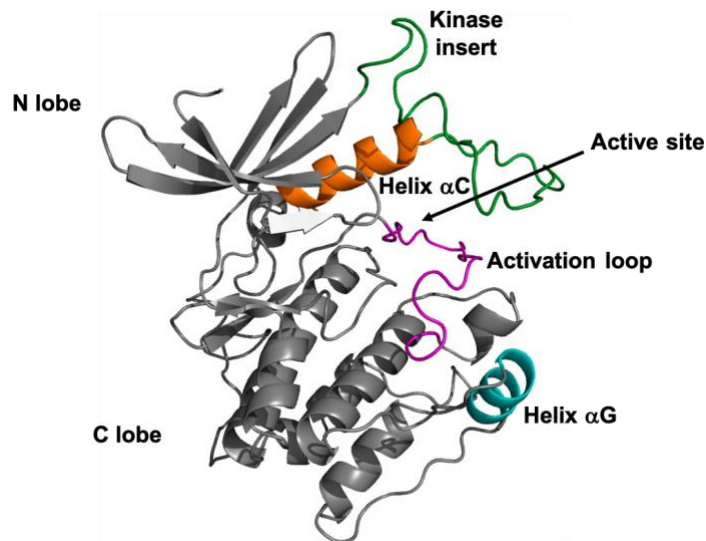


Figure 2.13 Ribbon representation of the predicted structure of Kin2 kinase domain

Kin2 kinase domain has a bilobal structure with an N lobe and a C lobe. The active site is in between. It has landmark regions just like other kinases - the helix α C in orange, the helix α G in cyan, and the activation loop in magenta. It has an extra region which we termed as the Kinase insert region depicted in green.

Mass spectrometric approach to identify phosphorylation sites on Kin2_{mini}

The *Saccharomyces* genome database (SGD) shows that protein kinases Kin1 and Kin2 are phosphorylated at more than 30 serine, threonine and tyrosine residues (some of which are common in both proteins), indicating that these kinases are regulated by a complex mechanism involving auto- and/or trans-phosphorylation. Next, we determined how many of these reported residues were phosphorylated in the Kin2_{mini} protein under conditions of ER stress. In order to do that, we purified Kin2_{mini} protein from cells grown under a condition of ER stress and analyzed the protein phosphorylation by mass spectrometry. The mass spectra analysis identified three major phosphorylated peptides with phosphorylated residues S151 (peptide 1), Y275 and T281 (peptide 2) and S328 and S329 (peptide 3). Other than these five kinase domain residues, there were eleven residues at the undefined domain (Kin2 residues T577, T608A, S609, S612, T629, S663, S706, S714, S1020, T1031 and T1037) which were conserved between Kin1 and Kin2 (Table 1).

Table 1 Phosphorylation sites on Kin1 and Kin2 proteins

#	Conserved phosphorylated residues		Kin2 mutations analyzed
	Kin1	Kin2	
1	S23	S24	
2	S25	T26	
3	-	S151	S151A
4	S296	Y275	Y275A
5	T302	T281	T281A
6	S349	S328	S328A
7	S350	S329	S329A
8	S569	T577	T577A
9	T592	T608	T608A

10	S593	S609	S609A
11	S596	S612	S612A
12	S612	T629	T629A
13	S647	S663	S663A
14	S677	S706	S706A
15	T700	S741	S741A
16	S966	S1020	S1020A
17	S973	T1031	T1031A
18	S979	T1037	T1037A

To determine if phosphorylation of these residues influenced the Kin2 kinase function we mutated these residues to non-phosphorylatable alanine (singly or in combination) and mutated proteins were expressed in the *kin1Δkin2Δ* strain. We found that mutations of 11 residues at the regulatory domain by alanine in a single protein (*i.e.* Kin2-11Ala) did not affect the ability of the full-length Kin2 to support cell growth on the tunicamycin medium. We also found that a single mutation of the residue S151 or double mutation of residues S328 and S329 within the kinase domain by alanine in the Kin2_{mini} protein (*i.e.*, Kin2_{mini}-S151A or Kin2_{mini}-S328A,S329A) did not impair yeast cell growth on the tunicamycin medium (**Fig 2.14**). These data suggested that phosphorylated residues S151, S328, S329, T577, T608A, S609, S612, T629, S663, S706, S714, S1020, T1031 and T1037 have insignificant impact on the ER stress response.

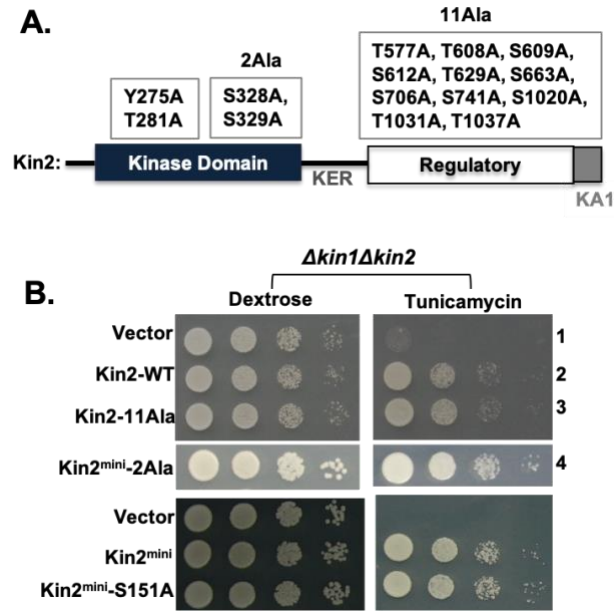


Figure 2.14 Mutational analysis of reported phosphorylation sites of Kin2

(A) The schematic representation of Kin2 protein with a kinase domain, kinase extension region (KER), regulatory domain and kinase associated domain 1 (KA1). The phosphorylated residues in the Kin2 protein as indicated were mutated by alanine. (B) Analysis of yeast growth test. A *kin1Δkin2Δ* strain harboring the indicated vector plasmid and the same vector containing the wild type or mutated Kin2 protein was tested for growth on the dextrose or tunicamycin medium.

Activation loop phosphorylation is important for kinase activity of Kin2^{mini}

Since we did not see any physiological significance of phosphorylation on the above-mentioned residues, we focused on activation loop residues Y275 and T281 in the Kin2 protein. Residues corresponding to Y275 and T281 in Kin2 are residues Ser296 (S296) and Thr302 (T302) in Kin1 (**Fig 2.15**). To determine the physiological relevance of Y275 or T281 phosphorylation, we individually mutated each one to alanine, generating Kin2^{mini}-Y275A and Kin2^{mini}-T281A constructs in the *Gal4-UAS* hybrid system. Kin2^{mini}-Y275A and Kin2^{mini}-T281A constructs were separately introduced in a *kin1Δkin2Δ* strain. The resulting strains were then tested for growth on dextrose, tunicamycin and galactose media and protein expressions were determined by Western blot (**Fig 2.15 B and C**). Cells expressing the Kin2^{mini}-Y275A, like wild-type Kin2^{mini}, grew on

the tunicamycin medium, but did not grow on the galactose medium (**Fig 2.15B**, rows 5 and 2). Similarly, cells expressing the Kin2_{mini}-T281A grew on the tunicamycin medium (**Fig 2.15B**, row 6). However, cells expressing Kin2_{mini}-T281A grew moderately on the galactose medium (**Fig 2.15B**, row 6). These growth phenotypes suggested that Kin2_{mini}-Y275A and Kin2_{mini}-T281A expressed functional kinases, the alanine mutation of Y275 or T281 did not impair the kinase activity, and the phosphorylation at either residue played insignificant role under physiological conditions.

To test if these residues act in combination, we mutated both residues Y275 and T281 to alanine in a single protein, generating a Kin2_{mini}-Y275A,T281A mutant. We also mutated both residues Y275 and T281 to glutamate in order to generate phospho-mimetic substitutions (*i.e.*, Kin2_{mini}-Y275A,T281E and Kin2_{mini}-Y275E,T281A). These Kin2_{mini}-Y275A,T281A, Kin2_{mini}-Y275E,T281A and Kin2_{mini}-Y275A,T281E mutants were then separately expressed in a *kin1Δkin2Δ* strain. We observed that the *kin1Δkin2Δ* cell expressing Kin2_{mini}-Y275A,T281A mutant protein, like kinase dead mutants Kin2_{mini}-K128R (K128 is the conserved Lys of the VAIK motif) and Kin2_{mini}-D248A (D248 is the conserved catalytic Asp of the HRD motif), did not grow on the tunicamycin medium (**Fig 2.15B**, rows 3, 4 and 7), but grew on the galactose medium (**Fig 2.15B**, galactose, compare rows 3, 4 and 7). These data suggested that Kin2_{mini}-Y275A,T281A expressed a non-functional protein like the catalytically inactive Kin2-K128R and Kin2-D248A mutants. Interestingly, we observed that the *kin1Δkin2Δ* cells expressing the Kin2_{mini}-Y275E,T281A or Kin2_{mini}-Y275A,T281E mutant protein, like the wild type Kin2_{mini}, grew on the tunicamycin medium (**Fig 2.15B**, Tunicamycin, rows 2, 8 and 9) and exhibited a lethal phenotype on the galactose medium (**Fig 2.15B**, galactose, compare rows 2, 8 and 9). These *in vivo* data suggested that Kin2_{mini}-Y275E,T281A and Kin2_{mini}-Y275A,T281E expressed active kinases in

which glutamate substitutions for Y275 and T281 likely mimicked the active phosphorylated state. Taken together, these data suggested that activation loop phosphorylation is important for the Kin2_{mini} kinase activity.

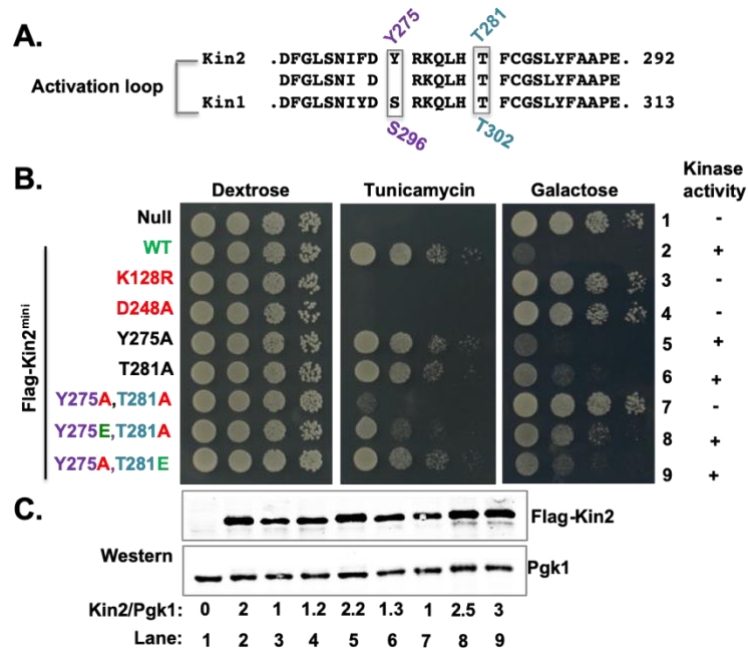


Figure 2.15 Activation loop phosphorylation is important for Kin2_{mini} kinase activity

(A) Comparison of the activation loop sequences of Kin1 and Kin2 kinases. The activation loop sequences of Kin1 (residues 287 to 313) and Kin2 (residues 267 to 292) were aligned. The phosphorylated residues are indicated on the top for Kin2 or at the bottom for Kin1. (B) Analysis of yeast cell growth. The *kin1Δkin2Δ* deletion strains containing a vector plasmid (null) or expressing a wild type Kin2_{mini} (WT) and its indicated derivatives were tested for growth on dextrose, tunicamycin and galactose media. The kinase activity is indicated as “+” (active) or “-” (inactive) signs. (C) Analysis of Kin2 protein expression. Whole cell extracts prepared from the yeast cells indicated in the panel (B) were subjected to SDS-PAGE followed by Western blot analyses using anti-Flag and anti-Pgk1 antibodies. The relative expressions (ratio of Flag-Kin2 and Pgk1 protein band intensities) are indicated at the bottom.

Activation loop phosphorylation is important for activity of full length Kin2

Next, we investigated the importance of activation loop phosphorylation in a full-length Kin2 protein. A *kin1Δkin2Δ* strain was separately transformed with an empty vector and the same vector bearing a wild type (WT) *KIN2* gene under its native promoter. We cloned the *KIN2* gene

to express a Flag-epitope at its N-terminal end. Transformants were streaked on both dextrose and tunicamycin media (**Fig 2.16**). We observed that transformants with the vector plasmid were able to grow on the dextrose medium but were unable to grow on the tunicamycin medium. However, the *kin1Δkin2Δ* cells containing the same plasmid bearing a Flag-tagged Kin2 gene were able to grow on both dextrose and tunicamycin media (**Fig 2.16**). These data suggested that the Flag-tag at the N-terminal end of Kin2 protein had no impact on its kinase function. Then, we mutated the catalytic residue Asp-248 of Flag-Kin2 protein, generating a kinase-inactive Kin2-D248A mutant. We also mutated the phosphorylated residues Y275 and T281 to generate several activation loop mutants (e.g., Kin2-Y275A, Kin2-T281A, Kin2-Y275A-T281A, Kin2-Y275E-T281A and Kin2-Y275A-T281E). These Kin2 mutants were separately transformed in the *kin1Δkin2Δ* strain and the resulting strains were tested for growth on both dextrose and tunicamycin media (see **Fig 2.16**).

The *kin1Δkin2Δ* strain containing a kinase-inactive Flag-Kin2-D248A mutant was sensitive to tunicamycin just like the vector. The *kin1Δkin2Δ* strain containing the Flag-Kin2-Y275A-T281E mutant was resistant to tunicamycin like the strain containing a wild-type Flag-Kin2. The resistance to tunicamycin was reduced when the *kin1Δkin2Δ* cells contained a Flag-Kin2-Y275A or Flag-Kin2-T281A mutant (**Fig 2.16**), and the resistance was further reduced when the *kin1Δkin2Δ* cells contained a Flag-Kin2-Y275A-T281A or Flag-Kin2-Y275E-T281A mutant. We were unable to detect the Flag-Kin2 protein by Western blot analysis in the whole cell extract containing 100μg of total protein, probably because of low expression from the native promoter. However, the obvious ER stress-resistant growth phenotype suggested that the kinase domain function was important to activate the ER stress response and the activation loop phosphorylation was important for full Kin2 kinase activity. Moreover, we found that the tunicamycin-resistant

phenotype of *kin1Δkin2Δ* cells containing the Flag-Kin2-Y275A-T281E derivative was comparable to cells containing a wild type Flag-Kin2 (Fig 2.16).

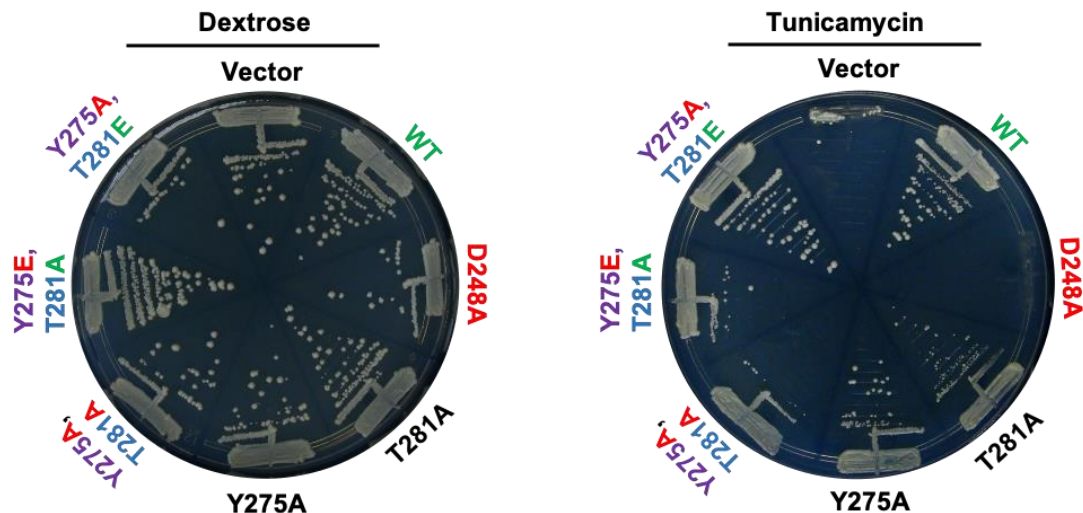


Figure 2.16 Activation loop mutations affect the protein function of full length Kin2

Analysis of yeast cell growth. The *kin1Δkin2Δ* deletion strains containing a vector plasmid (null), or the same vector plasmid bearing a wild type Flag-Kin2 (WT) or its indicated derivatives were streaked on the dextrose (upper panel) and tunicamycin (lower panel) media. Cells were then grown at 30°C for 48 hours.

To further confirm that the activation loop phosphorylation was important for the full kinase activity of Kin2, we performed *in vitro* kinase assays. Approximately 10 mg of total cellular proteins from the *kin1Δkin2Δ* cells expressing the Flag-Kin2-WT, Flag-Kin2-D248A or Flag-Kin2-Y275A-T281A were immunoprecipitated by anti-Flag M2-agarose. The immunoprecipitated proteins were washed with 5X kinase buffer and mixed with α -casein (0.5 μ g) and γ -³³P-ATP (1 μ Ci per reaction) like in Donovan *et al* (1994)¹⁶⁸. After 30 minutes, 2X SDS-dye was added to the reaction mixture to quench the kinase reaction. The reaction mixture was then heated at 90°C for 1 minute and loaded in an SDS-PAGE gel to separate the α -casein and M2-agarose precipitated proteins. The gel was stained to visualize the α -casein protein, dried and auto-radiographed (Fig 2.17).

Several phosphorylated protein bands (molecular mass ranging from 42-150 kDa) appeared in the reaction mixture containing the WT Flag-Kin2 (lane 3), indicating that Flag-Kin2 (molecular mass of Kin2 is 128.36 kDa) are autophosphorylated or they in turn phosphorylated other proteins in the immunoprecipitates. We also observed that α -casein was phosphorylated ~10-fold more in the reaction mixture containing the WT Flag-Kin2 protein than the reaction mixture containing the kinase-inactive Flag-Kin2-D248A protein (**Fig 2.17**, lanes 2 and 3). The Flag-Kin2-D248A is an inactive kinase, suggesting that phosphorylation in α -casein might occur by unknown kinases present in the immunoprecipitates. Moreover, we observed significant α -casein phosphorylation in the reaction mixture containing the Flag-Kin2-Y275A-T281A (**Fig 2.17**, lane 1) mutant, suggesting that Y275A and T281A mutations in a single protein did not completely abolish the kinase domain function. The relative phosphate incorporation in the α -casein showed that Flag-Kin2-Y275A-T281A mutant phosphorylated α -casein 5-fold less efficiently than the WT Flag-Kin2 (**Fig 2.17**, lanes 1 and 3). We were unable to detect the expression of Flag-Kin2 protein by Western blot analysis due to its extremely low expression. The data collectively suggested that Flag-Kin2-Y275A-T281A mutant expressed a weaker kinase and that the activation loop phosphorylation is important for the full kinase activity of Kin2.

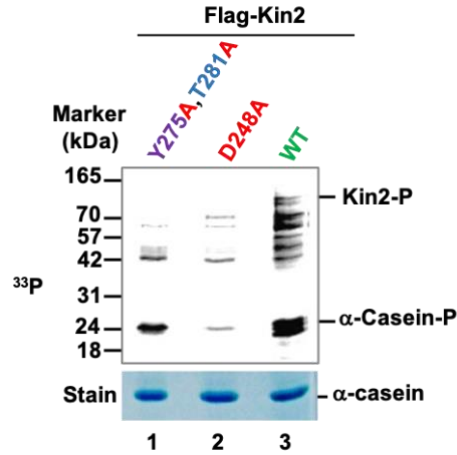


Figure 2.17 Activation loop phosphorylation is required for full Kin2 kinase function.

(A) Analysis of Kin2 kinase activity *in vitro*. Whole cell extracts (~10 mg) prepared from the *kin1* Δ *kin2* Δ deletion strains expressing a wild-type Flag-Kin2 (WT) and the indicated Kin2 derivatives mixed with anti-flag M2 agarose beads. The Flag-tagged Kin2 proteins were precipitated, washed with kinase buffer and mixed with α -casein (0.5 μ g) and γ - 33 P-ATP (1 μ Ci). The reaction mixture was then mixed with 2X SDS dye, heated at 90°C for 1 minute, centrifuged and loaded on an SDS-PAGE. The gel was stained, dried and auto-radiographed (33 P, upper panel). The α -casein protein bands are shown in the middle panel. Incorporations of 33 P in α -casein were determined by the relative band intensities and shown by bar diagram in the lower panel.

Activation loop phosphorylation is important for Kin1_{mini} kinase activity

Based on results of our experiments showing that phosphorylation of the activation loop is important for the activity of Kin2, we decided to perform similar studies on the related Kin1 kinase. The Kin2 residues Y275 and T281 correspond to Kin1 residues S296 and T302. Thus, we investigated whether or not substitution of glutamate for T302 activated the kinase function of Kin1_{mini} protein. We expressed the Kin1_{mini} and its derivatives Kin1_{mini}-D269A (kinase-inactive mutant), Kin1_{mini}-S296A,T302A (non-phosphorylatable mutant), Kin1_{mini}-S296A,T302E and Kin1_{mini}-S296E,T302A (phospho-mimetic mutants) in a *kin1Δkin2Δ* strain (**Fig 2.18**). The *kin1Δkin2Δ* strain containing a vector plasmid was unable to grow on the tunicamycin medium but was able to grow on the same medium when the vector plasmid contained a WT *KIN1*_{mini} gene (**Fig 2.18A**, rows 1 and 2). The *kin1Δkin2Δ* strain containing the Kin1_{mini}-S296A,T302E mutant, like WT Kin1_{mini}, was able to grow on the tunicamycin medium (**Fig 2.18A**, rows 2 and 5). In contrast, the *kin1Δkin2Δ* strain containing the Kin1_{mini}-D269A, Kin1_{mini}-S296A,T302A or Kin1_{mini}-S296E,T302A mutants, like the vector control, was unable to grow on the tunicamycin medium (**Fig 2.18A**, rows 1, 3, 4 and 6). Western analysis showed that all the mutant proteins were expressed at the levels comparable to WT (**Fig 2.18B**, lanes 1-6), suggesting that Kin1_{mini}-D269A, Kin1_{mini}-S296A,T302A and Kin1_{mini}-S296E,T302A mutants expressed non-functional kinases. These data further suggested that Kin1_{mini}-S296A,T281E likely expressed an active kinase in which the glutamate substitution for T302 mimicked a phosphorylated residue. Phospho-mimetic substitution at the Kin1 residue S296 (i.e., Kin1_{mini}-S296E,T302A), probably because the glutamate substitution, S296E, did not mimic the phosphorylated state, or phosphorylation of S296 had only a minor role for Kin1 kinase activity. Taken together, it appears that phosphorylation of

T302 in Kin1 or the corresponding T281 in Kin2 is important for the full Kin1 or Kin2 kinase domain function.

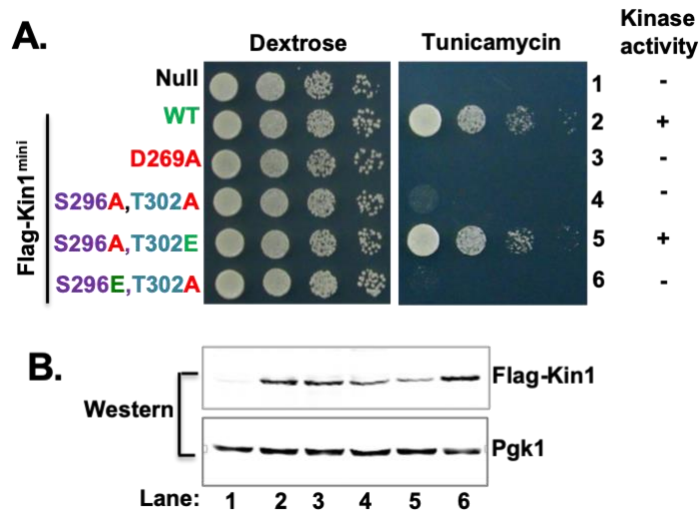


Figure 2.18 Activation loop phosphorylation is important for Kin1_{mini} kinase activity.

(A) The *kin1Δkin2Δ* deletion strains containing a vector plasmid (null) or expressing a wild-type Flag-Kin1 (WT) and the indicated derivatives were tested for their growth on dextrose and tunicamycin media. The kinase activity is indicated as “+” (active) or “-” (inactive) signs. (B) Whole cell extracts from the yeast cells indicated in the panel (A) were subjected to SDS-PAGE followed by Western blot analysis using anti-Flag and anti-Pgk1 antibodies.

Phosphorylation of the residue T302 in Kin1 or T281 in Kin2 occurs in *trans*

The inactive-to-active transition of kinases, in most cases, requires phosphorylation within the activation loop¹⁷⁸. Phosphorylation of the activation loop can occur by itself (*i.e.*, auto-phosphorylation) or may occur via other kinases (*i.e.*, trans-phosphorylation), or both¹⁷⁹. To address this question, we had an antibody raised against the phosphorylated T281 residue by GenScript. To determine how T281 phosphorylation occurs in cells, two catalytically inactive kinase mutants (*i.e.*, Kin2_{mini}-D248A and Kin2_{mini}-K128R) were expressed in a *kin1Δkin2Δ* strain (Fig 2.19A) and then examined the phosphorylation status of the T281 residue. Western blot analysis showed that expressions of Kin2_{mini}-K128R and Kin2_{mini}-D248A were similar to the wild

type Kin2_{mini} protein (**Fig 2.19A**, lanes 3,4 and 2). The residue T281 was phosphorylated in both Kin2_{mini}-K128R and Kin2_{mini}-D248A kinase-inactive proteins (**Fig 2.19A**, Western, lanes 3 and 4). We also observed that the level of T281 phosphorylation in Kin2_{mini}-K128R or Kin2_{mini}-D248A was much lower than in the Kin2_{mini} protein (**Fig 2.19A**, lanes 2,3 and 4) probably because of their susceptibility to de-phosphorylation by unknown phosphatases¹⁸⁰. The phosphorylation of T281 residue in kinase-dead mutants suggested that T281 phosphorylation likely occurred in a *trans* mechanism by an upstream kinase. To confirm that Kin2_{mini}-K128R was inactive kinase, we induced the expression of Flag-Kin1_{mini}, Flag-Kin2_{mini} and Flag-Kin2_{mini}-K128R proteins in yeast *Saccharomyces cerevisiae* cells. The recombinant proteins in *Saccharomyces cerevisiae* (referred to as the ScKin1_{mini}, ScKin2_{mini} and ScKin2_{mini}-K128R) were purified and subjected to *in vitro* kinase assays using α -casein as a substrate. We observed that the purified ScKin1_{mini} or ScKin2_{mini} readily phosphorylated α -casein, but the phosphorylation of α -casein was significantly lower when we used ScKin2_{mini}-K128R mutant protein (**Fig 2.19B**).

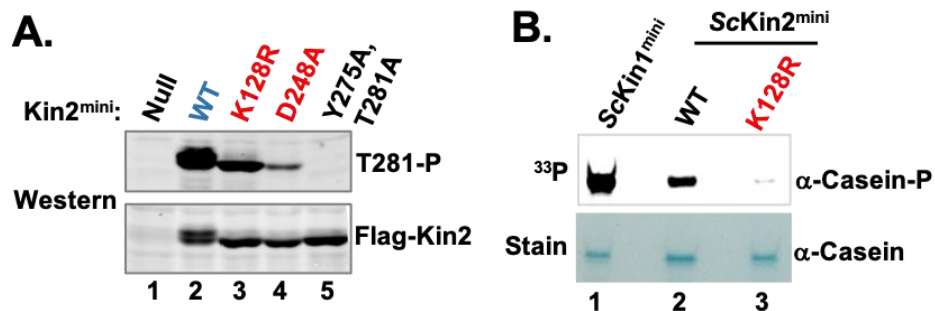


Figure 2.19 Mechanism of Kin2_{mini} phosphorylation on T281

(A) Western blot analysis. Whole cell extracts from the yeast cells expressing the wild-type Kin2_{mini} or its derivatives as indicated in (A) were subjected to SDS-PAGE followed by Western blot analysis using T281 phospho-specific and anti-Flag antibodies. (B) *In vitro* kinase assays. Partially purified ScKin1_{mini}, ScKin2_{mini} and ScKin2_{mini}-K128R proteins were mixed with α -casein in a kinase reaction buffer containing γ -³³P-ATP. The reaction mixture was quenched after 20 minutes by addition of 3X SDS-dye and resolved by gel-electrophoresis. The gel was stained to see protein bands (lower panel), dried and then subjected to autoradiography to detect the incorporation of ³³P in the α -casein.

To further confirm that T281 phosphorylation occurs in a *trans* mechanism, we performed an *in vitro* kinase assay using purified Kin2-KD from yeast and bacteria. The expression of the glutathione S-transferase (GST)-fused Kin2_{mini} (residues 94-526) protein in *E. coli* was extremely low. Thus, we made a GST-Kin2-(60-526)- Δ 40- Δ KI construct (D1386, plasmids list) in which 30 residues added at the N-terminal end of GST-Kin2_{mini} and residues 440-480 (the KER-II region) and residues 136-165 [the kinase insert (KI) region) were deleted. We performed a growth test just to ensure that the Kin2-(60-526)- Δ 40- Δ KI protein activated the UPR similar to the Kin2_{mini} protein (Fig 2.20).

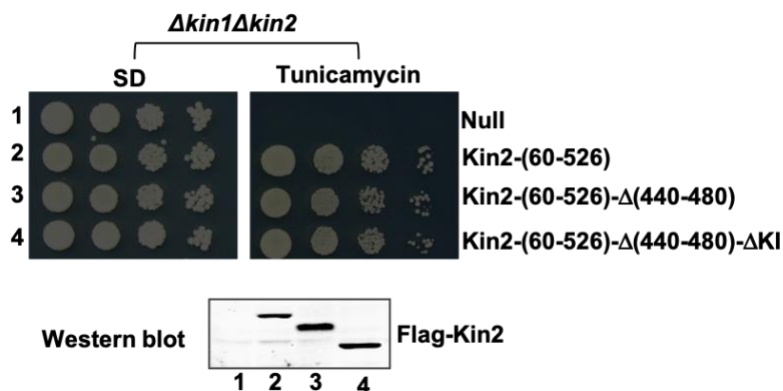


Figure 2.20 Growth test to ensure functionality of the Kin2 mutant used for kinase assays

The *kin1 Δ kin2 Δ* deletion strains containing a vector plasmid (null) or expressing a wild-type Flag-Kin1 (WT) and the indicated derivatives were tested for their growth on dextrose and tunicamycin media.

Then, we made derivatives of GST-Kin2_{mini} derivatives Kin2_{mini}-T281E (D1347, plasmids list) and Kin2_{mini}-Y275E (D1942, plasmids list) and expressed in *E. coli*. The recombinant proteins in *E. coli* (referred to as *Ec*GST-Kin2_{mini}, *Ec*GST-Kin2_{mini}-T281E or *Ec*GST-Kin2_{mini}-Y275E) was purified and mixed with the α -casein or histone in a reaction buffer containing γ -³³P-ATP [1 μ Ci per reaction). The reaction mixture was then resolved in an SDS-PAGE and the incorporation of ³³P in α -casein was detected by autoradiography (Fig 2.21A). A robust phosphorylation of

α -casein was observed in a reaction mixture containing GST-Kin2_{mini}-T281E protein, but not in the reaction mixture containing the *Ec*GST-Kin2_{mini} or *Ec*GST-Kin2_{mini}-Y275E (**Fig 2.21A**). These data suggested that the recombinant GST-Kin2_{mini}-T281E was an active kinase, whereas the recombinant *Ec*GST-Kin2_{mini} and *Ec*GST-Kin2_{mini}-Y275E proteins were inactive kinases, likely due to lack of the activating T281 phosphorylation. Collectively, our data suggest that glutamate substitution for T281, but not Y275, mimicked the phosphorylated state, thereby activating its kinase function.

To determine that T302 phosphorylation in Kin1 occurred in *trans*, we expressed GST-Kin1_{mini} and GST-Kin1_{mini}-T302E proteins in *E. coli*. The recombinant proteins in *E. coli* (referred to as the *Ec*GST-Kin1_{mini} and *Ec*GST-Kin1_{mini}-T302E) were purified and subjected to *in vitro* kinase assays as described above. We observed that the recombinant *Ec*GST-Kin2_{mini} was unable to phosphorylate the α -casein (**Fig 2.21B**). However, consistent with the *Ec*GST-Kin2_{mini}-T281E protein, the *Ec*GST-Kin1_{mini}-T302E readily phosphorylated α -casein (**Fig 2.21B**). These data suggested that the glutamate substitution for T302 mimicked the phosphorylated state, thereby activating its kinase function. Taken together, our data suggest that phosphorylation of T281 in Kin2 or T302 in Kin1 occurs in *trans*.

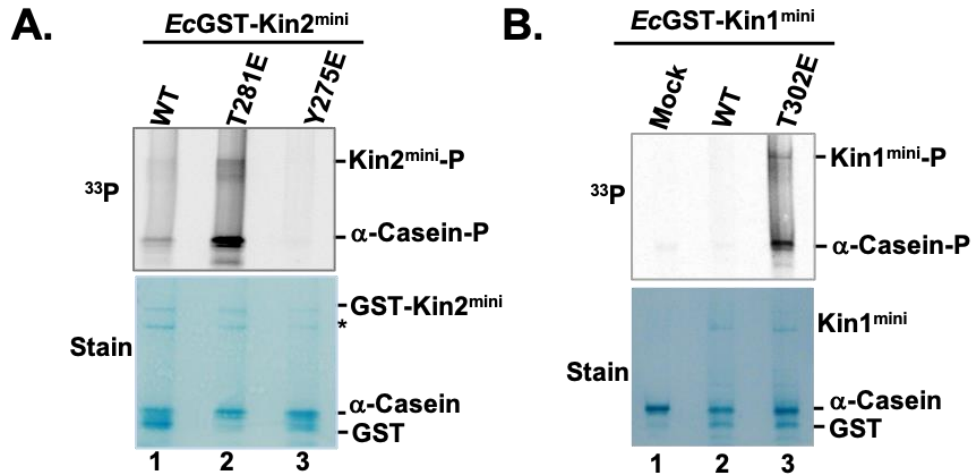


Figure 2.21 Phosphorylation of Kin2-T281 or Kin1-T302 occurs *in trans*.

(A) The recombinant *EcGST-Kin2_{mini}-T281E* protein phosphorylates α -casein *in vitro*. Partially purified recombinant *EcGST-Kin2_{mini}* (WT) or *EcGST-Kin2_{mini}-T281E* protein was subjected to *in vitro* kinase assay using γ -³³P-ATP and α -casein as a substrate. The *EcGST-Kin2_{mini}* and α -casein protein bands are shown at the lower panel, whereas the phosphoate (³³P) incorporation in the respective α -casein and *EcGST-Kin2_{mini}* proteins are shown at the upper panel. The sign “*” indicates a non-specific protein band bound with the *GST-Kin2_{mini}* protein. (B) The recombinant *EcGST-Kin1_{mini}-T302E* protein phosphorylates α -casein *in vitro*. Partially purified recombinant *EcGST-Kin1_{mini}* (WT) or *EcGST-Kin1_{mini}-T302E* protein was subjected to *in vitro* kinase assay using γ -³³P-ATP and α -casein as a substrate. The *EcGST-Kin1_{mini}* and α -casein protein bands are shown at the lower panel, whereas the phosphoate (³³P) incorporation in the respective α -casein and *EcGST-Kin1_{mini}* proteins are shown at the upper panel.

The glutamate substitution of T281 restores the defective ER-stress response associated with a mutation at the *HAC1-3'-UTR*

Since the Kin kinase was reported to modulate the translocation, splicing and translation of the *HAC1* mRNA, we therefore studied the effect of active *Kin2_{mini}-T281E* protein in *Hac1* expression from *HAC1* mRNA. In the *HAC1* mRNA it has been shown that an intra-molecular interaction between 5'-UTR and intron blocks the translation initiation^{181,182}, thus rendering *HAC1* mRNA translationally silent (Fig 2.22A). Under conditions of ER stress, *HAC1* mRNA associates with an ER-resident endonuclease *Ire1* that cleaves out the intron, thus releasing the translational block^{181,182}. Recently, our lab showed that a conserved sequence element (5'-G₁₁₄₀CGGG₁₁₄₄-3')

at the 3'-UTR has a significant contribution to translocation, splicing and translation of *HAC1* mRNA₁₃₇. Mutations of two consecutive guanine nucleotides (G₁₁₄₃ and G₁₁₄₄) at the 3'-UTR reduce the UPR (Fig 2.22B) induction due to defects in both splicing and translation of *HAC1* mRNA, which can be restored by over-expressing the protein kinase Kin1 or Kin2₁₃₇.

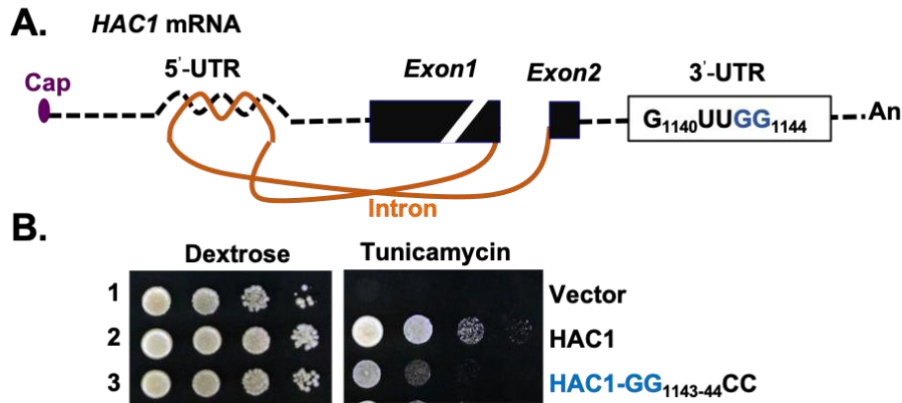


Figure 2.22 *HAC1* nucleotides GG (1143-44) play an important role in UPR

(A) The schematic representation of *HAC1* mRNA. The cap (closed oval), 5'- and 3'-UTRs (black dotted lines), exons (dark blue boxes), intron (solid orange line) and poly-adenine (An) tail are shown. The 5'-UTR•intron interaction and the consensus element at the 3'-UTR (i.e., 5'-G₁₁₄₀UUGG₁₁₄₄-3') are shown. (B) Analysis of yeast cell growth. A *hac1Δkin1Δ* deletion strain was transformed with the indicated *HAC1* or *KIN2* alleles. Transformants were then tested for growth on dextrose and tunicamycin media.

In order to provide additional direct *in vivo* evidence that the glutamate substitution of the residue T281 could activate the kinase domain, we overexpressed the Kin2_{mini}-T281E mutant protein in *kin1Δhac1Δ* yeast strain containing a *HAC1-GG₁₁₄₃₋₄₄CC* allele. The resulting strains were then tested for their growth on the tunicamycin medium. Yeast cells expressing a *HAC1-GG₁₁₄₃₋₄₄CC* allele grew slowly on the tunicamycin medium when compared with cells expressing a wild-type *HAC1* allele. The growth on tunicamycin was rescued when Kin2_{mini} or Kin2_{mini}-Y281A,T281E, but not Kin2_{mini}-Y281A,T281A, was overexpressed from a high-copy numbered vector (Fig 2.23A, rows 3 and 4) because of higher levels of Hac1 protein expression (Fig 2.23B,

lanes 2 and 4). These genetic and biochemical data collectively suggest that T281 phosphorylation within the activation loop of Kin2 is important for expression of Hac1 protein.

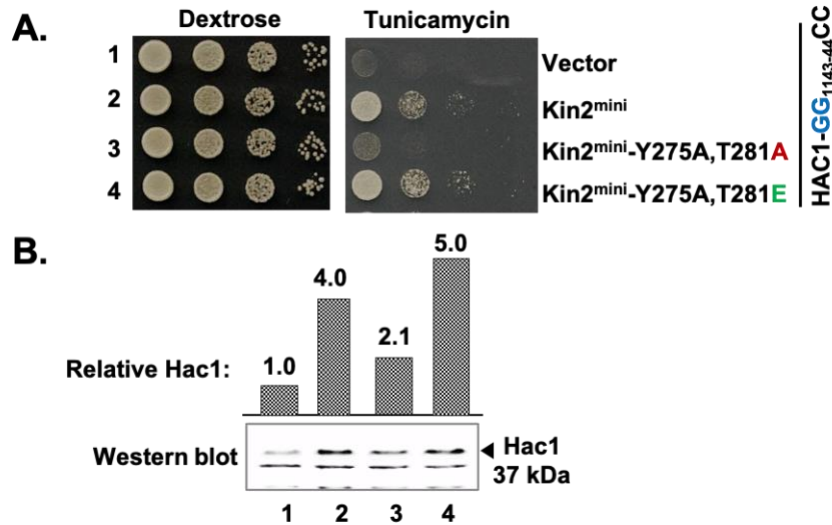


Figure 2.23 Thr-281 phosphorylation is required to suppress the defective alleles of *HAC1* mRNA.

(A) Analysis of yeast cell growth. A *hac1Δkin1Δ* deletion strain was transformed with the indicated *HAC1* or *KIN2* alleles. Transformants were then tested for growth on dextrose and tunicamycin media. (B) Analysis of Hac1 protein expression. Whole cell extracts from the yeast cells indicated in (C) were subjected to SDS-PAGE followed by Western blot analysis using an antibody of the recombinant Hac1 protein. Non-specific bands are indicated as loading controls and the relative amount of Hac1 protein was estimated as a ratio of each protein band density (ImageJ software) compared to the lane's loading control.

The list of plasmids and yeast strains used in this chapter are compiled in the Appendix I.

All materials and methods are listed under chapter 5.

Some of these findings are collectively published in Molecular and Cellular Biology as a Spotlight article. (DOI: 10.1128/MCB.00266-18).

3. Chapter 3: Phosphorylation of Pal2 by the Kinases Kin1 and Kin2 Modulates *HAC1* mRNA Splicing in the *Saccharomyces cerevisiae* Unfolded Protein Response

Introduction

Almost one third of cellular proteins fold and mature inside the endoplasmic reticulum (ER). Abiotic or biotic stresses cause protein misfolding in the ER leading to accumulation of these misfolded proteins in the ER, a condition called ER stress^{85,86}. ER stress triggers a network of signaling pathways collectively known as the unfolded protein response (UPR)⁸⁵⁻⁸⁸. Ire1 and Hac1 are key players of the UPR pathway in budding yeast⁸⁷. A major step in the yeast UPR pathway is the targeting of the *HAC1* pre-mRNA towards the Ire1 protein for splicing^{138,182,18}. Following colocalization, Ire1 splices the intron of *HAC1* mRNA that blocks translation initiation of the *HAC1* pre-mRNA. Eventually the mature *HAC1* mRNA is translated and the Hac1p which is a transcription factor that drives the expression of numerous proteins, including ER-resident chaperones, to enhance the protein folding capacity of the cell. The colocalization of Ire1 and *HAC1* mRNA requires a 3' bipartite element (3'BE), positioned at the 3'-UTR (untranslated region) of *HAC1*¹³⁸. Computer modelling predicts that the 3'-BE forms a helix-bulge-helix-bulge structure. Our lab showed that there are two guanine nucleotides (*GG1143,1144*) on one of the bulges on the 3'-BE that play an important role in the translocation and splicing of the *HAC1* mRNA¹³⁷. In an attempt to identify the genes that can suppress the growth defect of the guanine mutations, our lab discovered that over expression of Kin2 can restore the optimum UPR response in the GG mutant strain. This evidence was backed by the increased splicing of *HAC1* mRNA in the GG mutant strain when Kin2 was overexpressed¹³⁷. However, the detailed mechanism of this translocation is yet unknown. Based on observations, we speculate that

Kin kinases likely promotes the formation of a ribonucleoprotein (RNP) complex on the 3'-BE of *HAC1* mRNA, which facilitates co-localization of *HAC1* mRNA with Ire1 (Fig 3.1). Hence, identification of the RNP might shed light on the inner mechanisms of the translocation process.

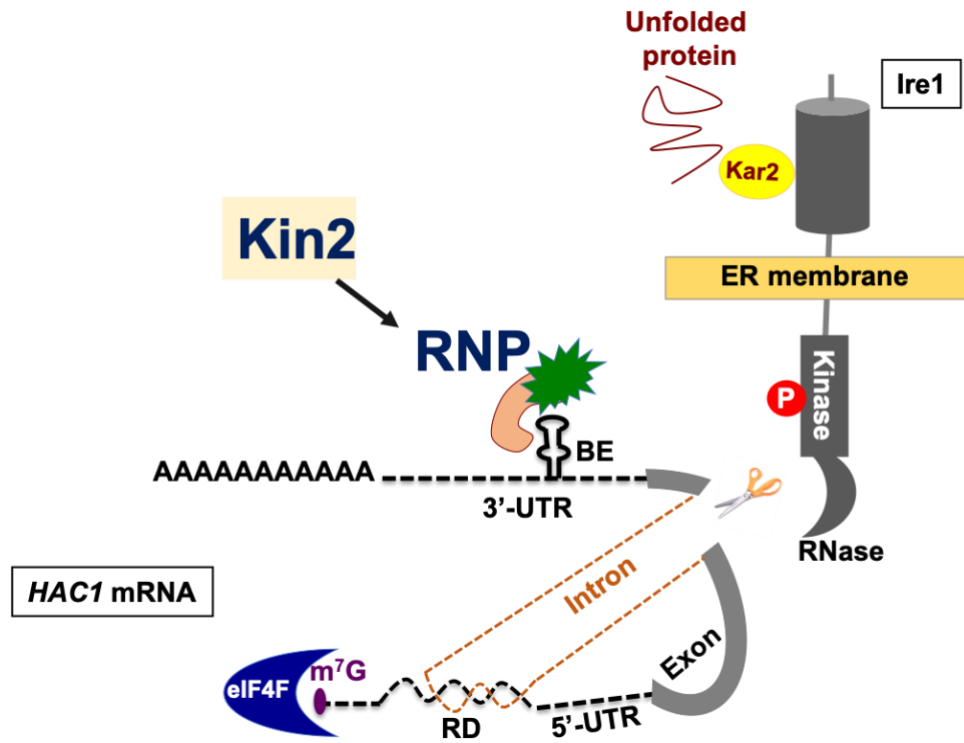


Figure 3.1 Working hypothesis: An RNA-Protein (RNP) Complex Assembles on the 3'-BE and Controls the *HAC1* mRNA Targeting

Unfolded protein (red scribbled line) accumulation in the ER causes ER stress and activates the ER resident transmembrane protein Ire1 (luminal domain and cytoplasmic kinase / RNase domain indicated in grey). Ire1 activation involves its dimerization, oligomerization and autophosphorylation (phosphorylation indicated as “P” in a red circle). The active Ire1 splices the *HAC1* pre-mRNA (mRNA cap indicated as a purple oval shape, 5'-UTR and 3'-UTR indicated in black dotted lines, exons in grey, intron is indicated by orange dotted line, cap binding complex eIF4F in blue). The intron remains base paired with the 5'-UTR and keeps the mRNA translationally silent. Following splicing the mature *HAC1* mRNA then, translates the Hac1 protein. Hac1p is an active transcription factor which enters the nucleus, binds to the UPR elements and drives the expression of the UPR target genes. UPR target genes are mainly protein folding enzymes and chaperones that assist with the protein folding capacity of the ER and thereby reduce ER stress. A key event in this Ire1-mediated UPR is the colocalization of the Ire1 with the *HAC1* mRNA. This colocalization is mediated by a cis-acting bipartite element (BE, indicated as a stem loop) located at the 3'-UTR of the *HAC1* mRNA. We hypothesize that there is a ribonucleoprotein (RNP) complex which assembles near the 3'-BE and targets the *HAC1* mRNA to the Ire1 foci. Kin2 is predicted to signal the RNP in order to generate an optimum stress response.

Results

Identification of the Ribonucleoprotein (RNP) complex

In order to identify the RNP, we developed a strategy using the *HAC1* mRNA 3'-UTR Bipartite element (BE) sequence. The 3'-BE nucleotides range from C₁₁₃₄ to A₁₁₉₂, where, adenine of the AUG codon is +1₁₃₈. We generated a construct where the 3'-BE sequence was conjugated with an RNA mimic of biotin (RMB) which is a 43-nucleotide RNA aptamer that mimics biotin₁₈₃. This was expressed from an *ADHI* constitutive promoter. For control, we generated a construct with the 5'-RD (RNA duplex)-RMB in which the 5'-UTR nucleotides U₋₁₉ to U₋₄₂ were linked with the intronic sequence from U₇₆₃ to A₇₈₃ and the RMB. This was also expressed under the control of the *ADHI* promoter. Since the intronic sequence of *HAC1* mRNA base pairs with the 5'-UTR₁₈₁, the prediction was that the control RNA would fold in a similar way (**Fig 3.2**).

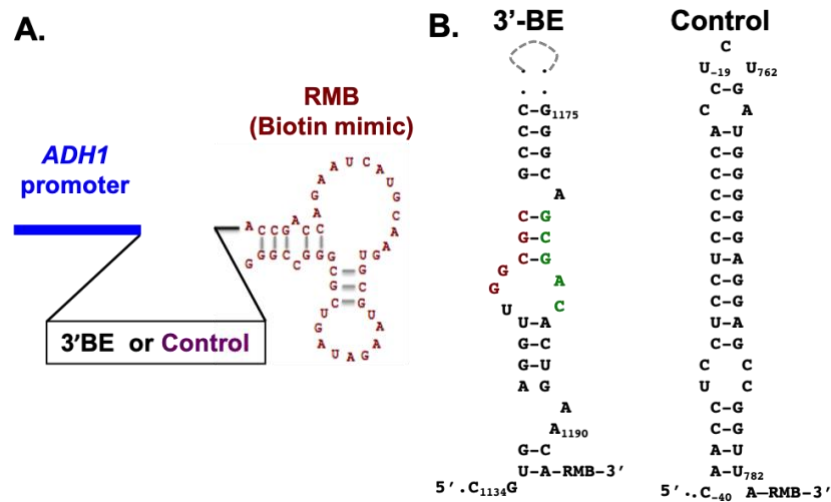


Figure 3.2 Construct designs for identification of RNP components

(A) The schematic representation of 3'-BE- and 5'-RD-RMB expression constructs. The template DNA sequence of the 3'-BE- or 5'-RD RNA was cloned under the constitutive *ADHI* promoter. The predicted structure of RNA mimic of biotin (RMB) has been shown. (B) The nucleotide composition of 3'-BE and 5'-RD mini RNA. The predicted secondary structure of 3'-BE and 5'-RD RNAs are shown. The conserved RNA motif within the 3'-BE is shown in brick red color. The 5'-RD consisting of 5'-UTR and intron are shown in black and red color, respectively. The numbers indicate the nucleotide positions.

Both 3'-BE-RMB and 5'-RD-RMB constructs were transformed into a *hac1Δ* strain, and expression of both RNAs was confirmed by RT-PCR (Fig 3.3A). Next, we grew yeast cells in the presence of 4-thiouridine (4sU) in order to label the uracil residues of these mini RNAs with thiol groups. The 4sU-labeled RNA and associated proteins were photo-crosslinked by UV-irradiation¹⁸⁴. RMB-conjugated RNAs were precipitated using streptavidin-agarose, and bound proteins were eluted. A fraction of the elute was separated on SDS-PAGE and another fraction was subjected to LC tandem mass spectrometry (LC-MS/MS) (Fig 3.3B).

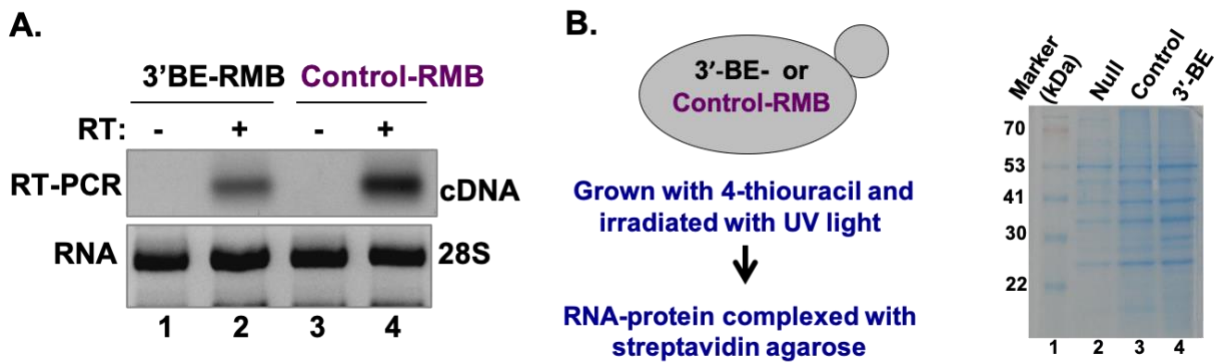


Figure 3.3 Analysis of 3'-BE specific proteomes of *HAC1* mRNA

(A) Analysis of mini RNA expression. Total RNA was isolated from the yeast cells containing the 3'-BE- or 5'-RD-RMB expression constructs. Then, cDNA was synthesized from the total RNA using gene-specific primer in the presence and absence of reverse transcriptase (RT). (B) Immunoprecipitation of 3'-BE-specific proteins. Yeast cells expressing the 3'-BE- or 5'-RD-RMB mini RNA was grown in the presence of 4-thiouracil and irradiated with UV-light. Total RNA was isolated and mixed with streptavidin agarose. The mixture was then washed thoroughly. An aliquot of the streptavidin agarose was run in an SDS-polyacrylamide gel. The gel was then stained.

Analysis of the 3'-BE specific proteomes identified Pal2 as a putative *HAC1* mRNA binding protein

The mass spectrometry data generated hundreds of proteins that were associated with the 3'-BE-RMB and the 5'-RD-RMB. Common mRNA binding proteins like proteins associated with the large and small subunit of ribosomes were identified. A comparative proteomic analysis

identified the list of proteins that were associated uniquely with either 3'-BE-RMB (**Table 2**) or 5'-RD-RMB. This list identified a protein of unknown function, Pal2.

Table 2 A list of putative 3'-BE and 5'-RD binding proteins

	Function	Protein
3'BE-specific proteins	Metabolic enzymes	Leu2, NTH1, FAA4, Frs1, PNC1, Ams1, Prs5, Cab3, Apa1, Pgm1
	Transporter	Vma8
	Transcription	Rpb2, Pbp4
	Endocytosis	Pan1
	Translational repressor	Ssd1
	mRNA export	Arx1
	mRNA localization	She3
	P-body	Xrn1
	Kinases	Cdc28, Bcy1, Ypk1
	Cytokinesis	Shs1, Cdc3, Vrp1
	Unknown	Pal2
5'RD-specific proteins	Metabolic enzymes	Mmf1, Snz1, NCE103, Arg5, Bna1, Sry1, TP11, Adk1, Met10, Cys3, Ade17, Sfa1, Spe3
	Transporter	Oac1, Pho88
	Chaperone	Phb2, Mge1, Ggc1
	V-ATPase	Vma10
	Phosphatase	Sac1
	Translocase	Tom70
	Unknown	Aim46

Previously, it was reported that Pal2 binds to *HAC1* mRNA¹⁸⁵. Another report shows that Pal2 contains the consensus sequence motif that is preferred by the Kin kinases (N-X-S-X-pT-X-L, where N is asparagine, X is any amino acid, S is serine, pT is phosphorylated threonine, L is

Role of Pal1 and Pal2 proteins in yeast UPR

Recent observations indicating the association of Pal2 with the yeast UPR components suggested that Pal proteins might be implicated in the UPR. To determine whether Pal2 and/or Pal1 were required for activation of ER stress, we generated a *pal1Δ pal2Δ* strain and examined its growth in the presence or absence of tunicamycin (Fig 3.5A). While yeast cells lacking both Pal1 and Pal2 grew slightly slower than wild-type (WT) cells on control medium, their growth was substantially reduced in the presence of tunicamycin (Fig 3.5A). Control strains lacking either Ire1 or Hac1 did not grow at all on medium containing tunicamycin (Fig 3.5A). Interestingly, the tunicamycin growth defect of *pal1Δ pal2Δ* cells was exacerbated when cells were grown on media containing galactose, a less preferred carbon source (Fig 3.5B). The advantage of using galactose medium was that, it allowed us to use lower concentration of tunicamycin which will avoid any non-specific toxicity.

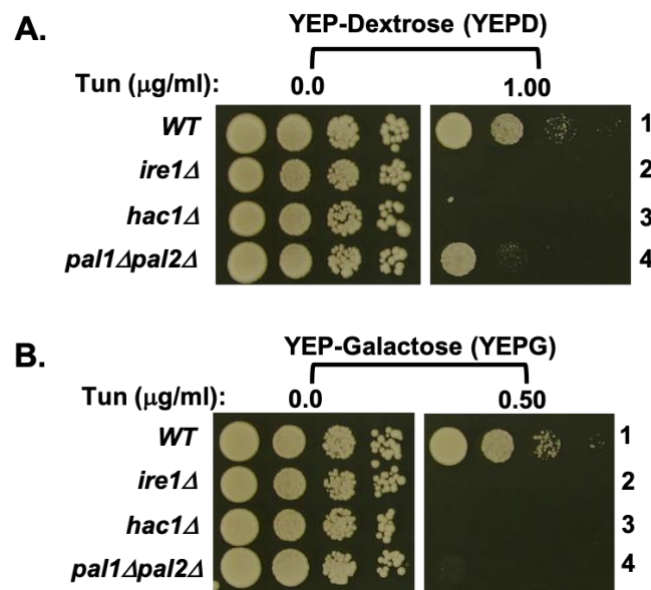


Figure 3.5 Pal1 and Pal2 double deletion strains is sensitive to Tunicamycin

(A) and (B) The indicated yeast strains were grown serially diluted and spotted on the YEPD (A) or YEPG (B) medium with or without tunicamycin.

We wanted to check if Pal1 or Pal2 by themselves (single mutant strains) affected the UPR. Deletion of *PAL1* alone had no effect on growth on tunicamycin medium, but the single deletion of *PAL2* showed a substantial growth defect (**Fig 3.6**).

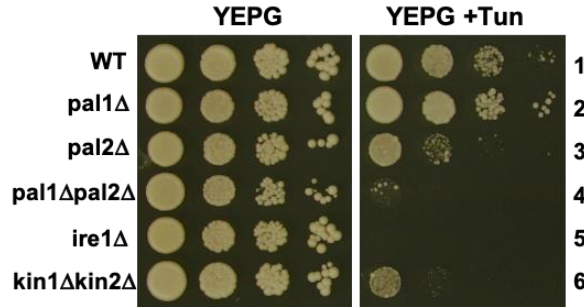


Figure 3.6 Pal2 deletion strain shows a severe UPR defect compared to Pal1 deletion

The indicated yeast strains were grown serially diluted and spotted on the YEPG medium with or without tunicamycin.

The *pal1Δ pal2Δ* yeast strain showed a slightly slower growth as compared to the WT strain on the YEPG media without tunicamycin (**Fig 3.6**, YEPG, rows 4 and 1). To confirm this phenotype, we grew the WT, *pal1Δ pal2Δ* and *kin1Δ kin2Δ* yeast cells in YEPG medium for 16 hours and measured O.D.₆₀₀ every 2 hours to plot a growth curve. From the growth curve it was evident that the *pal1Δ pal2Δ* exhibit a slow growth on YEPG medium (**Fig 3.7A**). We did not observe any apparent morphological abnormalities in the *pal1Δ pal2Δ* cells (**Fig 3.7B**).

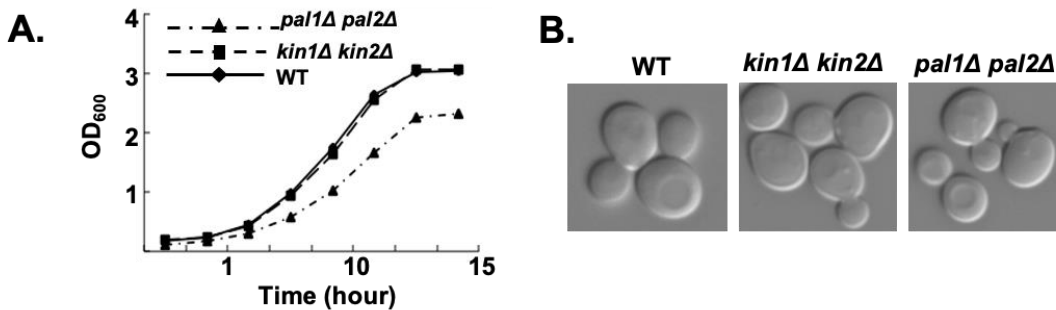


Figure 3.7 Pal1 and Pal2 double null strain displays slow growth phenotype

(A) The *pal1Δ pal2Δ* strain exhibited slow growth phenotype. Yeast cells were grown, OD₆₀₀ were measured, and plotted. (B) Confocal image of wild type (WT), *kin1Δ kin2Δ* and *pal1Δ pal2Δ* strains.

The tunicamycin sensitivity of the *pal1Δ pal2Δ* strain could be due to a defect in *HAC1* mRNA splicing, Hac1 protein expression, or impaired colocalization of *HAC1* mRNA with Ire1. To test if the *HAC1* splicing was defective, WT, *pal1Δ pal2Δ* and *kin1Δ kin2Δ* yeast cells were grown in the presence or absence of tunicamycin (Tun). Total RNA was extracted, and cDNA was synthesized from the total RNA. The synthetic cDNA was used to detect the spliced (*HAC1_s*) and un-spliced (*HAC1_u*) form of *HAC1* mRNA. Only unspliced *HAC1* mRNA (*HAC1_u*) was observed in WT cells grown in the absence of tunicamycin, whereas both un-spliced and spliced (*HAC1_s*) *HAC1* mRNAs were observed in the presence of tunicamycin. In the *pal1Δ pal2Δ* strain, the splicing of *HAC1* mRNA (**Fig 3.8**) was significantly reduced just like the reduced levels in *kin1Δ kin2Δ* strain.

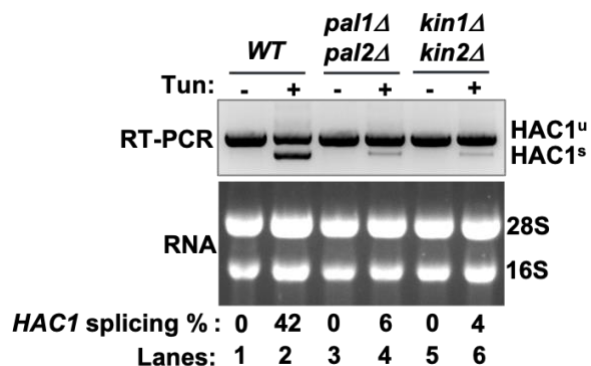


Figure 3.8 Splicing of *HAC1* mRNA is reduced in the *Pal1* and *Pal2* double deletion strain

The indicated yeast cells were grown in the presence or absence of tunicamycin (Tun). Total RNA was isolated (lower panel) and cDNA was prepared from the total RNA. The synthetic cDNA was used to detect the spliced (*HAC1_s*) and un-spliced (*HAC1_u*) form of *HAC1* mRNA.

In order to check the Hac1 protein expression, the WT and the *pal1Δ pal2Δ* yeast cells were grown in the presence or absence of tunicamycin (Tun). Whole cell extract was prepared and subjected to a Western blot analysis using anti-Hac1 antibody and to detect Hac1 protein expression and anti-Pgk1 antibody to detect Pgk1 for loading control. The expression of Hac1 protein from the spliced mRNA (**Fig 3.9A**) was significantly reduced (>50%). The single deletion

mutants were also tested for Hac1 expression. Hac1 protein expression was reduced (40%) in the *pal2*Δ strain but not in the *pal1*Δ strain (**Fig 3.9B**) which was consistent with the growth defect. Collectively, these data suggest that Pal1 and Pal2 significantly contribute to *HAC1* mRNA splicing and/or translation, with Pal2 playing the major role.

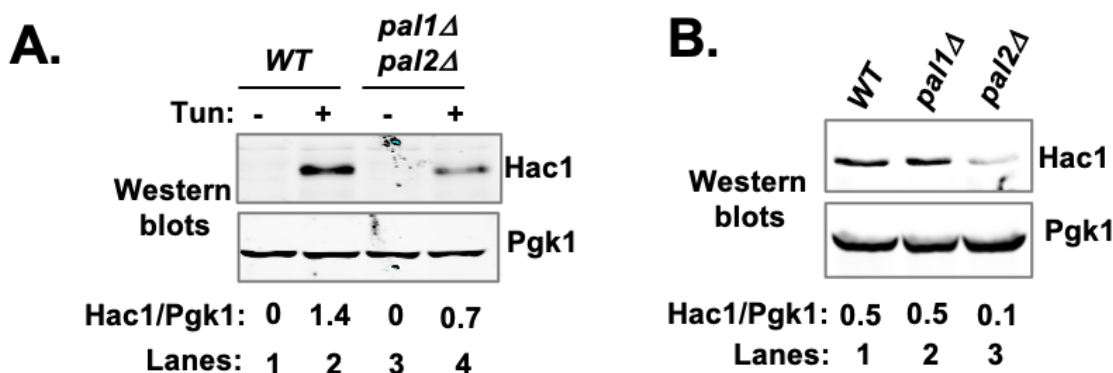


Figure 3.9 Hac1 protein production is reduced in the Pal1 and Pal2 double deletion strain

Whole cell extracts were isolated and subjected to Western blot analysis using antibodies against the Hac1 and Pgk1 proteins. The ratios of Hac1 and Pgk1 protein band signals are shown.

Another standard assay to test the UPR induction in yeast strains is by using the *LacZ* reporter assay¹⁸⁷. WT, *pal1*Δ *pal2*Δ and *kin1*Δ *kin2*Δ were transformed with a plasmid encoding beta-galactosidase under the control of an UPR element (UPRE) of the yeast *KAR2* gene¹⁸⁸. The transformants were grown with or without DTT (an ER stressor) and the cell lysates were prepared and used to check the beta-galactosidase activity. In WT cells, *UPRE*-driven *lacZ* expression was elevated about 6-fold when cells were treated with the ER stressor DTT, an effect that was reduced in the *pal1*Δ *pal2*Δ and *kin1*Δ *kin2*Δ strains (**Fig 3.10**).

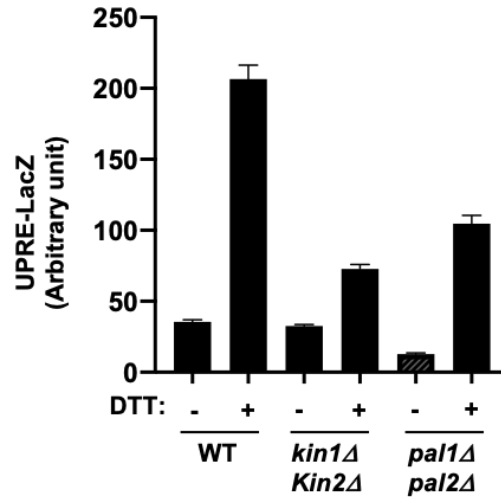


Figure 3.10 UPRE-driven LacZ reporter gene expression is reduced in the Pal1 and Pal2 double deletion strain

The yeast strain (wild type, *kin1Δkin2Δ* or *pal1Δpal2Δ*) was transformed with a plasmid carrying the UPRE-driven LacZ reporter gene. Transformants were grown in the presence (+) and absence (-) of DTT. Whole cell extract was prepared, and the β -galactosidase activity was measured.

To determine whether Pal1 and Pal2 act at the level of *HAC1* mRNA splicing, we examined growth on tunicamycin of strains expressing a plasmid-encoded intron-less *HAC1* construct. As anticipated, expression of the intron-less *HAC1* gene rescued the growth of an *ire1Δ* strain on tunicamycin medium (**Fig 3.11A**). Likewise, intron-less *HAC1* allowed the *pal1Δ pal2Δ* strain to grow in the presence of tunicamycin (**Fig 3.11A**), likely because it was able to translate the protein without Ire1-mediated splicing (**Fig 3.11B**). These data collectively suggest that Pal1 and Pal2 serve to promote *HAC1* mRNA splicing, likely by targeting mRNA to the ER stress site.

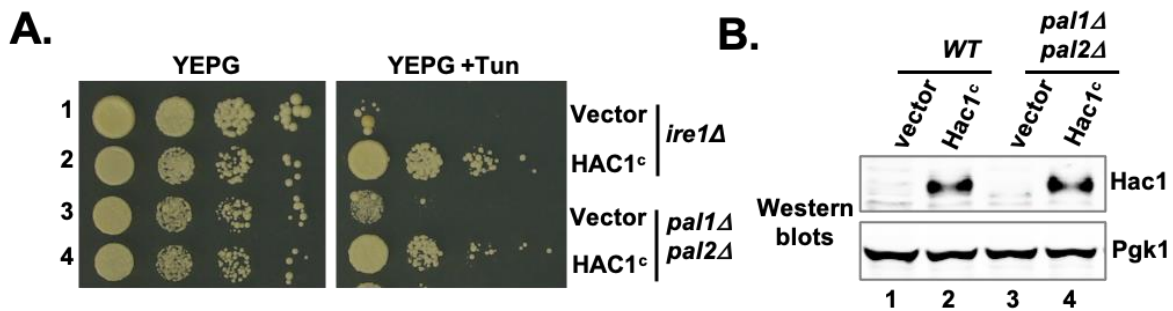


Figure 3.11 Analysis of Hac1 protein expression from the intron-less *HAC1* mRNA

(A) Analysis of yeast cell growth. The indicated yeast strains expressing a vector plasmid and the same vector containing an intron-less *HAC1* gene (*HAC1^c*) were grown serially diluted and spotted on the YEPG medium with or without tunicamycin. (B) Analysis of Hac1 protein expression. Yeast cells indicated in (A) were grown and whole cell extracts were isolated and subjected to Western blot analysis using antibodies against Hac1 and Pgk1 proteins. The ratios of Hac1 and Pgk1 protein band signals are shown.

Comparison of protein sequences of Pal protein from related fungal species

To study the conserved regions and the redundant domains in the Pal proteins, protein sequence of Pal2 homologs from *Saccharomyces cerevisiae* (Sc), *Torulaspora delbrueckii* (Td), *Kluyveromyces lactis* (Kl), *Lachancea quebecensis* (Lq), *Ashbya gossypii* (Ag) and *Eremothecium cymbalariae* (Ec) were aligned (**Fig 3.12**). Sequence comparison of Pal1 and Pal2 proteins indicate an overall 45% sequence identity, including a number of annotated phosphorylation sites. *S. cerevisiae* *PAL2* and its orthologs in other species contain an intron of variable length, whereas the paralogous *PAL1* gene does not have any intronic sequence (yeast genome database). Moreover, sequence comparison of Pal2 homologs among lower eukaryotes showed that the N-terminal region of Pal2 is highly variable (**Fig 3.12**)

3.13). However, Western blot analysis suggested that the basal expression of Pal2 in cells was extremely low.

The sequence alignment of Pal1 and Pal2 proteins showed that amino acid residues 165-499 of Pal1 are highly similar to residues 65-366 of Pal2 (**Fig 3.4**). To determine whether the N-terminal residues of Pal2 protein had any role in activating the UPR, we separately deleted the DNA sequences encoding residues 65 and 135 from the N-terminal end (**Fig 3.13**), generating Flag-tagged *PAL2 Δ intron- Δ N65* and *PAL2 Δ intron- Δ N135* constructs, respectively. Growth test on Tunicamycin showed that the minimum length of Pal2 that could activate the UPR was *PAL2 Δ intron- Δ N65* (**Fig 3.13B**). Western blot showed the protein expressions. These data suggest that the N-terminal 65 residues of Pal2 are dispensable for its function in the UPR, and that *PAL2 Δ intron- Δ N135* expressed a non-functional protein.

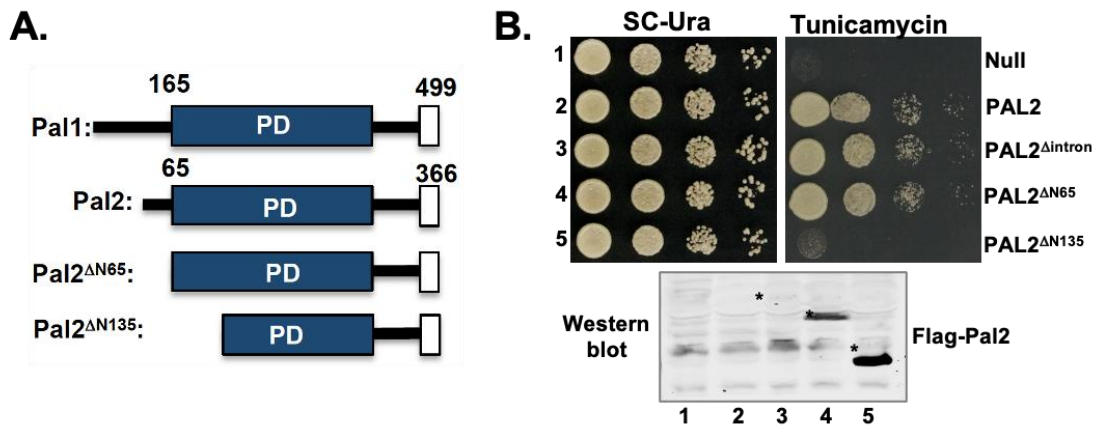


Figure 3.13 Truncation analysis of Pal2

(A) The schematic representation of Pal1 and Pal2 protein and its derivatives. The homologous Pal1 domains (PD) are indicated by dark blue boxes. Amino acid residue numbers are indicated. (B) Intron-less Pal2 can complement the Pal1 and Pal2 double deletion strain. The *pal1 Δ pal2 Δ* strains expressing the indicated wild type Pal2 or its derivatives were tested for growth on the complete synthetic (SC) without uracil (Ura) medium and the same medium containing tunicamycin. Whole cell extracts were prepared from yeast strain indicated in (B) and subjected to Western blot analysis using anti-Flag antibody. The symbol “*” indicates the Pal2 protein band.

We performed similar truncations on the paralog Pal1. Pal1 protein (residues 165-499, referred here to as *PAL1 ΔN*) could complement the tunicamycin growth defect of the *pal1 Δ pal2 Δ* strain (**Fig 3.14**). Hereafter, we used the *PAL2 Δ intron- Δ N65* and *PAL1 ΔN* derivatives for our studies to determine the physiological function of the respective proteins.

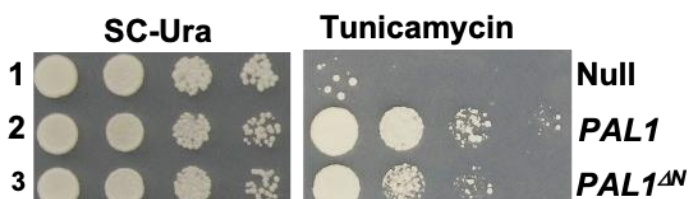


Figure 3.14 Truncation analysis of Pal1

Truncated Pal1 (residues 165-499) can complement the full length Pal1 protein. The *pal1 Δ pal2 Δ* strains expressing the indicated wild type Pal1 or its derivatives were tested for growth on the complete synthetic (SC) without uracil (Ura) and tunicamycin media.

Association of Pal1 and Pal2 proteins with *HAC1* mRNA

To determine if Pal1 and Pal2 proteins associate with *HAC1* mRNA *in vitro*, we employed the electrophoretic mobility shift assay (EMSA). Recombinant Pal1 or Pal2 protein was incubated with a fluorescein labeled 3'-BE (Flc-3'-BE from Sigma) and resolved on a native gel followed by fluorescence imaging. Both Pal1 and Pal2 induced an upward mobility shift of the Flc-3'-BE RNA (**Fig 3.15A**), suggesting that they indeed bind directly to the 3'-BE of *HAC1* mRNA. The gel shift of the fluorescein RNA was not observed when *HAC1* mRNA binding protein Ypt1₁₈₅ or a Met-tRNA binding protein eIF2 α ₁₈₉ was used. This indicated that Flc-3'-BE RNA binds selectively to Pal1 and Pal2, and that Ypt1 presumably interacts with other regions of the *HAC1* mRNA. To further confirm these data, we also found that co-incubation with unlabeled 3'-BE (synthesized by *in vitro* transcription) reduced the interaction of Pal2 with Flc-3'-BE (**Fig 3.15B**), further confirming that Pal1 and Pal2 specifically bind to the 3'-BE of *HAC1* mRNA.

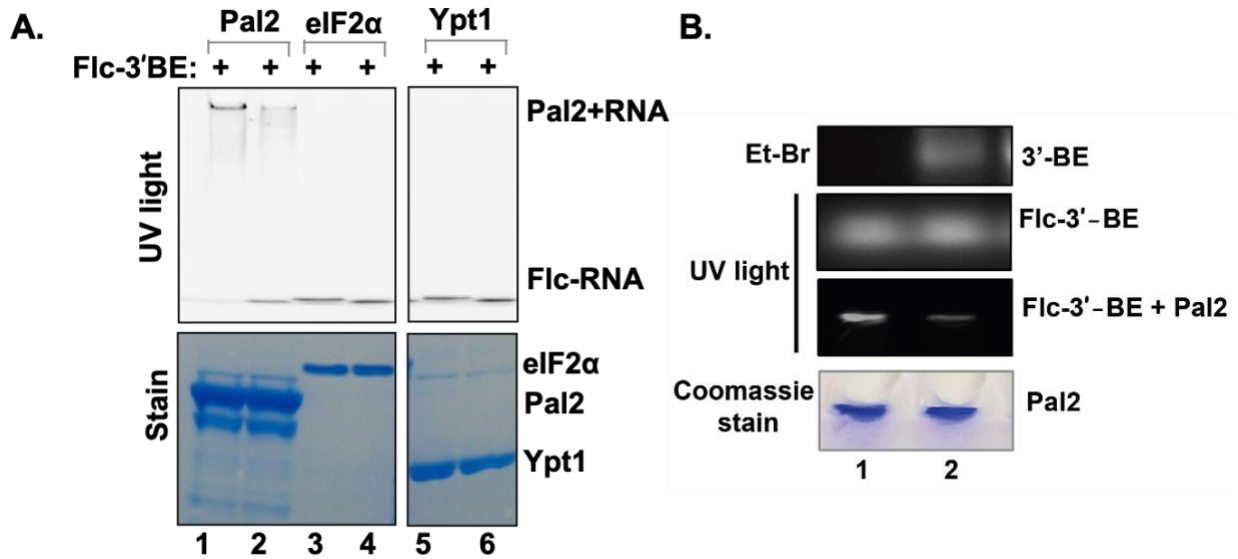


Figure 3.15 Truncated Pal proteins bind to the 3'-BE of *HAC1* mRNA *in vitro*.

(A) Electrophoretic mobility shift assay (EMSA) reveals that the recombinant proteins Pal1 and Pal2 bind to the 3'-BE of *HAC1* mRNA. A fluorescein-tagged synthetic RNA corresponding to the 3'-BE (Flc-3'-BE) was mixed with the recombinant protein His₆-Pal1, His₆-Pal2, His₆-eIF2 α or His₆-Ypt1 in a binding buffer. The reaction mixture was then resolved in a native gel followed by illumination with ultraviolet (UV)-light to see the RNA-protein interaction. (B) Competitive replacement of Flc-3'-BE RNA by the non-fluorescent 3'-BE RNA. The Flc-3'-BE (2nd panel) was mixed with the recombinant His₆-Pal2 protein (bottom panel) in a binding buffer with or without the non-fluorescent 3'-BE (top panel). The reaction mixture was then resolved in a native gel. The gel was illuminated with ultraviolet (UV)-light to see the Flc-3'-BE-Pal2 interaction. The portion of gel showing the Flc-3'-BE bound to Pal2 is shown (3rd panel).

Kin1 and Kin2 substrate identification

In budding yeast, Kin1 and Kin2 have dual roles in exocytosis¹³⁴ and the ER stress response¹³⁷. The Kin/Par-1/MARK kinases are reported to phosphorylate a variety of substrates. Kin1 kinase in the fission yeast *S. pombe* phosphorylates three polarity proteins (pal1, mod5, and tea4)¹⁹⁰. Par-1 in *C. elegans* phosphorylates Mex5, Mex6 and LIN-5¹⁹¹. Human MARK isoforms are known to phosphorylate the KXGS motifs in the repeat domain of Tau protein that stabilizes microtubules¹⁹². However, physiological substrate(s) of Kin kinases have not been identified.

Positional scanning-oriented peptide library (PSPL) analysis indicated that Kin kinases have a strong preference for sequences containing a conserved N-x-S-x-pT-x-L motif (**Fig 3.16**), where pT represents a phosphorylated threonine at the position +2 of the phosphorylation site¹. Previous analysis of the yeast phosphoproteomics data identified 36 proteins that contained an N-x-S-x-S/T-x-L motif (KINtide). Out of those 36 proteins, 12 proteins have been observed to be phosphorylated on the Ser or Thr residue found at position +2, which may “prime” the substrate for subsequent phosphorylation by Kin1 or Kin2. This list includes Pal2, Eap1 and a previously reported Kin substrate Sec9¹³⁴. To examine whether these candidates might be authentic Kin1 or Kin2 substrates, we overexpressed six of them (Sec9, Pal2, Kip3, Svl3, Mlf3 and Eap1) in yeast from a galactose-inducible high copy plasmid¹⁹³ and purified them via a C-terminal tandem affinity purification tag (**Fig 3.16B**). Partially purified proteins were subjected to kinase assays in the presence or absence of Kin1 purified from the same system in a reaction buffer containing radiolabeled γ -³²P-ATP (**Fig 3.16C**). In addition to Kin1 autophosphorylation, we observed robust phosphorylation of Sec9, Pal2, and Eap1 (**Fig 3.16C**). Svl3 and Mlf3 appeared to be phosphorylated to a lower level by Kin1, while Kip3 had substantial background phosphorylation in the absence of Kin1.

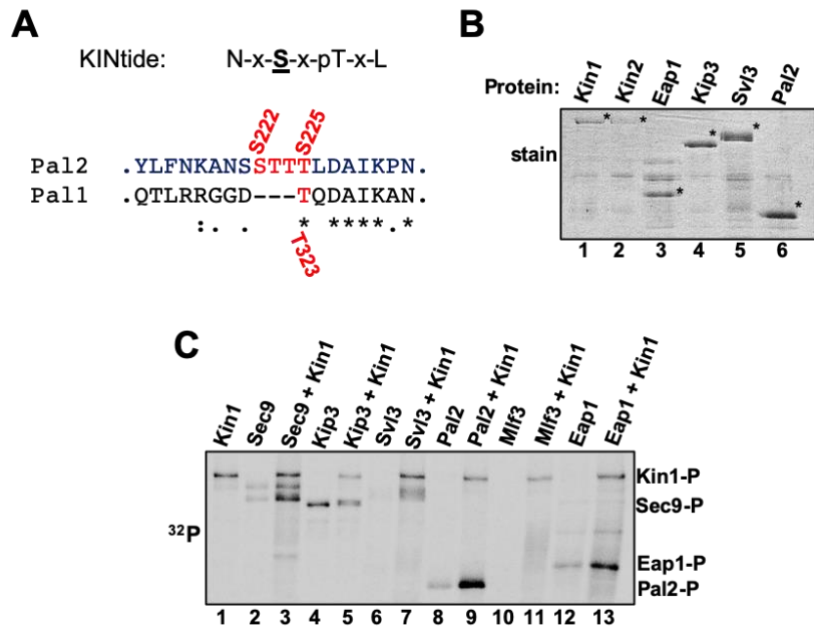


Figure 3.16 Kin1 phosphorylates Pal2 *in vitro*.

(A) Consensus element of Kin2 phosphorylation site motif (referred to as the Kintide). The conserved N-x-S-x-pT-x-L peptide sequence motif, where x indicates any amino acid and pT indicates a predicted primed phosphorylated threonine at the position +2 of the phosphorylated site (S). (B) Analysis of purified proteins from yeast. The indicated proteins were purified from yeast and subjected to SDS-PAGE analysis. Proteins are shown by the “*” symbols. (C) Phosphorylation of candidate substrates by Kin1. Purified proteins were mixed with Kin1 in a reaction mixture containing radiolabeled ATP (γ - 32 P-ATP). The reaction mixture was quenched by 2X SDS-dye and separated by SDS-PAGE. The gel was dried and subjected to autoradiography (32 P) to detect the incorporation of radioactive phosphate.

To further confirm that Pal2 is a substrate of Kin kinases, we expressed the Pal2 protein (residues 65-366) in bacteria. Circular dichroism (CD) spectroscopy indicated that recombinant Pal2 was composed of α -helices (10%), antiparallel β -sheet (25%), with the rest made up of turns and/or irregular structure (Fig 3.17). Thus, it appears that the overall fold of Pal2 protein likely consists of largely irregular structure, which is consistent with the predictions based on its amino acid sequence.

Next, we performed *in vitro* kinase assays using the same recombinant Pal2 protein as a substrate and Kin2 or PKR as a kinase. PKR is known to specifically phosphorylate the translation

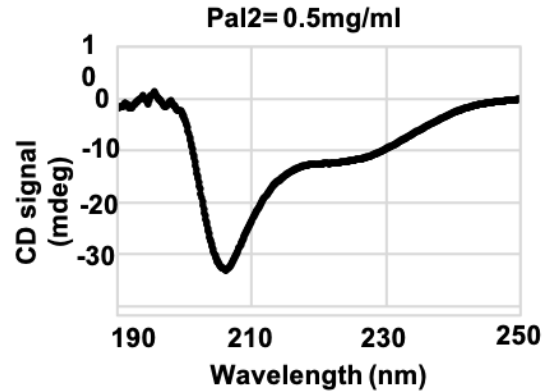


Figure 3.17 Circular dichroism spectroscopy of recombinant Pal2 protein

The recombinant Pal2 protein (0.5 mg/mL) was used to collect spectra in the wavelength range of 190–360 nm. CD spectra were collected in 0.1 cm path length quartz cells on a Jasco J-810 Spectropolarimeter. Spectra in the wavelength range of 190–360 nm were collected using the following acquisition parameters: 0.1 nm steps, 1 nm bandwidth, 4 s response, 100 millidegree sensitivity, and 50 nm/min scanning speed with an accumulation of 3. Secondary structure composition was estimated from the analysis of the CD spectrum by the BeStSel web server. (Wavelength used was 190-250nm)

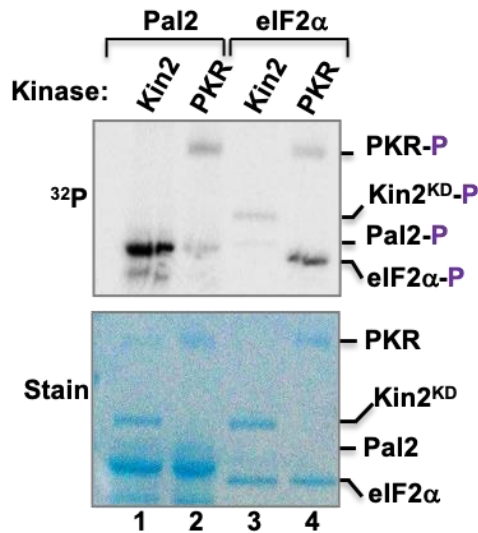


Figure 3.18 Kin2 specifically phosphorylates Pal2 *in vitro*

The recombinant His₆-Pal2 (residues 65-366) or eIF2 α protein was mixed with the purified Kin2 or PKR in a kinase reaction buffer containing γ -³²P-ATP. The reaction mixture was quenched by addition of 2X SDS-dye and resolved by gel-electrophoresis. The gel was stained to see protein bands (lower panel), dried and then subjected to autoradiography to detect the incorporation of ³²P in the respective protein (upper panel).

initiation factor eIF2 α (eIF2 α) to regulate cellular translation¹⁹⁴. As expected, we found that eIF2 α was readily phosphorylated by PKR, but not by Kin2 (**Fig 3.18**). Pal2 was phosphorylated by Kin2, but not by PKR. These results suggest that Pal2 is a specific substrate of Kin2.

Identification of specific Pal2 residues phosphorylated by Kin2

To map specific sites where Kin2 phosphorylates Pal2, Pal2 was mixed with Kin2 in kinase reaction buffer with ATP. Phosphorylated Pal2 was subjected to LC-MS/MS analysis (**Fig 3.19B**). We identified a major phosphorylated tryptic peptide (ANSSTTLDAAIKPNSK) that included the site predicted to be phosphorylated by Kin1/Kin2 (S222 within the N-x-S-x-T-x-L sequence motif) (**Appendix II**). Of six potential phospho-acceptor residues within this peptide, prior phosphoproteomics studies have found five of them (S221, S222, T223, T224, T225) to be phosphorylated *in vivo*¹⁹⁵ (**Fig 3.19A**).

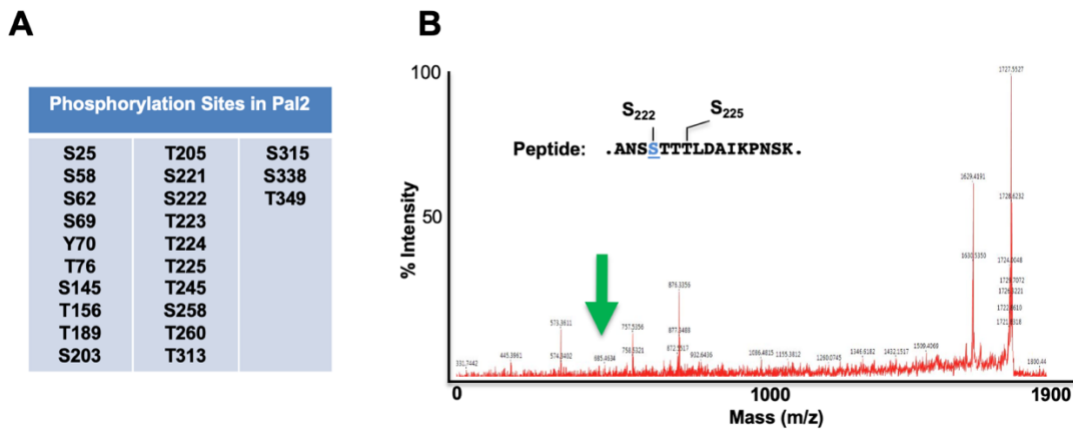


Figure 3.19 Pal2 is phosphorylated at multiple sites.

(A) Pal2 is phosphorylated at multiple sites. The reported phosphorylation sites from SGD are listed. (B) Mass spectrometric analysis of the Pal2 protein phosphorylated by Kin2 identified a single phosphorylated peptide.

To determine if the phosphorylation sites identified through the mass spectrometry results have any importance in Pal2 phosphorylation by Kin2, we performed *in vitro* kinase assays, using a series of Pal2 point mutants (**Fig 3.20**). Combined mutation of four putative phosphorylated residues (S222, T223, T224 and T225) to alanine (referred to as Pal2-4Ala) drastically reduced the level of Pal2 phosphorylation by Kin2 (**Fig 3.20**). By contrast, combined mutation of the three Thr residues (T223, T224 and T225, referred to as Pal2-3Ala) had a more modest effect, while mutation of S222 alone or in combination with T224 (referred as 2Ala) led to reduced phosphorylation by Kin2 (**Fig 3.20**). Collectively these data strongly suggest that S222 is the major site on Pal2 phosphorylated by Kin2 *in vitro*.

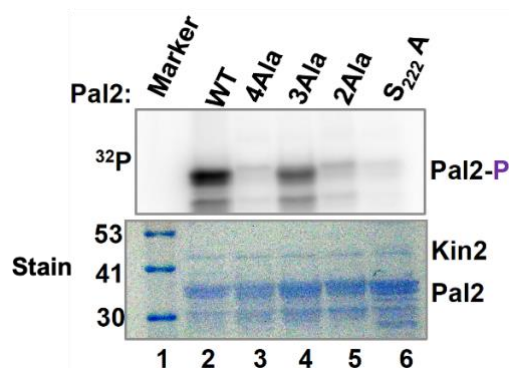


Figure 3.20 Kin2 phosphorylates Ser-222 of Pal2 *in vitro*

The recombinant His₆-Pal2 (residues 65-366) and its indicated derivatives were subjected to kinase assay. Pal2-4Ala = S222A, T223A, T224A and T225A. Pal2-3Ala = T223A, T224A and T225A. Pal2-2Ala = S222A and T224A. Protein markers (kDa) are indicated.

Next obvious question was whether Pal1 follows the same pattern. We observed that Pal1 lacks the Kin1/Kin2 consensus phosphorylation site sequence but does have a single threonine residue at position 323, analogous to Thr-225 of Pal2 (**Fig 3.16A**). We also found that the truncated Pal1 protein (residues 165-499) was weakly phosphorylated by Kin2 *in vitro* (**Fig 3.21**). This low

level of phosphorylation was unaffected by mutation of Thr-323 to Ala (**Fig 3.21**). These data suggest that unlike Pal2, Pal1 is not a substrate of Kin2.

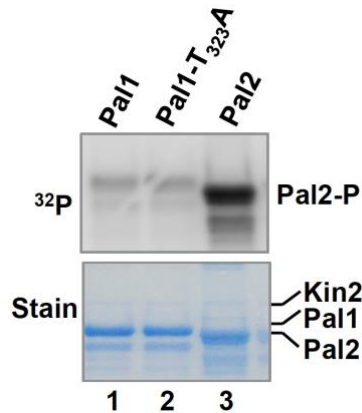


Figure 3.21 Pal1 is not a substrate of Kin2

Kin2 does not phosphorylate Pal1 *in vitro*. Recombinant His₆-Pal1 (residues 165-499) protein was subjected to kinase assay with purified Kin2 and γ -³²P-ATP

***In vitro* and *in vivo* phosphorylation of Pal2 by Kin2**

We next examined whether the Kin kinases phosphorylated Pal2 *in vivo*. We transformed the *pal1* Δ *pal2* Δ and *kin1* Δ *kin2* Δ strains with plasmids expressing Flag-tagged WT Pal2 protein. Transformants were grown under ER stress conditions, and whole cell extracts were subjected to either standard SDS-PAGE or phosphate affinity Phos-tag SDS-PAGE followed by Western blotting. On the Phos-tag gel, wild-type Pal2 was separated into at least three distinct species (**Fig 3.22**, lane 2), suggesting that Pal2 is phosphorylated at multiple sites. Notably, the slowest migrating protein band was absent from samples expressing the Pal2-4Ala mutant, in which two faster migrating protein bands were prominent. A similar pattern was seen when wild-type Pal2 was expressed in *kin1* Δ *kin2* Δ cells. Taken together, these data indicate that Pal2 is phosphorylated at one or more sites in the S222–T225 region in a manner dependent on Kin1 and/or Kin2. Collectively, our results suggest that Pal2 is a bona fide *in vivo* substrate of Kin1/Kin2.

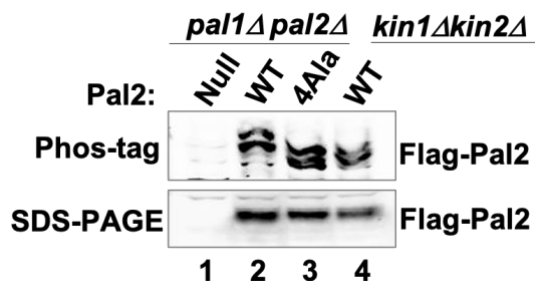


Figure 3.22 Kin1 or Kin2 phosphorylates Pal2 *in vivo*

Whole cell extracts were prepared from indicated yeast strains containing a vector plasmid (null) or the same plasmid containing the Flag-tagged wild type (WT) Pal2 or its 4Ala mutant. Samples were then subjected to normal SDS-PAGE or Phos-tag SDS-PAGE gel followed by Western blot analysis using anti-Flag antibody.

Importance of phosphorylation of Kin2 Thr-281 for its activation

Activation loop phosphorylation is a key event in the activation of a kinase. Our data showed that phosphorylation of Thr-281 within the activation loop of Kin2 is important for its activation¹⁹⁶. Thus, we wanted to determine if T281 phosphorylation controls the ability of Kin2 to phosphorylate Pal2. We purified the Flag-tagged Kin2 protein (residues 94-526) from yeast cells (i.e., *ScFlag-Kin2*). We also purified the GST-Kin2 (residues 94-526) and its derivatives GST-Kin2-T281E and GST-Kin2-ΔKI-T281E from *E. coli* (i.e., *EcGST-Kin2* and *EcGST-Kin2-ΔKI-T281E*). Then, we performed *in vitro* kinase assays with the recombinant Pal2 protein as a substrate using *ScFlag-Kin2*, *EcGST-Kin2* or *EcGST-Kin2-ΔKI-T281E* as the kinase. *ScFlag-Kin2* purified from yeast cells is presumably phosphorylated at T281¹⁹⁶, and was able to phosphorylate Pal2 (**Fig 3.23**, lane 2). The *EcGST-Kin2* protein purified from bacteria was unable to phosphorylate Pal2 (**Fig 3.23**, lane 3) likely because of the fact that the bacterially purified Kin2 protein was not phosphorylated at the activation loop residue T281. However, the *EcGST-Kin2-ΔKI-T281E* protein that contained a phospho-mimetic glutamate in place of T281 was able to phosphorylate

Pal2 (**Fig 3.23**, lane 4). Collectively, these results suggest that T281 phosphorylation within the activation loop of Kin2 is required for Pal2 phosphorylation, and that activation loop phosphorylation of Kin2 occurs *in trans* by another kinase.

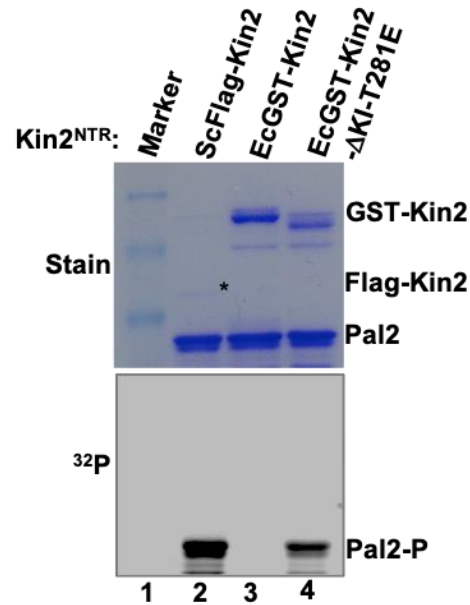


Figure 3.23 T281 phosphorylation of Kin2 is important for Pal2 phosphorylation

Recombinant His₆-Pal2 (residues 65-366) was subjected to kinase assay with Flag-tagged Kin2 purified from yeast (ScFlag-Kin2), GST-Kin2 purified from *E. coli* (EcGST-Kin2) and GST-Kin2-T281E purified from *E. coli* (EcGST-Kin2-T281E).

Effect of Pal2 Phosphorylation on ER stress response

In order to test if phosphorylation of Pal2 is important for ER stress response, we used a functional complementation approach. The WT Pal2 (Flag-Pal2 Δ intron- Δ N65) construct encodes a functional protein that complemented the *pal1* Δ *pal2* Δ double deletion strain (**Fig 3.24A**, row 2). Mutations were introduced in the context of this construct. Next, these constructs were transformed into the *pal1* Δ *pal2* Δ double deletion strain and the ability of the cells to grow in tunicamycin was tested. The mutation of S222 to Ala did not affect the ability of Pal2 to rescue the tunicamycin growth defect of a *pal1* Δ *pal2* Δ strain (**Fig 3.24A**, row 3). These data suggested that phosphorylation at S222 alone did not affect the resistance to tunicamycin. Accordingly, we combined mutations of nearby phosphorylated residues (i.e., T223, T224 and T225) with the S222A mutant. We observed that the *pal1* Δ *pal2* Δ strain expressing all double mutant combinations grew on tunicamycin medium (**Fig 3.24A**). However, the *pal1* Δ *pal2* Δ cells expressing the 4Ala quadruple mutant (Pal2 Δ N65-STTT222-225AAAA) exhibited a slow-growth phenotype compared to its isogenic wild type strain and were unable to grow on medium containing tunicamycin (**Fig 3.24A**). Western blot analysis showed expression of Pal2 protein from the 4Ala construct (**Fig 3.24B**, lane 9), suggesting that the growth defects were not due to defects in protein expression, but somehow these residues act together. We also observed that a phosphomimetic 4Glu quadruple mutant (Pal2 Δ N65-STTT222-225EEEE) grew on tunicamycin medium, suggesting that the functional impact of mutating these sites to Ala is due to ablating phosphorylation. It therefore appears that the phosphorylation of Pal2 at S222, T223, T224 and T225 are important for the tunicamycin resistant phenotype.

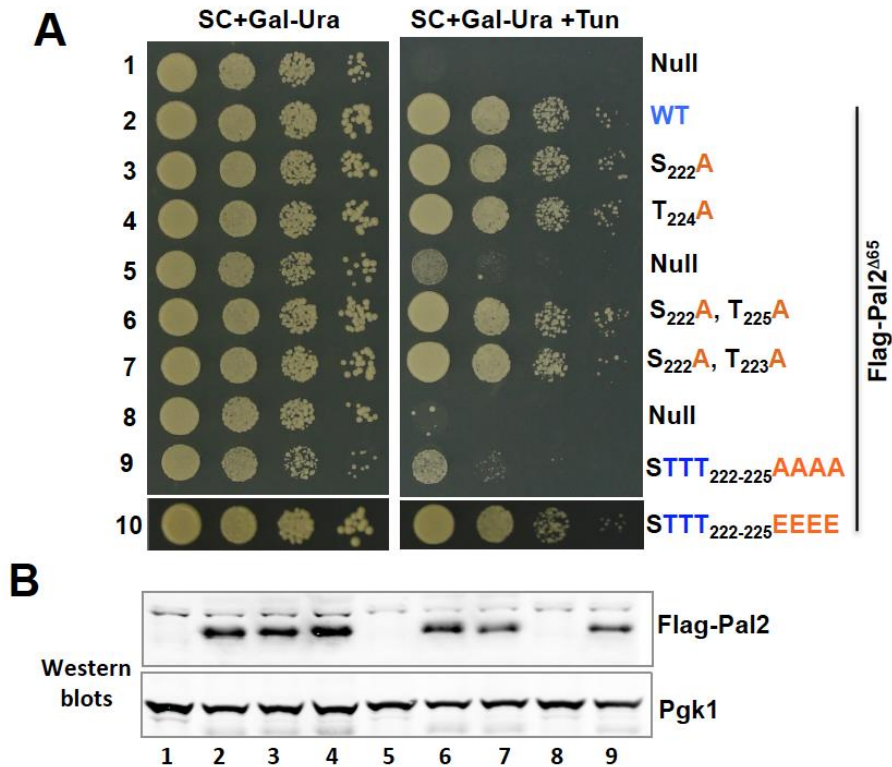


Figure 3.24 Phosphorylation of Pal2 is important for ER stress response

(A) The *pal1Δ pal2Δ* strains expressing wild type Pal2 and its derivatives were tested for growth on synthetic complete medium with and without tunicamycin. (B) Analysis of Pal2 protein expression. Whole cell extracts from the strains indicated were subjected to Western blot analysis using anti-Flag and Pgk1 antibody.

In order to test if the sensitivity to tunicamycin of the 4ala containing cells was due to Hac1 protein expression, we grew *pal1Δpal2Δ* cells harboring a vector, and the same vector expressing the WT-Pal2 and Pal2-4ala with tunicamycin. The cell lysates were subjected to western blot using antibody against Hac1. As expectation, the Hac1 expression in the 4ala mutant was drastically reduced (**Fig 3.25**).

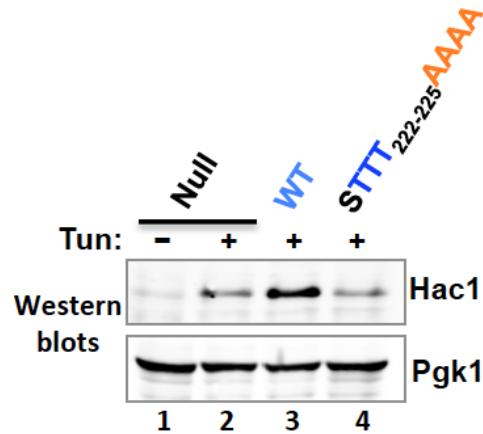


Figure 3.25 Hac1 protein expression is reduced in Pal2-4ala cells

pal1Δpal2Δ yeast cells harboring the indicated Pal2 alleles were grown in synthetic complete medium without uracil and whole cell extracts were isolated and subjected to Western blot analysis using antibodies against Hac1 and Pgk1 proteins.

Collectively, our data suggest that Kin2 phosphorylates Pal2 specifically at S222. We are yet to identify the unknown kinase(s) that might phosphorylate the residues T223, T224 and/or T225 (**Fig 3.26**).

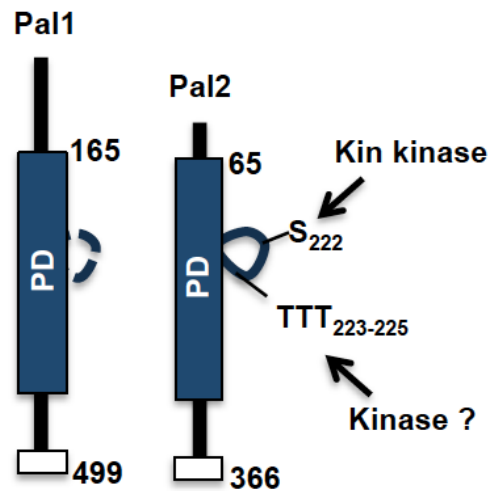


Figure 3.26 Schematic representation of Pal1 and Pal2 proteins

The homologous Pal1 domains (PD) are indicated by dark blue boxes. The phosphorylation loop of Pal2 is shown. The numbers indicate the amino acid residues.

Contribution of the Pal proteins in targeting *HAC1* mRNA to the ER stress site

So far, our data suggest that Pal proteins have a role in *HAC1* mRNA splicing and translation. During ER stress, *HAC1* mRNAs and Ire1 proteins aggregate and form discrete foci within the cytoplasm¹³⁸. Hence, we wanted to study if the Pal proteins have any effect on *HAC1* mRNA foci formation. We used a constructed a plasmid expressing the *HAC1* mRNA tagged with a nucleolin recognition element (NRE) at its 3'-UTR. Co-expression of this RNA with an NRE-binding domain (ND)-GFP fusion protein allows us to visualize *HAC1* mRNA localization¹³⁷. We transformed the WT and *pal1* Δ *pal2* Δ cells with these constructs and subjected the transformants to two-photon fluorescence microscopy. Cells co-expressing *HAC1*-NRE with ND-GFP grown in the presence of tunicamycin showed GFP signals distributed throughout the cytoplasm, with some discrete punctate structures suggestive of ER stress foci. The number of these punctate structures was reduced nearly two-fold in *pal1* Δ *pal2* Δ cells compared to the WT (**Fig 3.27**). These data suggest that Pal proteins likely play a significant role in *HAC1* mRNA foci formation.

Previously, it was shown that the Pal2 protein has a role in endocytosis and they localize near the cytoplasmic membrane¹⁹⁷. However, our data indicates that Pal2 has an important role in ER stress response. Based on our observations, we predict that Pal2 might localize near the ER stress sites to generate an optimum UPR signaling. Hence, we examined whether Ire1 and Pal2 co-localize at sites of ER stress. We expressed an Ire1-YFP (yellow fluorescent protein) fusion protein in a yeast strain expressing Pal2-GFP from its chromosomal locus, and visualized GFP and YFP by two-photon fluorescence microscopy (**Fig 3.28**).

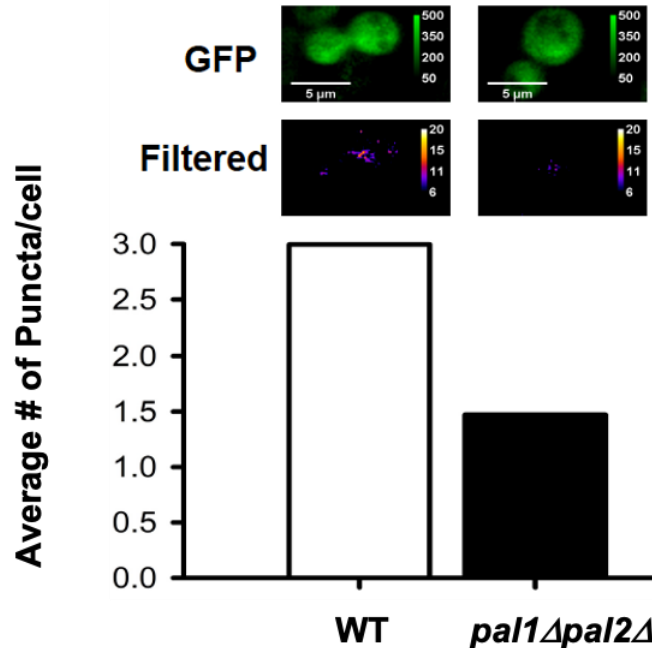


Figure 3.27 *HAC1* foci formation is reduced in Pal1 and Pal2 double deletion strain

Analysis of *HAC1* mRNA foci formation by two-photon micro-spectroscopy. The wild type or *pal1Δpal2Δ* cells expressing *HAC1-NRE* and ND-GFP were grown for two days at 30°C on a solid synthetic complete medium containing tunicamycin (1 μg/ml) and then imaged by two-photon microscopy. The GFP signal (top panel) was unmixed from the auto-fluorescence elementary spectra. The GFP intensity map was filtered (middle panel) to reveal the high-intensity punctate. Cells lacking both Pal1 and Pal2 protein deletion showed reduced punctate formation compared to its isogenic WT strain (bottom panel).

The Pal2-GFP fusion protein was observed throughout the cells, in contrast to a previous report that Pal2 localized strictly to the cell membrane¹⁹⁷. As expected, Ire1-YFP was basally distributed throughout the cytoplasm, whereas discrete punctae of Ire1 molecules were visualized when cells were treated with DTT. Ire1-YFP fusion protein was seen to co-localize with the GFP signal within the cytoplasm. In the presence of DTT, Ire1-YFP fusion protein formed an average of 3.86 foci per cell. The merged Pal2-GFP and Ire1-YFP intensity maps (lower panel of **Fig 3.28**) indicate that within the diffuse GFP signal there is some co-localization of the two molecules. Taken together, these data suggest a possible connection between Ire1 activation and Pal2 protein function.

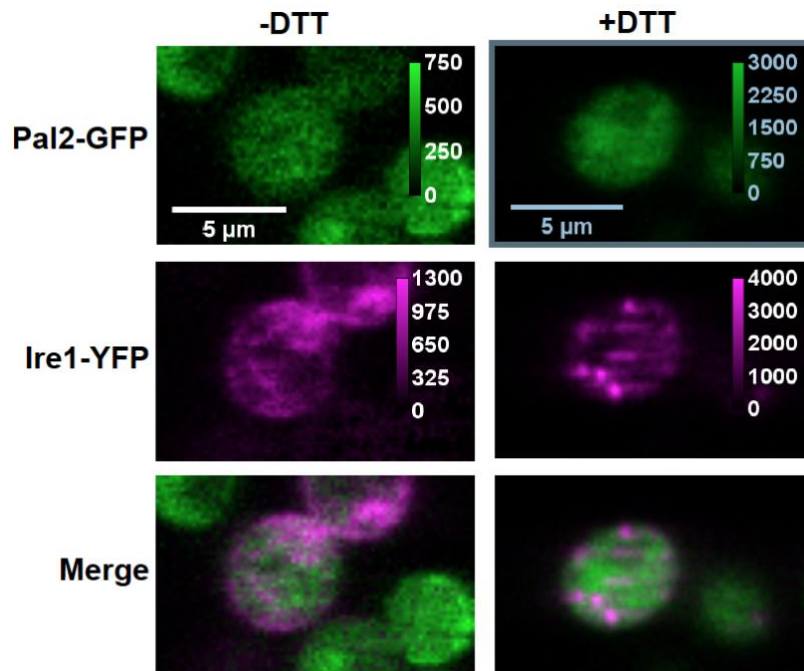


Figure 3.28 Analysis of Ire1-YFP and Pal2-GFP colocalization

Yeast cells co-expressing Pal2-GFP and Ire1-YFP was imaged by a two-photon micro-spectroscope. The signals were spectrally unmixed to obtain separate maps of GFP (top panels) and YFP (middle panels) in both the absence (left) and presence (right) of DTT. The images (bottom panel) were merged to show that Ire1-YFP foci overlapped with the Pal2-GFP.

The list of plasmids and yeast strains used in this chapter are compiled in the Appendix I.

All materials and methods are listed under chapter 5.

Mass spectrometry results are listed under Appendix II.

These findings have been compiled, revised and recommunicated to the journal Science Signaling.

4. Chapter 4: Discussion and future prospects

Protein kinases Kin1 and Kin2 belong to a family of serine/threonine kinases that have been shown to coordinate the cellular exocytosis as well as the ER-stress response. However, it is not known how Kin kinases are activated and how they transmit stress signals to the downstream components. In chapter 2, we investigated the molecular events that lead to activation of the Kin kinase domain under conditions of ER stress. We show that both Kin1 and Kin2 proteins minimally require a kinase domain (KD) and a short adjoining kinase extension region (KER) for their function. We refer to these mini functional Kin1 and Kin2 proteins as Kin1_{mini} and Kin2_{mini}, respectively. We further demonstrate that Kin2-KER is composed of two distinct subdomains (KER-I and KER-III) separated by a spacer of at least 40 amino acids. The computational analyses suggest that KER-I might fold and function like an UBA-like domain by yet unknown mechanisms.

Typically, most protein kinase domains are kept in an inactive state by means of intramolecular interaction(s) mediated by its own domain or inter-molecular interaction(s) mediated by other subunit(s), or both³³. For example, the KA1 domain in Kin kinases functions as an autoinhibitory domain¹³⁴, whereas a regulatory subunit of PKA inhibits its kinase activity¹⁹⁸. The inactive kinase domain must be activated in order to do its physiological function. Inactive-to-active transition requires release of the KD from its own domain or subunit, or both. But, in many cases, the isolated kinase domain is not functional. For example, we did not find any measurable Kin kinase activity when the isolated KD of Kin1 (residues 115-430) or Kin2 (residues 94-380) was expressed in yeast cells. For the kinase activity, Kin kinases required at least an adjoining extension region (i.e., KER) outside the kinase domain. However, the structural and functional role of KER is not yet clear. Most likely, KER increases the stability of protein by promoting a

specific intra-molecular interaction, binds a specific partner protein that activates the kinase domain, and/or targets the protein to a specific cell compartment.

Both Kin1 and Kin2 are shown to be phosphorylated proteins. Thus, it appears that each one is regulated by a complex mechanism involving auto- and/or trans-phosphorylation. Mutational analyses of several phosphorylated residues revealed that the substitution of phosphomimetic glutamate for the activation loop residues (Kin1 residue T302 or the Kin2-residues Y275 and T281) bypassed the requirement of phosphorylation in Kin1_{mini} or Kin2_{mini} proteins. The activation loop phosphorylation is a common mechanism by which protein kinases are activated²⁰. Interestingly, we found that the Kin2 residue T281 was phosphorylated in the Kin2_{mini}-K128R and Kin2_{mini}-D248A kinase-inactive mutants. Furthermore, we found that the bacterially expressed and purified GST-Kin1 or GST-Kin2 protein was unable to phosphorylate α -casein, likely due to lack of the activating T302 or T281 phosphorylation. Consistent with this notion, we observed that the glutamate substitution of the residue T302 or T281 in GST-Kin1 or GST-Kin2 protein led to phosphorylation of α -casein. Collectively, these data suggest that phosphorylation of the residue T302 in Kin1 or T281 in Kin2 occurs in a *trans* mechanism.

The Kin kinase domain shows a significant homology with the kinase domain of Snf1 (sucrose non-fermenting-1) in yeast and AMPK (AMP-activated protein kinase)-related kinase MARK in humans. Snf1 is phosphorylated and activated by a group of three upstream kinases Sak1, Tos3 and Elm1¹⁹⁹. If Sak1, Tos3 and Elm1 indeed were upstream kinase for the Kin2 T281 residue, we hypothesized that deletion strains lacking these kinases would result in a defective UPR. We performed a yeast growth test using the Sak1, Tos3 and Elm1 deletions in combination and test the growth on YEPD and YEPD with tunicamycin. We did not observe any growth defect

In another attempt to identify the Kin2 T281 upstream kinase, we analyzed the T281 phosphorylation status of Kin2 in certain kinase deletion strains. These kinase deletion strains were chosen on the following basis. Yeast has 129 reported kinases¹³. Out of these 19 are essential kinases, and among the non-essentials, 24 kinases have paralogs and the remaining do not. We made a list of non-essential kinases without paralogs and searched the database to check if any of these kinase deletion strains were reported to show tunicamycin sensitivity which would indicate a possible role of that kinase in the ER stress response pathway. However, we did not see much defect in the T281 phosphorylation in these kinase null strains (**Fig 4.3**).

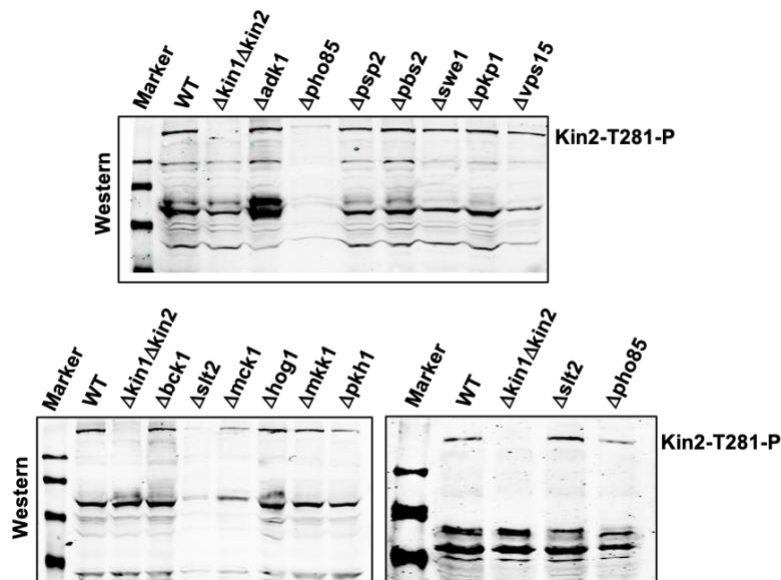


Figure 4.3 T281 phosphorylation status in non-essential kinase null strains

The indicated yeast strains were grown under ER stress conditions and the cellular extracts were collected and subjected to Western blotting using an antibody against the phosphorylated Kin2 T281 residue.

In future, it would be interesting to test the T281 phosphorylation status in the temperature sensitive mutants of the essential kinases and also in the deletion strains lacking the paralogous kinases. Collectively, these data suggest that T281 phosphorylation is mediated by a currently unknown kinase.

We also found that Kin2_{mini} protein associates with endomembrane when cells are under ER stress. Recently, Yuan et al. (2016) shows that Kin2 is predominantly located at the bud tip/neck¹⁷⁵. Thus, it appears that association of Kin2 with membrane regulates its kinase function, and the membrane association varies depending upon the cellular conditions. Still, molecular events leading to association of Kin kinases with endomembrane in specific cellular responses remain to be established. Moreover, roles of Kin kinases in ER proteostasis raise some intriguing questions: How, when and in what context do Kin kinases sense and transduce the ER stress signal? How do Kin kinases coordinate with the Ire1 pathway to produce an optimum UPR?

In Chapter 3, we show that the endocytic proteins Pal1 and Pal2, contributes to *HAC1* mRNA processing. We also show that Kin1 and Kin2 specifically phosphorylate Pal2, but not its isoform Pal1. Previously, we have shown that Kin kinases are required for optimal activation of the UPR¹³⁷. Thus, our work provides evidence of a previously unappreciated Kin2-Pal2 signaling pathway contributing to *HAC1* mRNA metabolism and ER homeostasis.

Under conditions of ER stress, the ER-resident endonuclease Ire1 cleaves the *HAC1* mRNA at two specific sites (G661 and G913), thus removing an intervening sequence that blocks the initiation of translation^{181,182}. Cleavage requires co-localization of *HAC1* mRNA with the Ire1 RNase domain, which is known to be mediated by a bipartite element (3'-BE) located within the 3'-UTR of its mRNA¹³⁸. We have shown previously that a conserved element (5'-G₁₁₄₃GCGC₁₁₄₇-3') within the 3'-BE of the *HAC1*-3'-UTR carries information that helps target the mRNA to ER

stress sites and subsequent co-localization with Ire1¹³⁷. We also have shown that overexpression of the Kin1 or Kin2 protein kinase suppresses the co-localization defect of the *HAC1-3'-BE* mutant with Ire1, implicating Kin kinase's role in the *HAC1* mRNA splicing and translation¹³⁷. However, the mechanism by which Kin1 and Kin2 controls these physiological processes has not been clearly defined. As *cis*-acting regulatory elements located at the 3'-UTR of mRNAs influence their localization by interacting with RNA binding proteins²⁰¹, we speculated that Kin kinases likely control the formation of an mRNA protein (RNP) complex on the 3'-BE or modulates an existing RNP complex, which drives *HAC1* mRNA targeting, splicing and/or translation. In an effort to identify the components of this RNP, we expressed a 3'-BE mini RNA and identified several 3'-BE-associated proteins, including Pal2 that has been recently reported to be one of the putative *in vitro* substrates of Kin2¹. The mass spectrometric approach to identify the 3'-BE associated proteins revealed several other proteins along with Pal2. In future, it would be fascinating to investigate the relation between Pal2 and these other proteins and study if and how they modulate each other's activities to drive the *HAC1* mRNA to the Ire1 foci for its splicing.

Pal2 has a paralog, Pal1. We tested the sensitivity of tunicamycin of *pal1Δ pal2Δ* strain in the medium exclusively containing glucose (the preferred carbon and energy source) and galactose (a less preferred carbon and energy source). Interestingly, we observed that the *pal1Δ pal2Δ* strain is severely sensitive to low concentration of tunicamycin on medium containing galactose. Tunicamycin inhibits the enzyme GlcNAc 1 (N-acetylglucosamine)-phosphotransferase that transfers GlcNAc-1-P from UDP-GlcNAc to dolichyl-phosphate, a step in the formation of N-linked glycosylation of nascent protein¹⁷⁰. Thus, it may be that the absence of exogenous glucose limits the pool of GlcNAc available for protein N-linked glycosylation, sensitizing cells to ER stress. The mechanistic details of galactose utilization are still being studied.

Kin2 uniquely phosphorylates Pal2 but not Pal1. Several prior reports also support unique paralog-specific functions of Pal1 and Pal2. For instance, Moorthy et al. recently showed that Pal2 associates with the endocytic coat factors to promote clathrin-mediated endocytosis¹⁹⁷, whereas Carroll et al. showed that Pal1 plays a critical role in the formation of endocytic sites¹⁸⁶. Pal1 is known to significantly contribute to cell polarity both in budding and fission yeast, a process essential for differentiation, morphogenesis and migration¹⁶⁹. Like budding yeast, the Pal1 ortholog in the fission yeast *S. pombe* has been shown to play an important role in maintaining cell morphology²⁰². The functional divergence between Pal1 and Pal2 can be attributed in part to differences in their primary sequence and patterns of expression. For instance, the *PAL2*, but not the *PAL1*, mRNA contains an intron sequence. Pal1 and Pal2 have only 45% sequence identity at the protein level. Most relevant to our study, only Pal2 harbors a consensus phosphorylation site sequence for Kin1 and Kin2, which is located within a group of phosphorylation sites that collectively are essential for its function in the UPR. More detailed functional analyses of Pal1 and Pal2 are necessary to fully determine how they buffer each other's function.

The circular dichroism spectrum suggests that Pal2 is likely a disordered protein, and likely stabilized by its partner proteins in order to be able to function as a protein with pleiotropic actions. It would be interesting to study if the other identified 3'-BE associated proteins interact with Pal2 and modulate its function.

The most well studied post-translational modification is reversible protein phosphorylation. Mutational studies on Pal2 suggested that single mutation of the phosphorylation site S222 was not sufficient to reduce the ER stress response; however, mutations of four consecutive phosphorylated residues (i.e., S222, T223, T224 and T225) by non-phosphorylatable alanine significantly reduced the ability of *pal1Δ pal2Δ* strain to induce the ER stress response.

These results demonstrate that phosphorylation of all four residues in Pal2 protein together play an important role in ER stress response. Kin kinases phosphorylate S222, but the kinase(s) that phosphorylates residues T223, T224 and/or T225 is yet to be identified. Taken, together, these data provide evidence of a previously unappreciated Kin2-Pal2 signaling pathway contributing to *HAC1* mRNA processing.

Recently, Jeschke et al. (2019) have shown that sucrose non-fermenting 1 (Snf1) kinase is a potential kinase engaging in priming a substrate (e.g., Sec9) for subsequent phosphorylation by Kin1/Kin21. To check if Pal2 is primed by Snf1 phosphorylation, we generated a *kin1Δ kin2Δ snf1Δ* strain and tested its ability to grow in the presence of tunicamycin. We found that the *kin1Δkin2Δsnf1Δ* strain grew on tunicamycin medium similarly to *kin1Δkin2Δ*, also confirmed by growth curves (**Fig 4.4**), in contrast to our expectation that the triple mutant would be more sensitive to tunicamycin. Also, the sequence surrounding the Pal2 priming site did not conform to the substrate recognition (L-x-R-x-x-S/T-x-x-x-L) motif of Snf1₂₀₃. Collectively, these results ruled out the possibility that Snf1 phosphorylates Pal2 under physiological conditions and contribute to the ER stress response. Kinases that phosphorylate T223, T224 and/or T225 remain to be identified.

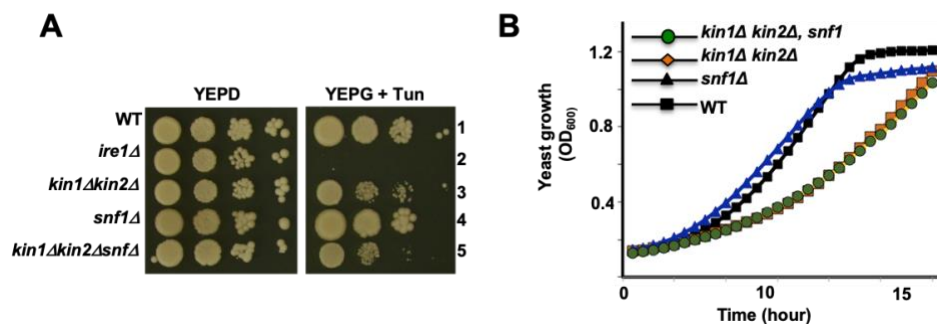


Figure 4.4 Snf1 does not contribute to the ER stress response

(A) Indicated yeast strains are tested for growth on the YEPG and tunicamycin media. (B) The indicated yeast cells were grown, OD₆₀₀ were measured, and plotted.

Previous reports show that mRNAs can be specifically targeted to distinct subcellular compartments²⁰⁴. mRNA localization signals are commonly found within their 3'-UTRs, like the 3'-BE in the *HAC1* mRNA that mediates co-localization with Ire1¹³⁸. This co-localization is evident in the formation of microscopic foci under conditions of ER stress^{137,138}. We have found that Pal2 partly localizes to these foci, suggesting that its interaction with the *HAC1* 3'-BE might be induced by ER stress. This is confirmed by the observation that *HAC1* mRNA foci are significantly reduced in yeast lacking Pal1 and Pal2. These data collectively suggest that Pal proteins likely contribute to the fine-tuning of Ire1 and/or *HAC1* mRNA foci formation. However, the specific role of Pal proteins in the formation of these foci is yet unknown.

In summary, our work unravels a Kin kinase signaling pathway that modulates the UPR signaling in budding yeast. The working model shows an integration of Kin-kinase and Ire1-mediated UPR signaling pathways (see **Fig 4.5**). During the ER stress, both Ire1 and Kin kinases are activated. Ire1 is activated by dimerization, oligomerization and auto-phosphorylation^{187,205}. The Kin kinases are activated when their kinase domain is released by an unknown mechanism from their kinase-associated domain 1 (KA1). Subsequently, the Kin2- kinase domain is activated by phosphorylation of its activation loop residue Kin2-T281 or Kin1-T302 in a *trans* mechanism¹⁹⁶. The active Kin kinase phosphorylates Pal2 that likely facilitates targeting of the translationally repressed *HAC1* mRNA to the active Ire1 to excise its intron. The translation of *HAC1* mRNA is then derepressed, resulting in production of an active transcription factor which activates expressions of several protein folding enzyme and chaperone genes to alleviate the ER stress.

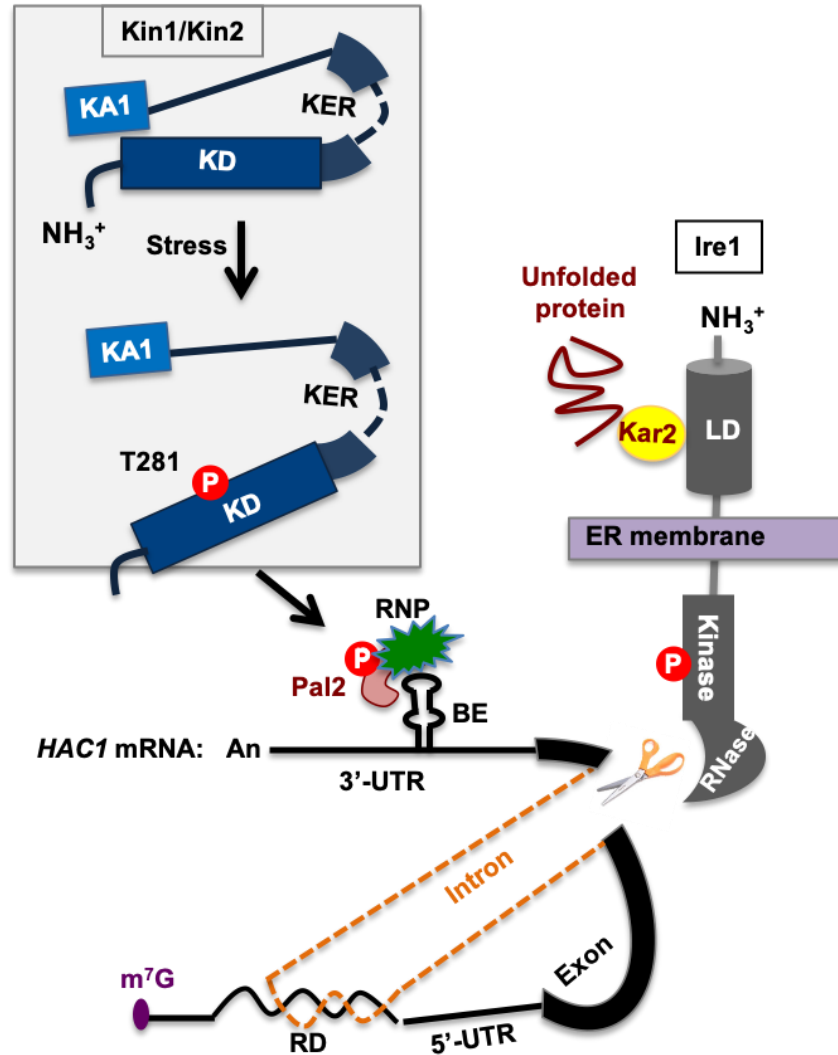


Figure 4.5 Model for Kin2-Pal2 pathway in promoting the UPR

The ER-resident chaperone Kar2 binds to the luminal domain (LD) of Ire1 and keeps it in an inactive form. During the ER stress, unfolded proteins (scribbled red line) accumulate inside the ER lumen and titrate Kar2, thus activating cytoplasmic kinase and RNase domain of Ire1. The exons (grey bars) of *HAC1* mRNA are separated by an intron (orange dashed line) that interacts with the 5'-UTR (solid black) line of mRNA to form an inhibitory RNA duplex (RD). The active RNase domain of Ire1 cleaves out the intron from the *HAC1* mRNA. The kinase associated domain 1 (KA1, light blue bar) binds to the kinase domain (KD, dark blue bar) of Kin1 or Kin2, thus keeping the kinase domain (KD) in an inactive form. An essential kinase extension region (KER) of Kin1/Kin2 is also shown. Under stress conditions, KD is activated by phosphorylation within the activation loop on residue T281 in a trans mechanism, shown here by the sign "P" encircled within a red circle. The active KD then phosphorylates Pal2, which is likely associated with the 3'-BE and 3'-BE-specific RNP (serrated green shape), thus targeting *HAC1* mRNA to the ER stress site.

5. Chapter 5: Materials and methods

Media, Buffers, Reagents and Stock Solutions

All chemicals and reagents were purchased from commercial suppliers Sigma-Aldrich, Acros Organics or Fisher Scientific unless otherwise noted. Restriction enzymes were purchased from NEB (New England Biolabs, USA). Protein assay reagent was obtained from Bio-Rad (USA).

1. Media

Agar plates were prepared by adding 2% Agar A (Bio Basic) to all media. Media was autoclaved at 15psi, 120°C for 20 mins. Ingredients were dissolved in double distilled water before autoclaving.

Luria Bertani (LB)

- 1% (w/v) Tryptone
- 0.5% (w/v) Yeast extract
- 1% (w/v) NaCl

Yeast Extract Peptone Dextrose (YEPD)

- 2% (w/v) Peptone
- 1% (w/v) Yeast extract
- 2% (w/v) Dextrose

Yeast minimal media (Synthetic Dextrose-SD)

- 0.142% (w/v) Yeast Nitrogen base (w/o ammonium sulfate)
- 0.5% (w/v) Ammonium sulfate
- 0.2% (w/v) Amino acid mixture
- 2% (w/v) Dextrose

Super Optimal Broth (SOC)

2% (w/v) Tryptone

0.5% (w/v) Yeast extract

10mM NaCl

2.5mM KCl

10mM MgCl₂ (added after sterilization)

20mM Glucose (added after sterilization)

2. Buffers

Volume of the buffers were adjusted by adding appropriate amount of double distilled water.

10X Tris-Glycine

30 g Tris Base

144 g Glycine

1L Water

Filter and store at 4°C.

10X Tris-Glycine SDS

30 g Tris Base

144 g Glycine

10 g Sodium dodecyl sulfate (SDS)

1L Water

Filter and store at 4°C.

50X Tris-Acetate EDTA (TAE)

242 g Tris Base

57.1 ml 100% Glacial acetic acid

100 ml 0.5 M EDTA (pH 8.0)

1L water

10X Tris-Borate EDTA (TBE)

108 g Tris base

55 g boric acid

40 mL 0.5 M EDTA (pH 8.0)

1L water

Filter and store at RT.

0.5 M EDTA (ethylenediaminetetraacetic acid)

186.1 g disodium EDTA.2H₂O

800 ml water

pH 8.0 adjusted by adding NaOH solution. Volume adjusted to 1L. Sterilized by autoclaving. Stored at RT.

1M Tri-HCl pH 8.0, pH 6.8, pH 7.5

121.2 g Tris base

800 ml water

pH adjusted by adding HCl solution. Volume adjusted to 1L. Sterilized by autoclaving. Stored at RT.

1.5 M Tri-HCl pH 8.8

181.7 g Tris base

800 ml water

pH adjusted by adding HCl solution. Volume adjusted to 1L. Sterilized by autoclaving. Stored at RT.

Ponceau Stain

0.5% (w/v) Ponceau stain

1% Acetic acid

Stored at 4°C.

5X Protein Loading Dye for SDS-PAGE

0.25% Bromophenol blue

50% Glycerol

10% SDS

0.25 M Tris-HCl (pH 6.8). Stored at RT.

5% β -mercaptoethanol (added right before use)

5X Protein Loading Dye for Native Gel

0.25% Bromophenol blue

50% Glycerol

0.25 M Tris-HCl (pH 6.8). Stored at RT.

10X Tris Buffered Saline (TBS)

24 g Tris base

88 g NaCl

800 ml water

pH adjusted to 7.6 by adding HCl solution. Volume adjusted to 1L. Sterilized by filtration. Stored at RT

Add 0.1% Tween 20 before storing.

To make TBST add 1ml Tween 20 in 1L 1X TBS.

5% Bovine Serum Albumin (BSA)

5 g BSA

100 ml 1X TBS

Sterilized by filtration. Stored at 4°C.

10% Polyacrylamide gel composition

Running gel	4 gels	Stacking gel	4 gels
water	15.2 ml	water	16.8 ml
Tris-Cl (1.5M) pH= 8.8	10.4 ml	Tris-Cl (1M) pH= 6.8	2.4 ml
Acrylamide (30%)	13.6 ml	Acrylamide (30%)	4 ml
10% SDS	400 μ l	10% SDS	240 μ l
TEMED	20 μ l	TEMED	20 μ l
10% APS	400 μ l	10% APS	240 μ l

50 μ M Phos-tag gel composition (10 ml, always made fresh)

8% Running gel	10 ml	4.5% Stacking gel	2 ml
water	4.47 ml	water	1.17 ml
Tris-Cl (1.5M) pH= 8.8	2.5 ml	Tris-Cl (1M) pH= 6.8	0.5 ml
Acrylamide (30%)	2.67 ml	Acrylamide (30%)	0.3 ml
10% SDS	100 μ l	10% SDS	20 μ l
TEMED	10 μ l	TEMED	2 μ l
10% APS	50 μ l	10% APS	10 μ l
Phos-tag (5.0 mmol/L)	100 μ l		
MnCl ₂ (10 mmol/L)	100 μ l		

10X MOPS

41.8 g 3-(N-morpholino) propanesulfonic acid (MOPS)

700 ml Diethyl pyrocarbonate (DEPC) treated water

pH 7.0 adjusted by adding NaOH solution.

20 ml 1M Sodium acetate

20 ml 0.5 M EDTA (pH 8.0)

Volume adjusted to 1L. Sterilized by filtration. Stored at RT.

Yeast cells breaking buffer for genomic DNA extraction

100 mM NaCl

10 mM Tris-HCl pH 8.0

1 mM EDTA

1 % SDS

Autoclaved and stored at RT.

Yeast cell breaking buffer for β -galactosidase assay

0.1 M Tris-HCl pH 8.0

20 % glycerol (v/v)

1 mM β -ME (added right before use)

Z-Buffer

16.1 g $\text{Na}_2\text{HPO}_4 \cdot 7\text{H}_2\text{O}$

5.5 g $\text{NaH}_2\text{PO}_4 \cdot 4\text{H}_2\text{O}$

0.75 g KCl

0.246 g $\text{MgSO}_4 \cdot 7\text{H}_2\text{O}$

2.7 ml β -ME

Volume adjusted to 1 lit, filter sterilized, aliquoted and stored at -20°C .

10X PBS

25.6 g Na₂HPO₄·7H₂O

80 g NaCl

2 g KCl

2 g KH₂PO₄

Volume adjusted to 1 lit, autoclaved and stored at RT.

3. Stock solutions

Ampicillin: 100 mg/ml. Stored at 4°C.

Kanamycin: 50 mg/ml. Stored at 4°C.

Tunicamycin: 1 mg/ml DMF. Stored at 4°C.

Dithiothreitol: 1M (154 mg/ml). Stored temporarily at 4°C.

Nourseothricin Sulfate: 5 mg/ml stock. 100 µl was used for one plate.

Hygromycin: 6 mg/ 30 ml media.

G418 Sulfate: 5 mg/ml stock. 500 µl was used for one plate.

4. Antibodies

Anti-Flag antibody was purchased from Sigma (cat # F-3165).

Anti-Pgk1 antibody was purchased from Thermo Fisher (cat # 459250).

Anti-actin antibody was purchased from Santa Cruz (Cat # SC-47778).

Anti-GST antibody was purchased from Invitrogen (cat # 13-6700).

Anti-PGK1 antibody monoclonal (Invitrogen; Cat #459250).

We had a polyclonal antibody raised against the recombinant Hac1 protein from Thermo Fisher Scientific (USA).

We had a monoclonal antibody raised against the T281-phospho-specific peptide (RKQLH**p**TFCGS) from Genscript, USA.

5. Agarose slurry for immunoprecipitation

M2-Flag agarose slurry was purchased from Sigma (M8823)

GST agarose beads was purchased from GE Healthcare (cat # 17-0756-01)

Protocols

1. Plasmid DNA Isolation

The Biobasic plasmid DNA isolation kit (BS614) was used for plasmid DNA preparation.

1. Single bacterial colony bearing the plasmid was grown in 5 ml of Luria broth overnight.
2. Tube containing overnight culture was centrifuged at 2,900 rpm (1630 X g) for 10 minutes. Liquid media was drained by and tube was dried by keeping inverted on a paper towel for 5-10 minutes.
3. 100 µl of Solution I (containing RNaseI) was added to the pellet, mixed well, and incubated in RT for 1 minute. Solution was transferred into a 1.5 ml microcentrifuge tube.
4. 200 µl of Solution II was added to the mixture and mixed gently by inverting the tube 10 times and incubated at room temperature for 1 minute.
5. 350 µl of Solution III was added and mixed gently by inverting tubes for 10 times and incubated at room temperature for 3 minutes.
6. Microcentrifuge tubes were centrifuged at 12,500 rpm (10,500 X g) for 7 minutes.
7. Supernatant was transferred to the EZ-10 column. Centrifuged at 10,000 rpm (6720 X g) for 1 minute.
8. Flow-through was discarded. 500 µl of Wash Solution was added to the column, incubated for 1 minute, and centrifuged at 6720 X g for 2 minutes.
9. Column was centrifuged at 6720 X g for 5 minutes for drying. Flow-through was discarded.
10. Column was transferred to a clean 1.5 ml microfuge tube. 100 µl of TE was added to the center part of the column, incubated at RT for 2 minutes. Centrifuged at 6720 X g for 2 minutes. Purified DNA was stored at -20°C for long-term use.

2. Yeast Genomic DNA Isolation

Reagents:

Yeast breaking buffer

Tris saturated phenol

Chloroform: Isoamyl alcohol (24:1)

1. 200 μ l of yeast breaking buffer was taken in a microcentrifuge tube and one yeast colony was resuspended in the buffer.
2. 100 μ l of zirconium beads was added to the tube. Break the cells at 4 °C by vortexing for 10 minutes.
3. 200 μ l of Tris saturated phenol was added to the broken cells and mixed by inverting the tube 5 times.
4. Tube was centrifuged at 10,500 X g for 10 minutes at 4 °C. Aqueous layer was transferred into a new tube.
5. 200 μ l of chloroform: isoamyl alcohol was added and the tube was centrifuged at 10,500 X g for 5 minutes.
6. Aqueous layer was transferred in a tube with 500 μ l of binding buffer. The mixture was transferred to an EZ- spin column and centrifuged at 6720 X g for 1 minute.
7. Flow through was discarded. 500 μ l of wash buffer was added and centrifuged at 6720 X g for 2 minutes.
8. Flow through was discarded and centrifuged at 6720 X g for 5 minutes.
9. Column was transferred to a 1.5 ml microcentrifuge tube. 40 μ l of TE was added and incubated in RT for 2 minutes.
10. Centrifuged at 6720 X g for 2 minutes. Genomic DNA was stored at -20 °C.

3. Chemical competent cells preparation

Reagents:

LB broth (4.5 liters)

Autoclaved distilled water (500ml)

Autoclaved 10 mM Calcium chloride in 10% Glycerol (100ml)

Day 1:

1. *E. coli* DH5 alpha cells were streaked on LB agar plate with and without Ampicillin.

Day 2:

2. 6 flasks containing 750 ml of Luria broth and one flask with 50 ml of LB broth was autoclaved along with 10 mM Calcium chloride in 10% Glycerol and centrifuge bottles.
3. Single colony of *E. coli* DH5 alpha from LB plate without ampicillin was inoculated in 50 ml of LB broth and grown overnight.

Day 3:

4. Absorbance of the 50 ml culture was recorded at A_{600} and cells equivalent to O.D.=0.05 was inoculated in 750 ml of broth.
5. Cells were grown till $A_{600} = 0.4- 0.5$. The culture was centrifuged at 4,500 rpm (3400 X g) for 5 minutes. The cell pellet was collected in centrifuge bottles.
6. Pellet was washed with cold autoclaved water twice.
7. Pellet was resuspended in 5-8 ml of calcium chloride and glycerol (10 mM calcium chloride in 10% glycerol).
8. 50 μ l cells were aliquoted into microcentrifuge tubes and snap-chilled in dry ice. Cells were immediately stored at $-80\text{ }^{\circ}\text{C}$.

4. Electro-competent cells preparation

Reagents:

LB broth (4.5 liters)

Autoclaved distilled water (500ml)

Autoclaved 10% Glycerol (100ml)

Day 1:

1. *E. coli* DH5 alpha cells were streaked on LB agar plate with and without Ampicillin.

Day 2:

2. 6 flasks containing 750 ml of Luria broth and one flask with 50 ml of LB broth was autoclaved along with 10% Glycerol and centrifuge bottles.
3. Single colony of *E. coli* DH5 alpha from LB plate without ampicillin was inoculated in 50 ml of LB broth and grown overnight.

Day 3:

4. Absorbance of the 50 ml culture was recorded at A_{600} and cells equivalent to O.D.=0.05 was inoculated in 750 ml of broth.
5. Cells were grown till $A_{600} = 0.4- 0.5$. The culture was centrifuged at 3400 X g for 5 minutes. The cell pellet was collected in centrifuge bottles.
6. Pellet was washed with cold autoclaved water twice.
7. Pellet was resuspended in 5-8 ml of 10% glycerol.
8. 50 μ l cells were aliquoted into microcentrifuge tubes and snap-chilled in dry ice.
Cells were immediately stored at -80 °C.

5. Bacterial transformation (heat-shock method)

Reagents:

SOC medium, LB plates with appropriate antibiotics, Dry bath

1. 1 vial of 50 μ l chemical competent cells were thawed on ice.
2. 50 ng - 100 ng of plasmid DNA was added to the cells.
3. Tubes were incubated on ice for 2 minutes.
4. Tubes were incubated on dry bath at 42 °C for 90 seconds.
5. Tube were incubated on ice for 2 minutes.
6. 500 μ l of SOC was added in the tube and incubated on shaker (850 rpm) at 37 °C for 1 hour.
7. Culture was plated on LB plate with appropriate antibiotic (Ampicillin/ kanamycin).
8. Plates were incubated at 37 °C overnight.

6. Bacterial transformation (electroporation)

Reagents:

SOC medium, LB plates with appropriate antibiotics, Dry bath, Electroporator

1. 1 vial of 50 μ l electro-competent cells were thawed on ice.
2. 10 ng of plasmid DNA was added to the cells.
3. Competent cells with plasmid mixture was transferred to electro cuvettes.
4. Cells were pulsed in the electroporator.
5. 500 μ l of SOC was added in the cuvette and the entire mixture was transferred to an microcentrifuge tube.
6. The microcentrifuge tube was incubated on shaker (850 rpm) at 37 °C for 1 hour.

7. Culture was plated on LB plate with appropriate antibiotic (Ampicillin/ kanamycin).
8. Plates were incubated at 37 °C overnight.

7. Yeast transformation

Reagents:

1X TE

0.1 M Lithium acetate in TE

PEG

Calf thymus DNA (CT DNA)

Selection media

Preparation of reagents:

1. 1 M Lithium acetate stock solution was prepared by dissolving 6.6 g of Lithium acetate in water and filter sterilized. 1 ml of 1 M lithium acetate was added in 9 ml of TE to make 0.1 M Lithium acetate in TE.
2. 110 g of PEG-3550 (Sigma) was dissolved in 150 ml of TE and autoclaved. After autoclaving, volume increases to 225 ml. 25 ml of 1 M Lithium acetate was added after autoclaving.

Day 1:

1. Yeast colonies were inoculated in 5 ml of YEPD or in appropriate minimal media and grown overnight.

- O.D.₆₀₀ of starter culture was measured and amount required for inoculation in 30 ml YEPD such that the O.D. of the secondary culture is 0.2 was calculated.

To check O.D. primary culture was diluted 1:20 {50µl culture and 950µl water}.

O.D. calculated by multiplying with dilution factor.

Calculation:

Amount of primary culture to be inoculated in secondary = $(0.2 \times 30) / [\text{O.D.}_{600}]$

- Culture was grown till O.D. (~0.6-0.8)
- When desired O.D. was obtained, culture was harvested in a falcon tube at 1630 X g for 6 mins.
- Cells were washed with 750 µl of 1X TE and transferred to microfuge tubes.
- Cells were pelleted down (10,500 X g, 1 min) and supernatant thrown.
- In the same way wash the cells were again washed with 750µl 0.1 M Li-Ac (diluted in 1X TE).
- Cells were resuspended in 750 µl (1X TE + Li-Ac) and incubated in shaker at 30°C for 1 hour.
- Following was taken in a microfuge tube:
Plasmid DNA-5 µl (if concentration is >200ng/ml)
Carrier DNA-5 µl
Yeast Cells-100 µl
This mix was incubated for 1 hour at 30°C (static)
- 750 µl PEG-LiOAc was added to tubes and incubated for 1 hour at 30°C (static).
- Heat shock at 42°C for 8 mins.
- Kept at RT for 1 min.

13. Cells were pelleted at 10,500 X g for 1min and supernatant thrown.
14. 500 μ l SD media was added to resuspend the cells.
15. 3000 μ l was plated on minimal media and grown for 2-3 days.

8. Total protein precipitation from yeast

Reagents:

- 100% TCA (Sigma)
- 20% TCA (diluted in distill water from 100% TCA)
- 5% TCA (diluted in distill water from 100% TCA)
- 0.5 mm zirconium beads
- 1 M Trizma Base (pH not adjusted)

Day 1:

1. Single yeast colony was inoculated in 5-10 ml of appropriate liquid medium and grown overnight.

Day 2:

2. 0.5 ml of overnight culture was inoculated in 25 ml of liquid medium. Cells were grown till O.D.₆₀₀ ~ 0.6-0.8.
3. Cells were treated with 5 mM DTT for 2 hours for the detection of Hac1 protein expression on Western blot.
4. Cells equivalent to O.D. = 15 was harvested. Cells were transferred to a microcentrifuge tube and spun down to separate the media.
5. 200 μ l of 100 % TCA was added to the pellet and incubated overnight at 4°C.

Day 3:

6. Tubes were centrifuged for 4 mins at 1075 X g at RT. Pellets contain protein sample.
7. Supernatant was discarded and re-suspend in 200 μ l 20% TCA.
8. Zirconium beads were added to the 100 μ l mark. Cells were disrupted by vortexing using Vortex-Genie at 4°C: 2 cycles of 1 min each.
9. 200 μ l of cell suspension was collected in a fresh tube.
10. 400 μ l 5% TCA was added and vortexed for 1 min. Total collection is now 600 μ l.
11. Tubes were centrifuged at 605 X g for 10 mins at RT.
12. Supernatant was discarded. Proteins are in the pellet.
13. For western blot, 50 μ l 2X LSB was added. The color is supposed to turn yellow from the acid.
14. Titration was performed with 50 μ l 1 M Trizma-base. Color should turn blue.
15. Tubes were incubated at 95°C and tapped in-between to dissolve the cell pellets.
16. Tubes were centrifuged at 10,500 X g for 1 min at RT.
17. 15 μ l of protein sample was loaded on protein gel.

9. Western Blot analysis

Reagents:

Transfer buffer	
10X Tris Glycine	50 ml
Methanol	100 ml
Cold water	350 ml

Day 1:

Polyacrylamide gel electrophoresis (PAGE)

1. 15 μ l of protein sample isolated using TCA method was loaded in the 10 % SDS-PAGE gel, run for 70 minutes on 150 Volts (Bio-Rad PowerPac 1645050). 4 μ l protein ladder (Bulldog-Bio) was used.

Transfer

2. Transfer setup was prepared using Nitrocellulose membrane.
3. Overnight transfer at 4°C using transfer buffer. Run at 25 V for 12 hours (Invitrogen XCell II™ Blot Module EI 9051).

Day 2:

4. Nitrocellulose membrane was stained with Ponceau dye to check transfer.
5. Ponceau dye was washed off with 1X TBST.
6. 5% BSA was used to block the membrane for 1 hour at RT.
7. Primary antibody was added and incubated overnight on a nutator shaker at 4°C.

Day 3:

8. Membrane was washed with 1X TBST 5 times (each wash should be for 10 mins).
9. Membrane was incubated with secondary antibody (0.5 μ l in 5ml BSA).
10. Membrane was washed with 1X TBST 5 times (each wash should be for 10 mins).
11. Membrane was scanned in LICOR Odyssey IR Imaging system to visualize protein bands.

10. Total RNA isolation from yeast

The PureLink™ RNA mini kit (Invitrogen 12183018A) was used for RNA preparation.

Reagents:

1. Elution buffer

1X TE 300 μ l

RNase free water 700 μ l

2. 0.1% DEPC water

MiliQ water 1 lit

DEPC (from Sigma) 1 ml

Shaken gently and kept at RT overnight (DEPC is carcinogenic, handled with care).

Autoclaved next day.

3. Formaldehyde RNA running gel (1.4%)

Agarose 0.7 g

Formaldehyde 730 μ l

Ethidium bromide 1.0 μ l

10X MOPS 5 ml

DEPC water 45 ml

Agarose was dissolved in the DEPC water with MOPS, formaldehyde was added in the fume hood followed by EtBr.

Protocol:

1. 10 μ l of β -ME (Sigma) was added in 1 ml lysis buffer and kept on ice.
2. 600 μ l of lysis buffer was added in the microcentrifuge tubes containing yeast cells.

3. Cells were thawed on ice.
4. Zirconium beads were added approximately equivalent to volume of 100 μ l.
5. Cells were disrupted by vortexing for 10 minutes at 4°C.
6. Centrifuged for 12K for 5 minutes.
7. 600 μ l supernatant was collected in a tube containing 600 μ l of chilled 70% ethanol.
Thus, total volume was 1200 μ l.
8. 600 μ l was added on a column (Ambion kit), centrifuged (10 K for 2 min), and liquid discarded from collector.
9. Remaining 600 μ l was added to the same column step 8 was repeated.
10. 500 μ l wash buffer was added to the column and washed twice.
11. Centrifuged at 12K for 5 minutes for drying.
12. RNA was eluted with 40 μ l of elution buffer. Stored at -80 °C.
13. RNA concentration was measured using a Nanodrop (Thermo Scientific NanoDrop 1000 Spectrophotometer) and quality was examined by RNA gel electrophoresis.

11. Reverse Transcriptase PCR

Reagents:

10mM dNTP – NEB Biolabs dNTP mix- #N0447S (make aliquots of 20 μ l and store)

100uM random primer – Biolabs #1254S (aliquots of 10 μ M stored)

DEPC-treated water – prepared in lab

5X first strand buffer – Invitrogen- P/N y02321 (aliquots of 20 μ l stored)

0.1M DTT – Invitrogen -- P/N y00147 (aliquots of 20 μ l stored)

RNase OUT – Invitrogen- P/N 100000840

Reverse Transcriptase III - Invitrogen 18080-093

Protocol:

1. First strand cDNA synthesis reaction. Primer-dNTP reaction mixture:

	<u>1 reaction</u>	<u>5 reactions</u>
10 mM dNTP	1.0 μ l	5.0 μ l
10 μ M Random primer	0.5 μ l	2.5 μ l
DEPC water	8.5 μ l	32.5 μ l
Total	9.5 μ l	47 μ l

2. 9.5 μ l of total mix was dispensed in microcentrifuge tubes.

3. 2000 ng of RNA was added.

4. Mixture was heated at 70 °C for 3 minutes and transferred to ice immediately (this is to break secondary structures of RNA).

5. Reaction mixture with Reverse transcriptase:

	<u>1 reaction</u>	<u>5 reactions</u>
5X First strand buffer	4.0 μ l	20 μ l
0.1 M DTT	1 μ l	5 μ l
RNase out	0.2 μ l	1 μ l
Reverse transcriptase	0.2 μ l	1 μ l

6. 5.4 μ l reaction mixture was added to each tube containing RNA mix and incubated:

Temperature	Time
50 °C	45 minutes
65 °C	10 minutes

7. Synthetic cDNA was stored at -80°C.

12. *In vitro* transcription

1. DNA template 200 ng-(5'-GGGGCGTAATACGACTCACTATAGGGCGTGAGGTT GGCGCGCCCTCCTACAATTATTTGTGGCGACTGGGCAGCGACACTGAACA-3')

1X T7 reaction buffer, 1mM rNTP mix, 1 U RNase OUT, 1 U T7 RNA polymerase (NEB M0251S). Reactions were incubated at 37 °C for 2 hours and run on a 1.5% agarose gel to quantify the amount of RNA product.

13. Detection of *HAC1* mRNA splice variants

1. PCR master mix for testing the *HAC1* mRNA splicing

PCR super mix (Invitrogen)	44 µl
10 µM Primer omd 1225 (5'-CGCAATCGAACTTGGCTATCCCTACC-3')	2 µl
10 µM Primer omd 1226 (5'-CCCACCAACAGCGATAATAACGAG-3')	2 µl
Synthetic cDNA	2 µl

PCR conditions:

Temperature	Time	
94 °C	4 minutes	
94 °C	1 minute	} 20 cycles
55 °C	45 Sec	
72 °C	30 Sec	
72 °C	5 minutes	
4 °C	∞	

2. 10 µl PCR products were separated on a 1.5 % DNA gel.
3. Quantities of *HAC1_s* and *HAC1_u* were measured using ImageJ. Percent splicing was calculated as $Hac1_s / (HAC1_s + HAC1_u) * 100\%$.

14. β -galactosidase assay

Reagents:

1. Z-buffer
2. ONPG (o-nitrophenyl- β -D-galactopyranoside) stock solution.

ONPG	4 g
Z- buffer	1000 ml

Filter sterilized, aliquoted and stored at -20°C .

3. β -galactosidase breaking buffer
4. 1M sodium carbonate (5.3 g in 50 ml water)

Protocol:

1. Yeast cells were grown in minimal media till O.D. = 0.6. Cells were treated with 5mM DTT for 30 minutes to 2 hours as required.
2. Cultures were harvested, cells washed with TE and transferred to microcentrifuge tubes. Cells can be stored at -20°C or subjected to breaking using breaking buffer.
3. 200 μl of β -galactosidase breaking buffer was added in cell pellet (5 μl β -ME was added in 10 ml lysis buffer) on ice.
4. About 100 μl of zirconium beads was added, tubes were vortexed in 4°C for 10 min, spun down at 4°C for 10,500 X g , 5 min.
5. Supernatant was transferred into a clean tube.
6. ONPG and Z-buffer aliquots were thawed at 28°C for at least 1 hour.
7. 2 μl of protein sample was added to 1 ml of 1X Bradford reagent. A_{600} for each sample was recorded.

8. 1ml Z-buffer was added to 5 ml glass test tube and equilibrated at 28°C water bath.
(Three tubes per sample)
9. 25µl protein supernatant was added, briefly vortexed to mix.
10. 200 µl ONPG was added and vortexed. Time was recorded.
11. Tubes were incubated in 28°C as it takes 5-30 minutes for the of yellow color to develop. Reaction was stopped after yellow color saturated by adding 500 µl of 1 M sodium carbonate.
12. A₄₂₀ was recorded for each sample.
13. The β-galactosidase units are calculated by using the following formula:

$$\text{Beta galactosidase Units} = \frac{(\text{OD}_{420} \times 1000)}{\text{Concentration} \times 1.7 \times 0.0045 \times \text{time (min)} \times \text{volume (}\mu\text{l)}}$$

OD₄₂₀ = Take 1 ml of assay reaction mixture to read the OD₄₂₀

Concentration = 1 µl /protein concentration, µg/ml

Time (min) = Incubation time (20 min)

Volume (µl) = 25 µl

15. Protein purification from Yeast cells

Reagents:

Breaking buffer (40 ml) (prepared under cold conditions)

1M Tris-Cl (pH= 7.5)	800 µl
2. 5 M NaCl	8 ml
Ammonium sulfate	1.6 g
100 mM PMSF (in ethanol)	400 µl

Protease inhibitor tablet	1
(Thermo Scientific A32963)	
25 % Triton X-100	40 μ l
Water to volume	40 ml

20 ml buffer was kept aside for washing agarose beads after immunoprecipitation.

To the rest 20 ml, the following phosphatase inhibitors were added:

Sodium fluoride	1 mg
Sodium orthovanadate	1 mg
β - Glycerophosphate	150 mg

Protocol:

1. 750 μ l breaking buffer with phosphatase inhibitors were added to cells. Cells were thawed on ice.
2. Glass beads were added to the 200 μ l mark. Cells were disrupted by vortexing in 4°C for 10 minutes. Tubes were centrifuged at 10,500 X g for 10 minutes.
3. Supernatant was transferred to a fresh tube. 500 μ l breaking buffer was added and the cells were disrupted under the same conditions.
4. Tubes were centrifuged at 10,500 X g for 10 minutes. Supernatant was pooled in a single tube.
5. Bradford assay for protein quantification: 1ml 1 X Bradford reagent was dispensed in microcentrifuge tubes. 5 μ l cell lysate was added to 1 ml of Bradford reagent. OD₆₀₀ was recorded. OD₆₀₀ = 0.1 is equivalent to 1 μ g of protein.

6. 100 μ l 50% agarose bead (slurry) was equilibrated with the breaking buffer by washing the beads 3 times in 500 μ l breaking buffer. Centrifugation was carried out at 4°C 270 X g for 1 minute.
7. Cell lysate was added to the equilibrated beads and kept in the nutator shaker (Clay Adams 421105) for 1 hour at 4°C.
8. To remove unbound protein, the beads were washed either in microcentrifuge tubes or in columns (BioRad PolyPrep Columns 7311550) with the buffer without phosphatase inhibitors. Beads were washed a minimum of 5 times.
9. Protein was eluted in 100 μ l elution buffer:

50 mM Tris pH= 8.00, 10% glycerol	900 μ l
Flag peptide/ reduced Glutathione	1 mg/ 3.5 mg
1 M DTT	100 μ l
10. 100-150 μ l of elution buffer was added to washed beads. Incubated in ice for 10 minutes with intermittent tapping. Centrifuged at 10,500 X g for 1 minute at 4°C. 5 μ l of elute was used to measure protein concentration using Bradford reagent.
11. ~0.5 μ g protein was mixed with 2X or 3X SDS dye, heated for 5 mins and separated on SDS-PAGE.

16. Site Directed Mutagenesis (ABM SDM kit E088)

Primers were designed to incorporate diagnostic restriction site.

Recently purified plasmid DNA was used (this ensures higher success rates.)

PCR reaction:

	Experiment	Control
Plasmid template (10ng/ μ l)	2 μ l	2 μ l
Primer 1 (10 μ M)	1 μ l	0
Primer 2 (10 μ M)	1 μ l	0
2 X PCR Mix	20 μ l	20 μ l
Water	16 μ l	18 μ l

Extension time was set according to template size and PCR run for 30 cycles. PCR products were run in DNA gel to check for amplification.

PCR treatment:

0.5 μ l Assembly Enhancer and 1 μ l Cloning Optimizer was added to 40 μ l PCR.

Reaction was set up for 5 mins at 37°C followed by 20 mins at 80°C.

10 μ l 2X Ligation Free Master mix was added to 10 μ l treated PCR and incubated at 50°C for 15 mins.

2 μ l was used for electroporation.

Transformants were selected on appropriate Antibiotics. In case of extremely high transformation efficiency, the ligations mixtures were treated with DpnI followed by electroporation.

Plasmids were digested with diagnostic restriction sites, followed by sequencing to confirm mutation(s).

17. Electrophoretic Mobility Shift Assay (EMSA)

Reagents:

8% non-denaturing polyacrylamide gel (2 gels)

40% polyacrylamide	4 ml
10X TBE buffer	11.3 ml
10 % APS	0.2 ml
Water	4.5 ml
TEMED	10 μ l

Binding buffer (stock)

100 mM Tris-HCl (pH 7.0)
200 mM MgCl ₂

Loading Dye

50 % Glycerol
1 mg/ml Xylene Cyanol

Protocol:

1. Protein and fluorescein tagged RNA was thawed in ice.
2. Binding buffer was prepared for 5 or 10 reactions:

	5 reactions	10 reactions
100 mM Tris-HCl pH 7.0	20 μ l	40 μ l
200 mM MgCl ₂	1.25 μ l	2.5 μ l

3. EMSA reaction was set up as follows:

<u>Reaction:</u>	1	2	3
RNA oligomer	5 μ l	5 μ l	0
Protein	0	5 μ l	5 μ l
Buffer	4 μ l	4 μ l	4 μ l
Water	21 μ l	16 μ l	21 μ l

4. Tubes were incubated in 30°C for 45 mins with taping every 15 mins.
5. 5X loading dye was added and samples were separated on TBE gel with the following running conditions:

20 mins at 120 V at RT, then 3 hrs at 120 V at 4°C.

6. Fluorescein tagged RNA was visualized under UV and protein bands were visualized by staining and destaining the protein gel.

18. Protein purification from BL21 bacterial cells

A. GST-tagged protein purification

1. Cells were grown in LB broth with Ampicillin at 37°C. At O.D.₆₀₀ ~0.6, 1 mM IPTG was added and culture was grown in RT overnight. Cells were collected in 50 ml falcon tubes (Corning 352070), centrifuged and media discarded. Cells were either processed for protein purification or stored at -20°C.
2. 50 ml 10X PBS cell lysis buffer was prepared with 1 Protease inhibitor tablet.
3. Following stock solutions were prepared:

DNase	10 mg/ml
Lysozyme	10 mg/ml
DTT 1 M	1 ml
MgCl ₂	1 ml

4. To each tube containing cells, the following were added:

2X PBS lysis buffer	2 ml
DNase	20 μ l
Lysozyme	20 μ l
DTT 1 M	20 μ l
MgCl ₂	20 μ l

5. Cells were either thawed in this buffer or dissolved by pipetting gently.

6. To the rest 30 ml buffer 300 μ l 25 % Triton X-100, and 300 μ l 1 M DTT was added.

This served as the equilibration and washing buffer for agarose beads.

7. Cells were sonicated 6-8 times to ensure cell lysis. Frothing avoided.

8. Cell debris was separated by centrifugation at 11,350 X g for 15 mins at 4°C.

9. Clear cell lysate was pooled in a falcon tube and protein concentration measured by using Bradford reagent.

10. Glutathione conjugated agarose beads (from Gold Bio G-250) were equilibrated with the buffer by washing the beads 3 times in 500 μ l buffer. Centrifugation was carried out at 4°C 270 X g for 1 minute. [Gold Bio GST beads capacity = 8 mg GST protein / 1 ml gel]

11. Cell lysate was added to the equilibrated beads and kept in the nutator shaker for 1 hour at 4°C. Either falcon tubes can be used or Bio Rad columns (731-1550).

12. To remove unbound protein, the beads were washed either in microcentrifuge tubes or in columns (BioRad) with the buffer. Beads were washed a minimum of 6 times.

13. Protein was eluted in 300 μ l elution buffer:

50 mM Tris pH= 8.00, 10% glycerol	900 μ l
Reduced Glutathione	3 mg
1 M DTT	100 μ l

300 µl of elution buffer was added to washed beads. Incubated in ice for 10 minutes with intermittent tapping. Centrifuged at 10,500 X g for 1 minute at 4°C. 5µl of elute was used to measure protein concentration using Bradford reagent.

14. ~0.5 µg protein was mixed with 2X or 3X SDS dye with β-ME, heated for 5 mins and separated on SDS-PAGE.
15. Gel was fixed (50% methanol and 10% glacial acetic acid), stained for 20 minutes in a staining solution (0.1% Coomassie Brilliant Blue R-250, 50% methanol and 10% glacial acetic acid) and de-stained overnight in a de-staining solution (40% methanol and 10% glacial acetic acid) to visualize protein bands.

B. His-tagged protein purification

1. Cells were grown in LB broth with Ampicillin at 37°C. At O.D. ~0.6, 1 mM IPTG was added and culture was grown in RT overnight. Cells were collected in 50 ml falcon tubes, centrifuged and media discarded. Cells were either processed for protein purification or stored at -20°C.
2. Lysis buffer was prepared using 1X NaHPO₄ (50 mM) and NaCl (300 mM) pH 8.0 with 1 Protease inhibitor tablet (per 40 ml) and 10 mM Imidazole.
3. 5 ml lysis buffer was added to thaw the cells.
4. Cells were sonicated 6-8 times to ensure cell lysis. Frothing avoided.
5. Cell debris was separated by centrifugation at 11,350 X g for 15 mins at 4°C.
6. Clear cell lysate was pooled in a falcon tube and protein concentration measured by using Bradford reagent.

7. Ni-NTA conjugated agarose beads (ThermoFisher 88221) were equilibrated with the buffer by washing the beads 3 times in 500 μ l buffer. Centrifugation was carried out at 4°C 270 X g for 1 minute.
8. Cell lysate was added to the equilibrated beads and kept in the nutator shaker for 1 hour at 4°C. Either falcon tubes can be used or Bio Rad columns (731-1550).
9. To remove unbound protein, the beads were washed either in microcentrifuge tubes or in columns (BioRad) with the same buffer but containing 20 mM Imidazole. Beads were washed a minimum of 6 times.
10. Protein was eluted in 300 μ l elution buffer:

50 mM Tris pH= 8.00, 10% glycerol	900 μ l
Imidazole	34 mg
1 M DTT	100 μ l

300 μ l of elution buffer was added to washed beads. Incubated in ice for 10 minutes with intermittent tapping. Centrifuged at 10,500 X g for 1 minute at 4°C. 5 μ l of elute was used to measure protein concentration using Bradford reagent.
11. ~0.5 μ g protein was mixed with 2X or 3X SDS dye with β -ME, heated for 5 mins and separated on SDS-PAGE.
12. Gel was fixed, stained and destained to visualized protein bands.

19. Proteolysis

1 ml protein was incubated with 100 μ l 10 X HRV 3C Protease Buffer and 10 μ l Protease (ThermoFisher 88946) and incubated in 4°C for 1 hour. Mixture was dialyzed.

20. Dialysis

1. Protein with protease mix was injected into a cassette (Thermo Scientific 66380)
2. Cassette kept in dialysis buffer (50 mM Tris-HCl pH 8.0, 10 % glycerol, 1mM DTT) overnight at 4°C.
3. Sample was taken out next morning and stored in -80°C or separated in SDS-PAGE.

21. *In-vitro* radiolabeled kinase assay

Reagents:

5X Kinase Buffer (aliquoted and stored at 4°C)

1 M Tris-HCl pH 8.0	2 ml
1 M KCl	5 ml
1 M MgCl ₂	2.5 ml
50 % Glycerol	20 ml
Water to volume	100 ml

ATP [γ -³²P] (gloves and lab coat worn at all times with ionizing detector badge)

SDS-PAGE gel was cast on disposable cassettes (Novex mini gel 1.5 mm cassettes NC2015).

Protocol:

1. Purified kinase, substrate and ATP [γ -³²P] were thawed in ice.
2. Geiger counter was kept ON, to monitor ionizing radiation throughout workflow.

3. Reactions were prepared in the following manner:

Reaction	Kinase	Substrate	5 X KB + 0.5 μ l 32 P	H ₂ O
1	5 μ l	0	4 μ l	11 μ l
2	0	5 μ l	4 μ l	11 μ l
3	5 μ l	5 μ l	4 μ l	6 μ l

4. After carefully adding proteins and buffer with ATP, the tubes were centrifuged and tapped a few times to mix.
5. Reaction was incubated in RT for 20 mins.
6. Reaction was stopped using 5 μ l 5 X SDS dye containing β -ME.
7. Samples were heated at 95°C, centrifuged, and loaded on a denaturing gel.
8. 1/3 of the gel was run at 120 V for 90 mins.
9. Gel was fixed, stained and destained to visualize protein bands.
10. Gel was dried (BioRad Gel Dryer 583) for 1.5 hours at 80°C.
11. Dried gel was exposed on a Phosphorimager for 30 mins.
12. The Phosphorimager was scanned using the STORM 860 Molecular Imager.

22. Membrane fractionation

1. Yeast cells were harvested and lysed by glass beads in a microfuge tube with 400 μ l of lysis buffer (25mM Tris-phosphate pH 6.7, 1mM β -mercaptoethanol (β -ME), 1mM PMSF and 1 protease tablet per 25 ml buffer).
2. The whole-cell lysate was clarified by centrifugation at 5000 rpm (2655 X g) for 10 minutes at 4°C. The clear supernatant was divided into two separate tubes (150 μ l each).
3. The first tube with 150 μ l of lysate was used to precipitate the total soluble and insoluble proteins as follows. 37.5 μ l of 100% TCA was added and kept in ice for 10

- minutes. Total protein was collected by centrifugation at 2400 X g for 10 minutes and solubilized in a buffer (40 μ l of 1M Tris-HCl pH 8.0 and 10 μ l of 5X SDS-dye) at 90°C. This fraction was considered as the “input”.
4. The second tube containing 150 μ l of lysate was further centrifuged at 14,000 rpm (20,817 X g) for 30 minutes at 4°C in order to pellet the insoluble fraction (the membrane fraction).
 5. The supernatant containing the soluble proteins was then collected in a fresh tube and total protein was precipitated and solubilized in a buffer as described above (the soluble protein fraction).
 6. The pellet containing the insoluble membrane fraction was solubilized in a buffer (40 μ l of Tris-HCl pH 8.0 and 10 μ l of 5X SDS-dye) at 90°C.
 7. The “input”, “soluble” and “insoluble” protein fractions were subjected to Western analysis.
 8. The pellet containing the membrane fraction was also solubilized in a buffer (50mM Tris-HCl pH 8.0, and 1mM DTT) containing 0, 0.5% or 1% of TritonX-100. The pellet and supernatant fractions were separated by centrifugation at 20,817 X g for 20 min at 4°C. The pellet and supernatant fractions were then separated on an SDS-PAGE and subjected to Western blot analyses using an anti-Flag antibody.

23. Pull down of biotinylated RNA and protein

1. Yeast cells expressing the 3'-BE-RMB or 5'-RD-RMB were grown in SC-uracil medium, until OD₆₀₀ reached 0.8. Then, 4-thiouracil (20 mM) and DTT (5 mM) were added together and cells were grown for another 3 hours. The 200 ml culture was then harvested and washed with 1X PBS (phosphate buffered saline).
2. Cells were re-suspended in 1X PBS in a 15 cm petri dish and exposed to UV light inside a UV-Stratalinker-1800 (Stratagene), twice for 2.5 minutes each (auto-crosslink setting).
3. Cells were pelleted by centrifugation at 4°C and lysed in 20 mM Tris-HCl, pH 7.4, 1 mM EDTA, 50 mM LiCl, 1% β-mercaptoethanol, 1 mg/ml heparin, 0.5mM phenylmethyl-sulfonyl fluoride (PMSF), 10 mM vanadyl adenosine.
4. The RMB-conjugated RNAs were immobilized on Streptavidin agarose and bound proteins were eluted by 2X SDS dye (100 mM Tris-HCl pH 6.8. 4% SDS. 0.2% bromophenol blue).
5. A fraction of the RNA elution was separated on SDS-PAGE and another fraction was sent to the Center of Biotechnology (Madison, WI, USA) for LC-MS/MS to identify associated proteins.

23. Circular dichroism (CD) spectroscopy (collaboration with Dr. Pokkuluri, Argonne Laboratory, Chicago)

Protein samples were analyzed at a concentration of 0.5 mg/mL in 20 mM sodium phosphate, pH 8.0. CD spectra were collected in 0.1 cm path length quartz cells on a Jasco J-810 Spectropolarimeter. Spectra in the wavelength range of 190–360 nm were collected using the following acquisition parameters: 0.1 nm steps, 1 nm bandwidth, 4 s response, 100 millidegree

sensitivity, and 50 nm/min scanning speed with an accumulation of 3. Secondary structure composition was estimated from the analysis of the CD spectrum by the BeStSel web server²⁰⁶ (wavelength range used for analysis is 190-250 nm).

24. *In vivo* imaging of yeast cells by a confocal microscope

1. Cells were grown under ER stress conditions using DTT.
2. Cells were pelleted and resuspended in minimal media. An aliquot of cells was used for *in vivo* imaging studies.
3. Images were recorded using Leica TCS SP2 confocal microscope equipped with HCX PL APO 63X/1.2 NA water immersion objective lens.
4. The GFP was excited at 458 nm, and emissions were recorded at 466-526 nm.

25. *In vivo* imaging of yeast cells by a two-photon micro-spectroscopy (collaboration with Dr. Valerica Raicu, Physics, UWM)

1. We used an optical micro-spectroscopy (OptiMiS, Aurora Spectral Technologies, Milwaukee, WI). The OptiMiS consists of a two-photon microscope with spectral resolution²⁰⁷ and a Nikon Ti-E Inverted Microscope (Nikon Instruments Inc., New York) equipped with a high NA (=1.45) and 100x objective. A tunable femtosecond Ti:Sapphire laser (MaiTai™ HR, Newport) was used to provide light of wavelength of 930 nm in order to excite yeast cells expressing the YFP and/or GFP.

2. About 200 μL of yeast cell suspension was placed onto 35 mm glass-bottom dishes (Cellvis D35-14-1.5-N, California), allowed to settle for 5 minutes, washed with 1 mM KCl and then taken to the microscope for imaging.
3. Spectrally resolved images were acquired for emission wavelengths ranging from 400 nm to 600 nm with a resolution of 5 nm using an average laser power of 400mW for the entire line of 500 pixels, with a line-integration time²⁰⁷ of 100ms.
4. Spectral unmixing was then performed on acquired images of co-expressed the Ire1-YFP and Pal2-GFP using separately acquired elementary spectra of GFP and YFP, using a procedure previously described²⁰⁸.
5. Briefly, the average emission spectra obtained from several cells containing only the GFP or the YFP fluorescent species were normalized to their maximum values to obtain elementary spectra of GFP and YFP, respectively.
6. An automatic computer algorithm was used to separate the composite spectra originating from co-expressing cells.
7. Intensity maps were generated for both GFP and YFP signals, and YFP images were filtered to remove intensity counts less than 750 A.U. to isolate and distinguish relatively bright Ire1-YFP foci.
8. Individual maps of the Ire1-YFP and Pal2-GFP fluorescence were assigned false colors and then overlaid to determine co-localization.
9. The average number of foci per cell and the number of cells displaying foci were calculated for samples both treated and untreated with DTT.

10. For punctate counting experiments of GFP in yeast strains (WT and *pal1Δ pal2Δ*) treated with DTT, the same imaging system described above was employed using excitation light of 800nm and an average laser power of 500mW for the entire line of 500 pixels. Elementary spectra separately obtained for ND-GFP and auto-fluorescent signals were used to unmix composite spectra.
11. An algorithm written in MATLAB filtered the intensity maps such that GFP punctate become visible above the nearly uniform fluorescence background. The first filter removed pixels that showed GFP intensity lower than 50 A.U. (to exceed background level) or more than 500 A.U., to remove cells that have so much GFP expression that would saturate any information from punctate. A second filter required a minimum ratio of GFP to auto-fluorescent intensity greater than 6, in order to avoid incorrect assignment of auto-fluorescent to the GFP channel due to possible errors in spectral unmixing. The use of auto-fluorescent maps alongside with GFP also leads to correct identification of cell boundaries.
12. We required that a minimum of 3 pixels be immediately adjacent to one another in the filtered image in order for it to be counted as a punctate. The average number of punctate per cell was computed in the presence of DTT.

APPENDIX I

Table 3 List of yeast strains used in this study

Chapter 2

Yeast strain	Genotype	Reference
WT(BY4741)	MATa his3-Δ1 leu2-Δ0 met5-Δ0 ura3-Δ0	Research Genetics
<i>kin1Δkin2Δ</i>	MATa his3-Δ1 leu2-Δ0 met5-Δ0 ura3-Δ0 <i>kin1::NatMX kin2::KanMX</i>	Anshu et al. (2015)
<i>hac1Δkin1Δ</i>	MATa his3-Δ1 leu2-Δ0 met5-Δ0 ura3-Δ0 <i>hac1::NatMX kin1::kanMX</i>	Anshu et al. (2015)
<i>ste2Δ</i>	MATa leu2-3,112 ura3-52 his3-Δ1 trp1 <i>ste2::leu2 sst1-Δ5</i>	Stoneman et al. (2017)

Chapter 3

Standard *S. cerevisiae* media was used to grow and analyze the yeast strains. To construct the *pal1Δ pal2Δ* strain, we first replaced The *KanMX* cassette in the *pal1::KanMX* strain with the *NatMX* gene by the standard PCR-mediated gene disruption protocol. In the resulting *pal1::NatMX* strain, the *PAL2* gene was disrupted by *KanMX* to generate the double deletion strain. To generate the *kin1Δ kin2Δ snf1Δ* strain we first disrupted the *KanMX* gene of the *snf1Δ* strain (*MATa his3-Δ1 leu2-Δ0 met5-Δ0 ura3Δ0 snf1::KanMX*, yeast deletion collection) with the *hphMX4* cassette (to generate *MATa his3-Δ1 leu2-Δ0 met5-Δ0 ura3-Δ0 snf1::hphMX*). The genomic DNA of this strain (*snf1::hphMX*) was used as a template to amplify the *hphMX* cassette using primers annealing ~200-bases upstream and downstream of the *SNF1* open reading frame. The amplified

PCR product was used to disrupt the *SNF1* gene of the *kin1Δ kin2Δ* strain (*MATa his3-Δ1 leu2-Δ0 met5-Δ0 ura3-Δ0 kin1::NatMX kin2::kanMX*).

Yeast strain	Genotype	Reference
<i>WT</i>	<i>MATa his3-Δ1 leu2-Δ0 met5-Δ0 ura3-Δ0</i>	Deletion collection
<i>ire1Δ</i>	<i>MATa his3-Δ1 leu2-Δ0 met5-Δ0 ura3-Δ0 ire1::kanMX</i>	Deletion collection
<i>hac1Δ</i>	<i>MATa his3-Δ1 leu2-Δ0 met5-Δ0 ura3-Δ0 hac1::kanMX</i>	Deletion collection
<i>pal1Δ</i>	<i>MATa his3-Δ1 leu2-Δ0 met5-Δ0 ura3-Δ0 pal1::kanMX</i>	Deletion collection
<i>pal2Δ</i>	<i>MATa his3-Δ1 leu2-Δ0 met5-Δ0 ura3-Δ0 pal2::kanMX</i>	Deletion collection
<i>pal1Δ pal2Δ</i>	<i>MATa his3-Δ1 leu2-Δ0 met5-Δ0 ura3-Δ0 pal1::natMX, pal2::kanMX</i>	This study
<i>kin1Δ kin2Δ</i>	<i>MATa his3-Δ1 leu2-Δ0 met5-Δ0 ura3-Δ0 kin1::NatMX kin2::kanMX</i>	Anshu et al. (2015)
<i>snf1Δ</i>	<i>MATa his3-Δ1 leu2-Δ0 met5-Δ0 ura3-Δ0 snf1::kanMX</i>	Deletion collection
<i>kin1Δ kin2Δ snf1Δ</i>	<i>MATa his3-Δ1 leu2-Δ0 met5-Δ0 ura3-Δ0 kin1::NatMX kin2::kanMX snf1::HphMx</i>	This study
<i>PAL2-GFP: NatMX6</i>	<i>MATa leu2 ura3-52 trp1 his3Δ200 GAL2 PAL2-GFP: NatMX6</i>	Moorthy et al., 2019

Table 4 List of plasmids used in this study.

Chapter 2

Plasmid	Details	Reference
D1	pRS313, low copy <i>HIS3</i> vector	Low copy vector
D8	pRS426, high copy <i>URA3</i> vector	High copy vector
D18	pEMBLyeX4 expression vector	High copy vector
D197	Kin2 in 2 μ <i>URA3</i> vector	Patrick Brennwald
D619	Kin1 in pBG1805 expression vector	Benjamin Turk
D1163	pGEX-2T-TEV HTa expression vector	Kean et al. (2011)
D1400	Kin2 (1-1147) in D18	This study
D1129	Kin2 (94-526) in D18	Anshu et al. (2015)
D1186	Kin2 (94-400) in D18	This study
D1184	Kin2 (94-440) in D18	This study
D1182	Kin2 (94-480) in D18	This study
D1220	Kin2 (94-526)- Δ (400-440) in D18	This study
D1191	Kin2 (94-526)- Δ (440-480) in D18	This study
D1742	Kin2-(94-510) in D18	This study
D1181	Kin2-(94-500) in D18	This study
D1221	Kin2 (94-526)- D ₂₄₈ A in D18	This study
D1239	Kin2 (94-526)-Y ₂₇₅ A,T ₂₈₁ A in D18	This study
D1514	Kin2 (94-526)-Y ₂₇₅ A,T ₂₈₁ E in D18	This study
D1353	Kin1-KD in D18	This study
D1534	Kin1 (115-515)-Y ₂₉₄ F,S ₂₉₆ A,T ₃₀₂ A in D18	This study

D1535	Kin1 (115-515)-Y ₂₉₄ F,S ₂₉₆ A,T ₃₀₂ E in D18	This study
D1507	Kin2 (94-526)-K ₁₂₈ R in D18	This study
D1386	Kin2 (60-526) Δ40, ΔKI in D1163	This study
D1347	Kin2 (60-526) Δ40, ΔKI, T ₂₈₁ E in D1163	This study
D1688	Hac1 WT in D1	This study
D1689	Hac1 GG1143-1144CC in D1	This study
D1459	GFP-Kin2 (1-526) in D8	This study
D1258	GFP-KA1 in D8	This study
D1882	Kin1 (115-430) in D18	This study
D1963	Ste2-YFP in a high copy <i>TRPI</i> vector	Stoneman, et al. (2017)
D1237	Kin2 (94-526)-Y ₂₇₅ A in D18	This study
D1238	Kin2 (94-526)-T ₂₈₁ A in D18	This study
D1570	Kin2 (94-526)-Y ₂₇₅ E,T ₂₈₁ A in D18	This study
D852	Kin2 in D8	This study
D853	Kin2-D ₂₄₈ A in D8	This study
D1950	Kin2-T ₂₈₁ A in D8	This study
D1949	Kin2-Y ₂₇₅ A in D8	This study
D1946	Kin2-Y ₂₇₅ A,T ₂₈₁ A in D8	This study
D1947	Kin2-Y ₂₇₅ E,T ₂₈₁ A in D8	This study
D1948	Kin2-Y ₂₇₅ A,T ₂₈₁ E in D8	This study
D1968	Kin1 (115-515)-D ₂₆₉ A in D18	This study
D1955	Kin1 (115-515)-S ₂₉₆ E,T ₃₀₂ A in D18	This study
D1942	Kin2 (60-526) Δ40, ΔKI, Y ₂₇₅ E in D1163	This study

D1379	Kin1 (58-515) Δ KI in D1163	This study
D1380	Kin1 (58-515) Δ KI, T ₃₀₂ E in D1163	This study

Chapter 3

Plasmid	Description	Reference
D3	pRS315, low-copy-number. <i>LEU2</i> vector	Lab collection
D4	pRS316, low-copy-number. <i>URA3</i> vector	Lab collection
D8	pRS426, high-copy-number. <i>URA3</i> vector	Lab collection
D18	pEMBLyeX4 expression vector	Lab collection
D23	pET15b expression vector	Lab collection
D49	UPRE-LacZ in <i>URA3</i> vector	Lab collection
D1163	pGEX-2T-TEV HTa expression vector	Lab collection
D774	Hac1 bipartite element with Biotin aptamer- under ADH1 promoter and terminator in p1379	This study
D844	Hac1 5'-UTR-intron with Biotin aptamer- under ADH1 promoter and terminator in p1378	This study
D1951	HAC1 exon1 in D4	This study
D1096	Pal2-(77-364) in D23	This study
D1525	Ypt1 in D23	This study
D1536	Pal2 (1-366) with intron in D4	This study
D1537	Pal2 (1-366) in D4	This study
D1538	Pal2 (65-366) in D4	This study

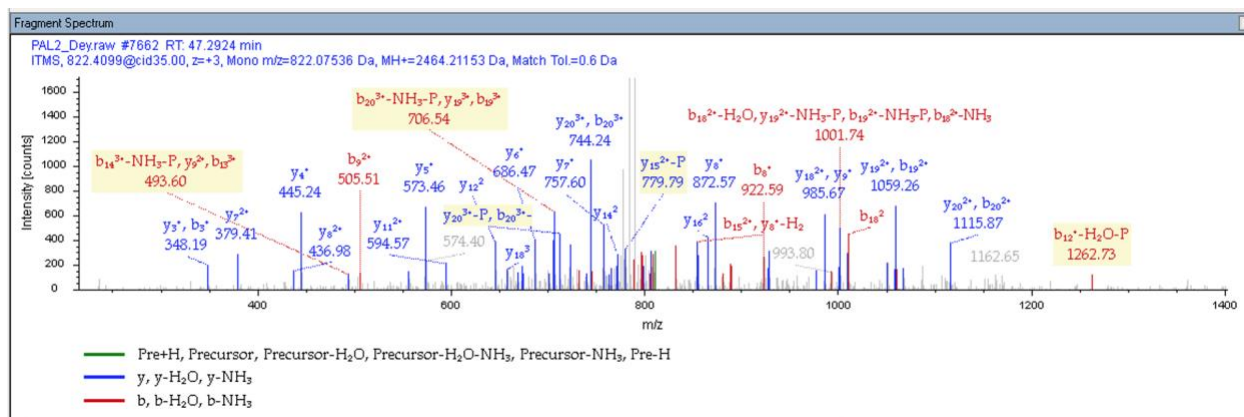
D1539	Pal2 (135-366) in D4	This study
D1129	Kin2 (94-526) in D18	Ghosh et al. (2018)
D619	Kin1 in pBG1805	MORF collection
D624	Kin2 in pBG1805	MORF collection
D665	Eap1 in pBG1805	MORF collection
D676	Kip3 in pBG1805	MORF collection
D651	Svl3 in pBG1805	MORF collection
D675	Pal2 in pBG1805	MORF collection
D666	Sec9 in pBG1805	MORF collection
D647	Mlf3 in pBG1805	MORF collection
D109	PKR wild type in p2734	Lee et al. (2015)
D2199	Pal1 (162-499) in D23	This study
D1637	Pal1 (162-499) T323A in D23	This study
D1443	Pal2 (65-366) S221A in D23	This study
D1428	Pal2 (65-366) S222A in D23	This study
D2200	Pal2 (65-366) S222A, T224A in D23	This study
D2201	Pal2 (65-366) T223A, T224A, T225A in D23	This study
D2202	Pal2 (65-366) S222A, T223A, T224A, T225A in D23	This study
D1427	Pal2 (65-366) S221A, S222A in D23	This study
D1386	Kin2-(60-526)- Δ 40, Δ KI in D1163	Ghosh et al. (2018)
D1347	Kin2-(60-526)- Δ 40, Δ KI, T281E in D1163	Ghosh et al. (2018)
D1551	Pal2 (65-366) S222A in D4	This study
D2142	Pal2 (65-366) T224A in D4	This study

D1559	Pal2 (65-366) S222A, T225A in D4	This study
D2144	Pal2 (65-366) S222A, T223A in D4	This study
D1695	Pal2 (65-366) S222A, T223A, T224A, T225A in D4	This study
D1649	Pal1 (162-499) in D4	This study
D1620	Pal1 (1-499) in D4	This study
D2264	Pal2 (65-366) S222E, T223E, T224E, T225E in D4	This study
D2239	HAC1-NRE in D4	This study
D995	ND-GFP2 in D3	Anshu, et.al. 2015
D800	Ire1-YFP in D8	This study

APPENDIX II

Mass spectrometry results to identify phosphorylated peptide on Pal2. Shown below is the MS/MS spectrum of the Pal2 phospho-peptide.

Ion Series	Phosphorylation Losses			Neutral Losses	Multiple Neutral Losses	Precursor Ions			
#1	b ⁺	b ²⁺	b ³⁺	Seq.	y ⁺	y ²⁺	y ³⁺	#2	
1	72.04439	36.52583	24.68631	A				22	
2	235.10772	118.05750	79.04076	Y	2393.17483	1197.09105	798.39646	21	
3	348.19178	174.59953	116.73545	L	2230.11150	1115.55939	744.04202	20	
4	495.26020	248.13374	165.75825	F	2117.02744	1059.01736	706.34733	19	
5	609.30312	305.15520	203.77256	N	1969.95903	985.48315	657.32453	18	
6	737.39809	369.20268	246.47088	K	1855.91610	928.46169	619.31022	17	
7	808.43520	404.72124	270.14992	A	1727.82114	864.41421	576.61190	16	
8	922.47813	461.74270	308.16423	N	1656.78402	828.89565	552.93286	15	
9	1009.51016	505.25872	337.17490	S	1542.74109	771.87419	514.91855	14	
10	1176.50852	588.75790	392.84102	S-Phospho	1455.70907	728.35817	485.90787	13	
11	1277.55619	639.28174	426.52358	T	1288.71071	644.85899	430.24175	12	
12	1378.60387	689.80557	460.20614	T	1187.66303	594.33515	396.55919	11	
13	1479.65155	740.32941	493.88870	T	1086.61535	543.81131	362.87663	10	
14	1592.73561	796.87145	531.58339	L	985.56767	493.28747	329.19407	9	
15	1707.76256	854.38492	569.92570	D	872.48361	436.74544	291.49939	8	
16	1778.79967	889.90347	593.60474	A	757.45666	379.23197	253.15707	7	
17	1891.88374	946.44551	631.29943	I	686.41955	343.71341	229.47803	6	
18	2019.97870	1010.49299	673.99775	K	573.33549	287.17138	191.78335	5	
19	2117.03146	1059.01937	706.34867	P	445.24052	223.12390	149.08503	4	
20	2231.07439	1116.04083	744.36298	N	348.18776	174.59752	116.73410	3	
21	2318.10642	1159.55685	773.37366	S	234.14483	117.57605	78.71980	2	
22				K	147.11280	74.06004	49.70912	1	



Bibliography

1. Jeschke, G. R. *et al.* Substrate priming enhances phosphorylation by the budding yeast kinases Kin1 and Kin2. *J. Biol. Chem.* **293**, 18353–18364 (2018).
2. Mann, M. & Jensen, O. N. Proteomic Analysis of post-translational modifications. *Nature* **21**, 255–261 (2003).
3. Graves, J. D. & Krebs, E. G. Protein phosphorylation and signal transduction. *Pharmacol. Ther.* **82**, 111–121 (1999).
4. Manning, G., Plowman, G. D., Hunter, T. & Sudarsanam, S. Evolution of protein kinase signaling from yeast to man. *Trends Biochem. Sci.* **27**, 514–520 (2002).
5. Manning, G., Whyte, D. B., Martinez, R., Hunter, T. & Sudarsanam, S. The protein kinase complement of the human genome. *Science (80-.)*. **298**, 1912–1934 (2002).
6. Ardito, F., Giuliani, M., Perrone, D., Troiano, G. & Muzio, L. Lo. The crucial role of protein phosphorylation in cell signaling and its use as targeted therapy. *Int. J. Mol. Med.* **40**, 271–280 (2017).
7. Burnett, G. & Kennedy, E. The Enzymatic Phosphorylation of Proteins. *J. Biol. Chem.* **211**, (1954).
8. Ponomarenko, E. A. *et al.* The Size of the Human Proteome: The Width and Depth. *Int. J. Anal. Chem.* **2016**, (2016).
9. Duong-Ly, K. C. & Peterson, J. R. The human kinome and kinase inhibition as a therapeutic strategy. *Curr. Protoc. Pharmacol.* **60**, (2013).
10. Hanks, S. K., Quinn, a M. & Hunter, T. The protein kinase family: conserved features and deduced phylogeny of the catalytic domains. *Science* **241**, 42–52 (1988).
11. Taylor, S. S., Keshwani, M. M., Steichen, J. M. & Kornev, A. P. Evolution of the eukaryotic protein kinases as dynamic molecular switches. *Philos. Trans. R. Soc. B Biol. Sci.* **367**, 2517–2528 (2012).
12. Dey, M., Mann, B. R., Anshu, A. & Mannan, M. A. U. Activation of protein kinase PKR requires dimerization-induced cis-phosphorylation within the activation loop. *J. Biol. Chem.* **289**, 5747–5757 (2014).
13. Hunter, T. & Plowman, G. D. The protein kinases of budding yeast: Six score and more. *Trends in Biochemical Sciences* **22**, 18–22 (1997).
14. Knighton, D. R. *et al.* Crystal Structure of the Catalytic Subunit of Cyclic Adenosine Monophosphate-Dependent Protein Kinase. (1991).
15. Knighton, D. R. *et al.* Structure of a peptide inhibitor bound to the catalytic subunit of cyclic AMP dependent protein kinase. *Science (80-.)*. **253**, 414–420 (1991).
16. Hanks, S. K. & Hunter, T. The eukaryotic protein kinase superfamily : kinase (catalytic) domain structure and classification. *FASEB J.* **9**, 576–596 (1995).

17. Huse, M. & Kuriyan, J. The Conformational Plasticity of Protein Kinases. *Cell* **109**, 1–8 (2002).
18. Bossemeyer, D. Protein kinases-structure and function. *FEBS Lett.* **369**, 57–61 (1995).
19. Adams, J. a & Taylor, S. S. Divalent metal ions influence catalysis and active-site accessibility in the cAMP-dependent protein kinase. *Protein Sci.* **2**, 2177–86 (1993).
20. Nolen, B., Taylor, S. & Ghosh, G. Regulation of protein kinases: Controlling activity through activation segment conformation. *Mol. Cell* **15**, 661–675 (2004).
21. Levinson, N. M. *et al.* A Src-like inactive conformation in the Abl tyrosine kinase domain. *PLoS Biol.* **4**, 753–767 (2006).
22. Hubbard, S. R., Mohammadi, M. & Schlessinger, J. Autoregulatory Mechanisms in Protein-tyrosine Kinases. 11987–11990 (1998).
23. Hubbard, S. R. Crystal structure of the activated insulin receptor tyrosine kinase in complex with peptide substrate and ATP analog. *EMBO J.* **16**, 5572–5581 (1997).
24. Vogtherr, M. *et al.* NMR characterization of kinase p38 dynamics in free and ligand-bound forms. *Angew. Chemie - Int. Ed.* **45**, 993–997 (2006).
25. Jura, N. *et al.* Catalytic Control in the EGF Receptor and Its Connection to General Kinase Regulatory Mechanisms. *Mol. Cell* **42**, 9–22 (2011).
26. Dar, A. C., Dever, T. E. & Sicheri, F. Higher-order substrate recognition of eIF2a by the RNA-dependent protein kinase PKR. *Cell* **122**, 887–900 (2005).
27. Skamnaki, V. T. *et al.* Catalytic mechanism of phosphorylase kinase probed by mutational studies. *Biochemistry* **38**, 14718–14730 (1999).
28. Matte, A., Tari, L. W. & Delbaere, L. T. How do kinases transfer phosphoryl groups? *Ann. Diagn. Pathol.* **6**, 413–419 (1998).
29. Tari, L. W., Matte, A., Pugazhenthii, U., Goldie, H. & Delbaere, L. T. J. Snapshot of an enzyme reaction intermediate in the structure of the ATP-Mg²⁺-oxalate ternary complex of Escherichia coli PEP carboxykinase. *Nat. Struct. Biol.* **3**, 355–363 (1996).
30. Tari, L. W., Matte, A., Delbaere, L. T. J. & Goldie, H. Mg²⁺-2⁺ clusters in enzyme-catalyzed phosphoryl-transfer reactions. *Nat. Struct. Biol.* **4**, 990–994 (1997).
31. Schulz, G. E. Binding of nucleotides by proteins. *Curr. Biol.* **2**, 81 (1992).
32. Bossemeyer, D., Engh, R. A., Kinzel, V., Ponstingl, H. & Huber, R. Phosphotransferase and substrate binding mechanism of the cAMP-dependent protein kinase catalytic subunit from porcine heart as deduced from the 2.0 Å structure of the complex with Mn²⁺ adenylyl imidodiphosphate and inhibitor peptide PKI(5-24). *EMBO J.* **12**, 849–859 (1993).
33. Johnson, L. N., Noble, M. E. M. & Owen, D. J. Active and inactive protein kinases: Structural basis for regulation. *Cell* **85**, 149–158 (1996).
34. Arencibia, J. M., Pastor-Flores, D., Bauer, A. F., Schulze, J. O. & Biondi, R. M. AGC protein kinases: From structural mechanism of regulation to allosteric drug development for

- the treatment of human diseases. *Biochim. Biophys. Acta - Proteins Proteomics* **1834**, 1302–1321 (2013).
35. Zhang, H. *et al.* Phosphoprotein analysis using antibodies broadly reactive against phosphorylated motifs. *J. Biol. Chem.* **277**, 39379–39387 (2002).
 36. Bayascas, J. R. *PDK1: The Major Transducer of PI 3-Kinase Actions.* (2010). doi:10.1007/82
 37. Pearce, L. R., Komander, D. & Alessi, D. R. The nuts and bolts of AGC protein kinases. *Nat. Rev. Mol. Cell Biol.* **11**, 9–22 (2010).
 38. Balendran, A. *et al.* PDK1 acquires PDK2 activity in the presence of a synthetic peptide derived from the carboxyl terminus of PRK2. *Curr. Biol.* **9**, 393–404 (1999).
 39. Biondi, R. M. *et al.* Identification of a pocket in the PDK1 kinase domain that interacts with PIF and the C-terminal residues of PKA. *EMBO J.* **19**, 979–988 (2000).
 40. Frödin, M. *et al.* A phosphoserine/threonine-binding pocket in AGC kinases and PDK1 mediates activation by hydrophobic motif phosphorylation. *EMBO J.* **21**, 5396–5407 (2002).
 41. Swulius, M. T. & Waxham, M. N. Ca(2+)/calmodulin-dependent protein kinases. *Cell. Mol. Life Sci.* **65**, 2637–57 (2008).
 42. Bhattacharyya, M., Karandur, D. & Kuriyan, J. Structural Insights into the Regulation of Ca²⁺/Calmodulin-Dependent Protein Kinase II (CaMKII). *Cold Spring Harb. Perspect. Biol.* a035147 (2019). doi:10.1101/cshperspect.a035147
 43. Varjosalo, M. *et al.* The Protein Interaction Landscape of the Human CMGC Kinase Group. *Cell Rep.* **3**, 1306–1320 (2013).
 44. Malumbres, M. Cyclin -dependent kinases. *Nature* **424**, 228–232 (2003).
 45. Morgan, D. O. Principles of CDK regulation. *Nature* **374**, 131–134 (1995).
 46. Fisher, R. P. & Morgan, D. O. A novel cyclin associates with M015/CDK7 to form the CDK-activating kinase. *Cell* **78**, 713–724 (1994).
 47. Ullrich, A. & Schlessinger, J. Signal transduction by receptors with tyrosine kinase activity. *Cell* **61**, 203–212 (1990).
 48. Superti-Furga, G. & Courtneidge, S. A. Structure-function relationships in Src family and related protein tyrosine kinases. *BioEssays* **17**, 321–330 (1995).
 49. Roussel, R. R., Brodeur, S. R., Shalloway, D. & Laudano, A. P. Selective binding of activated pp60(c-src) by an immobilized synthetic phosphopeptide modeled on the carboxyl terminus of pp60(c-src). *Proc. Natl. Acad. Sci. U. S. A.* **88**, 10696–10700 (1991).
 50. Matsuda, M., Mayer, B. J., Fukui, Y. & Hanafusa, H. Binding of transforming protein, P47gag-crk, to a broad range of phosphotyrosine-containing proteins. *Science (80-)*. **248**, 1537–1539 (1990).
 51. Young, M. A., Gonfloni, S., Superti-Furga, G., Roux, B. & Kuriyan, J. Dynamic coupling

- between the SH2 and SH3 domains of c-Src and Hck underlies their inactivation by C-Terminal tyrosine phosphorylation. *Cell* **105**, 115–126 (2001).
52. Gonfloni, S., Weijland, A., Kretzschmar, J. & Superti-Furga, G. Crosstalk between the catalytic and regulatory domains allows bidirectional regulation of Src. *Nat. Struct. Biol.* **7**, 281–286 (2000).
 53. Braakman, I. & Bulleid, N. J. Protein Folding and Modification in the Mammalian Endoplasmic Reticulum. *Annu. Rev. Biochem.* **80**, 71–99 (2011).
 54. Westrate, L. M., Lee, J. E., Prinz, W. A. & Voeltz, G. K. Form Follows Function: The Importance of Endoplasmic Reticulum Shape. (2015). doi:10.1146/annurev-biochem-072711-163501
 55. Schwarz, Dianne. S., Blower, M. D. The endoplasmic reticulum: structure, function and response to cellular signaling.
 56. Fagone, P. & Jackowski, S. Membrane phospholipid synthesis and endoplasmic reticulum function. doi:10.1194/jlr.R800049-JLR200
 57. Walter, P., Gimlore, R., Muller, M., Blobel, G. The protein translocation machinery of the endoplasmic reticulum. *Phil. Trans. R. Soc. Lond. B* **300**, 225–228 (1982).
 58. Walter, P. & Blobel, G. Signal recognition particle contains a 7S RNA essential for protein translocation across the endoplasmic reticulum. *Nature* **299**, 691–8 (1982).
 59. Keenan, R. J., Freymann, D. M., Stroud, R. M. & Walter, P. THE SIGNAL RECOGNITION PARTICLE. *Annu. Rev. Biochem* **70**, 755–75 (2001).
 60. Grudnik, P., Bange, G. & Sinning, I. Protein targeting by the signal recognition particle. *Biol. Chem.* **390**, 775–782 (2009).
 61. VON HEIJNE, G. Patterns of Amino Acids near Signal-Sequence Cleavage Sites. *Eur. J. Biochem.* **133**, 17–21 (1983).
 62. Gilmore, R., Blobel, G. & Walter, P. Protein Translocation Across the Endoplasmic Reticulum. I. Detection in the Microsomal Membrane of a Receptor for the Signal Recognition Particle.
 63. Gilmore, R., Walter, P. & Blobel, G. Protein Translocation Across the Endoplasmic Reticulum. II. Isolation and Characterization of the Signal Recognition Particle Receptor.
 64. Connolly, T. ;, Rapiejko, P. J. & Gilmore, R. Requirement of GTP Hydrolysis for Dissociation of the Signal Recognition Particle from Its Receptor. *Sci. Earth, Atmos. Aquat. Sci. Database* pg **252**, (1991).
 65. Nan Chang, C., Model, P. & Blobel, G. Membrane biogenesis: Cotranslational integration of the bacteriophage f1 coat protein into an Escherichia coli membrane fraction. *Cell Biol.* **76**, 1251–1255 (1979).
 66. Blobel, G. Intracellular protein topogenesis. *Proc. Natl. Acad. Sci. U. S. A.* **77**, 1496–500 (1980).

67. Ellgaard, L., McCaul, N., Chatsisvili, A. & Braakman, I. Co- and Post-Translational Protein Folding in the ER. *Traffic* **17**, 615–638 (2016).
68. Woolhead, C. A., McCormick, P. J. & Johnson, A. E. Nascent Membrane and Secretory Proteins Differ in FRET-Detected Folding Far inside the Ribosome and in Their Exposure to Ribosomal Proteins. *Cell* **116**, 725–736 (2004).
69. Ellgaard, Lars and Helenius, A. Quality Control in the Endoplasmic Reticulum. *Nat. Rev. Mol. Cell Biol.* **4**, 181–191 (2003).
70. Braakman, I. & Hebert, D. N. Protein Folding in the Endoplasmic Reticulum. doi:10.1101/cshperspect.a013201
71. Hendershot, L. The ER Chaperone BiP Is a Master Regulator of ER Function. *October* 289–297 (2004).
72. Alder, N. N., Shen, Y., Brodsky, J. L., Hendershot, L. M. & Johnson, A. E. The molecular mechanisms underlying BiP-mediated gating of the Sec61 translocon of the endoplasmic reticulum. *J. Cell Biol.* **168**, 389–399 (2005).
73. Matlack, K. E. S., Misselwitz, B., Plath, K. & Rapoport, T. A. BiP acts as a molecular ratchet during posttranslational transport of prepro- α factor across the ER membrane [2]. *Cell* **97**, 553–564 (1999).
74. Haas, Ingrid, Wabl, M. Immunoglobulin heavy chain binding protein.
75. Puig, A. & Gilbert, H. F. Anti-chaperone Behavior of BiP during the Protein Disulfide Isomerase-catalyzed Refolding of Reduced Denatured Lysozyme*. *J. BIOUXICAL Chem.* **269**, 25889–25896 (1994).
76. Liè vremon, J.-P., Rizzuto, R., Hendershot, L. & Meldolesi, J. BiP, a Major Chaperone Protein of the Endoplasmic Reticulum Lumen, Plays a Direct and Important Role in the Storage of the Rapidly Exchanging Pool of Ca²⁺.
77. Kabani, M. *et al.* Dependence of Endoplasmic Reticulum-associated Degradation on the Peptide Binding Domain and Concentration of BiP. *Mol. Biol. Cell* **14**, 3437–3448 (2003).
78. Mccracken, A. A. & Brodsky, J. L. Assembly of ER-Associated Protein Degradation In Vitro: Dependence on Cytosol, Calnexin, and ATP.
79. Vembar, S. S. & Brodsky, J. L. One step at a time: endoplasmic reticulum-associated degradation. doi:10.1038/nrm2546
80. Kerscher, O., Felberbaum, R. & Hochstrasser, M. Modification of Proteins by Ubiquitin and Ubiquitin-Like Proteins. *Annu. Rev. Cell Dev. Biol* **22**, 159–80 (2006).
81. Thibault, G. & Ng, D. T. W. The endoplasmic reticulum-associated degradation pathways of budding yeast. *Cold Spring Harb. Perspect. Biol.* **4**, 1–15 (2012).
82. Amm, I., Sommer, T. & Wolf, D. H. Protein quality control and elimination of protein waste: The role of the ubiquitin–proteasome system.
83. Hampton, R. Y. ER-associated degradation in protein quality control and cellular regulation.

- Curr. Opin. Cell Biol.* **14**, 476–482 (2002).
84. Ruggiano, A., Foresti, O. and & Carvalho, P. ER-associated degradation: Protein quality control and beyond. *Rockefeller Univ. Press J. Cell Biol* **204**, 869–879 (2014).
 85. Schroder, M. Endoplasmic reticulum stress responses. *Cell. Mol. Life Sci.* **65**, 862–894 (2008).
 86. Xu, C., Bailly-Maitre, B. & Reed, J. C. Endoplasmic reticulum stress : cell life and death decisions. **115**, (2005).
 87. Walter, P. & Ron, D. The Unfolded Protein Response: From Stress Pathway to Homeostatic Regulation. *Science (80-.)*. **334**, 1219–1243 (2011).
 88. Ron, D. & Walter, P. Signal integration in the endoplasmic reticulum unfolded protein response. *Nat. Rev. cell Biol.* **8**, 519–529 (2007).
 89. Wu, H., Ng, B. S. H., Thibault, G. & Kong, L. Endoplasmic reticulum stress response in yeast and humans. *Biosci. Rep* **34**, 321–330 (2014).
 90. Lin, J. H., Walter, P. & Benedict Yen, T. Endoplasmic Reticulum Stress in Disease Pathogenesis. doi:10.1146/annurev.pathmechdis.3.121806.151434
 91. Bernales, S., Papa, F. R. & Walter, P. Intracellular Signaling by the Unfolded Protein Response. *Annu. Rev. Cell Dev. Biol* **22**, 487–508 (2006).
 92. Tabas, I. & Ron, D. Integrating the mechanisms of apoptosis induced by endoplasmic reticulum stress. doi:10.1038/ncb0311-184
 93. Bertolotti, A., Zhang, Y., Hendershot, L. M., Harding, H. P. & Ron, D. Dynamic interaction of BiP and ER stress transducers in the unfolded- protein response. *Nat. Cell Biol.* **2**, 326–332 (2000).
 94. Credle, J. J., Finer-Moore, J. S., Papa, F. R., Stroud, R. M. & Walter, P. On the mechanism of sensing unfolded protein in the endoplasmic reticulum. *Proc. Natl. Acad. Sci. U. S. A.* **102**, 18773–84 (2005).
 95. Cox, J. S., Shamu, C. E. & Walter, P. Transcriptional induction of genes encoding endoplasmic reticulum resident proteins requires a transmembrane protein kinase. *Cell* **73**, 1197–206 (1993).
 96. Tirasophon, W., Lee, K., Callaghan, B., Welihinda, A. & Kaufman, R. J. The endoribonuclease activity of mammalian IRE1 autoregulates its mRNA and is required for the unfolded protein response. *Genes Dev.* **14**, 2725–2736 (2000).
 97. Lee, K. P. K. *et al.* Structure of the dual enzyme Ire1 reveals the basis for catalysis and regulation in non-conventional RNA splicing. *Cell* **132**, 89–100 (2008).
 98. Korennykh, A. V. *et al.* The unfolded protein response signals through high-order assembly of Ire1. *Nature* **457**, 687–693 (2009).
 99. Lu, S. J. *et al.* Conservation of IRE1-regulated bZIP74 mRNA unconventional splicing in rice (*Oryza sativa* L.) involved in ER stress responses. *Mol. Plant* **5**, 504–514 (2012).

100. Shen, X. *et al.* Complementary signaling pathways regulate the unfolded protein response and are required for *C. elegans* development. *Cell* **107**, 893–903 (2001).
101. Sidrauski, C. & Walter, P. The transmembrane kinase Ire1p is a site-specific endonuclease that initiates mRNA splicing in the unfolded protein response. *Cell* **90**, 1031–1039 (1997).
102. Nojima, H. *et al.* Hac1: A novel yeast bZIP protein binding to the CRE motif is a multicopy suppressor for *cdc10* mutant of *Schizosaccharomyces pombe*. *Nucleic Acids Res.* **22**, 5279–5288 (1994).
103. Cox, J. S. & Walter, P. A Novel Mechanism for Regulating Activity of a Transcription Factor That Controls the Unfolded Protein Response. *Cell* **87**, 391–404 (1996).
104. Sidrauski, C., Cox, J. S. & Walter, P. tRNA Ligase Is Required for Regulated mRNA Splicing in the Unfolded Protein Response. *Cell* **87**, 405–413 (1996).
105. Bertolotti, A. *et al.* Increased sensitivity to dextran sodium sulfate colitis in IRE1 β -deficient mice. *J. Clin. Invest.* **107**, 585–93 (2001).
106. Martino, M. B. *et al.* The ER stress transducer IRE1 β is required for airway epithelial mucin production. *Mucosal Immunol.* **6**, 639–54 (2013).
107. Yoshida, H., Matsui, T., Yamamoto, A., Okada, T. & Mori, K. XBP1 mRNA Is Induced by ATF6 and Spliced by IRE1 in Response to ER Stress to Produce a Highly Active Transcription Factor. *Cell* **107**, 881–891 (2001).
108. Kosmaczewski, S. G. *et al.* The RtcB RNA ligase is an essential component of the metazoan unfolded protein response. *EMBO Rep.* **15**, 1278–1285 (2014).
109. Calton, M. *et al.* IRE1 couples endoplasmic reticulum load to secretory capacity by processing the XBP-1 mRNA. *Nature* **415**, 92–96 (2002).
110. Yoshida, H., Oku, M., Suzuki, M. & Mori, K. pXBP1(U) encoded in XBP1 pre-mRNA negatively regulates unfolded protein response activator pXBP1(S) in mammalian ER stress response. *J. Cell Biol.* **172**, 565–75 (2006).
111. Harding, H. P., Zhang, Y. & Ron, D. Protein translation and folding are coupled by an endoplasmic-reticulum- resident kinase. *Nature* **397**, (1999).
112. Hinnebusch, A. G. Translational Regulation of GCN4 and the General Amino Acid Control of Yeast. *Annu. Rev. Microbiol.* **59**, 407–450 (2005).
113. Hinnebusch, A. G. Translational regulation of yeast GCN4. *J. Biol. Chem.* **272**, 21661–4 (1997).
114. Marciniak, S. J. *et al.* CHOP induces death by promoting protein synthesis and oxidation in the stressed endoplasmic reticulum. *Genes Dev.* **18**, 3066–77 (2004).
115. Zinszner, H. *et al.* CHOP is implicated in programmed cell death in response to impaired function of the endoplasmic reticulum. *Genes Dev.* **12**, 982–95 (1998).
116. Schindler, A. J. & Schekman, R. In vitro reconstitution of ER-stress induced ATF6 transport in COPII vesicles. *Proc. Natl. Acad. Sci. U. S. A.* **106**, 17775–80 (2009).

117. Haze, K., Yoshida, H., Yanagi, H., Yura, T. & Mori, K. Mammalian transcription factor ATF6 is synthesized as a transmembrane protein and activated by proteolysis in response to endoplasmic reticulum stress. *Mol. Biol. Cell* **10**, 3787–99 (1999).
118. Ye, J. *et al.* ER stress induces cleavage of membrane-bound ATF6 by the same proteases that process SREBPs. *Mol. Cell* **6**, 1355–64 (2000).
119. Tassan, J. P. & Le Goff, X. An overview of the KIN1/PAR-1/MARK kinase family. *Biol. Cell* **96**, 193–199 (2004).
120. Drewes, G., Ebneith, A. & Preuss, U. MARK, a Novel Family of Protein Kinases That Phosphorylate Microtubule-Associated Proteins and Trigger Microtubule Disruption. *Cell* **89**, 297–308 (1997).
121. Drubin, D. G. & Nelson, W. J. Origins of Cell Polarity. *Cell* **84**, 335–344 (1996).
122. Sammak, P. J. & Borisy, G. G. Direct observation of fluorescent microtubules in living cells. *Lett. to Nat.* **332**, 724–726 (1988).
123. Hurov, J. & Piwnicka-Worms, H. The Par-1/MARK family of protein kinases: From polarity to metabolism. *Cell Cycle* **6**, 1966–1969 (2007).
124. Gustke, N. *et al.* The Alzheimer-like phosphorylation of tau protein reduces microtubule binding and involves Ser-Pro and Thr-Pro motifs. *FEBS Lett.* **307**, 199–205 (1992).
125. Biernat, J., Gustke, N., Drewes, G., Mandelkow, E. & Mandelkow, E. Phosphorylation of Ser262 strongly reduces binding of tau to microtubules: Distinction between PHF-like immunoreactivity and microtubule binding. *Neuron* **11**, 153–163 (1993).
126. Drewes, G. MARKing tau for tangles and toxicity. *Trends Biochem. Sci.* **29**, 548–555 (2004).
127. Guo, S. & Kemphues, K. J. par-1, a gene required for establishing polarity in *C. elegans* embryos, encodes a putative Ser/Thr kinase that is asymmetrically distributed. *Cell* **81**, 611–620 (1995).
128. Kemphues, K. J., Priess, J., Morton, D. & Cheng, N. S. Identification of Genes Required for Cytoplasmic Localization in Early *C. elegans* Embryos. *J. Cell. Biochem.* **52**, 311320 (1988).
129. Kemphues, K. PARsing Embryonic Polarity. *Cell* **101**, 345–348 (2000).
130. Derenzo, C., Reese, K. J. & Seydoux, G. Exclusion of germ plasm proteins from somatic lineages by cullin-dependent degradation. *Nature* **424**, 685–689 (2003).
131. Cox, D. N., Lu, B., Sun, T. Q., Williams, L. T. & Jan, Y. N. *Drosophila* par-1 is required for oocyte differentiation and microtubule organization. *Curr. Biol.* **11**, 75–87 (2001).
132. Shulman, J. M., Benton, R. & St Johnston, D. The *Drosophila* homolog of *C. elegans* PAR-1 organizes the oocyte cytoskeleton and directs oskar mRNA localization to the posterior pole. *Cell* **101**, 377–388 (2000).
133. Riechmann, V., Gutierrez, G. J., Filardo, P., Nebreda, A. R. & Ephrussi, A. Par-1 regulates

- stability of the posterior determinant Oskar by phosphorylation. *Nat. Cell Biol.* **4**, 337–342 (2002).
134. Elbert, M., Rossi, G., Brennwald, P. The Yeast Par-1 Homologs Kin1 and Kin2 Show Genetic and Physical Interactions with Components of the Exocytic Machinery. *Mol. Biol. Cell* **16**, 532–549 (2004).
 135. Drewes, G. & Nurse, P. The protein kinase kin1, the fission yeast orthologue of mammalian MARK/PAR-1, localises to new cell ends after mitosis and is important for bipolar growth. *FEBS Lett.* **554**, 45–49 (2003).
 136. Murphy, J. M. *et al.* Conformational instability of the MARK3 UBA domain compromises ubiquitin recognition and promotes interaction with the adjacent kinase domain. *Proc. Natl. Acad. Sci. U. S. A.* **104**, 14336–14341 (2007).
 137. Anshu, A., Mannan, M. A.-U., Chakraborty, A., Chakrabarti, S. & Dey, M. A Novel Role for Protein Kinase Kin2 in Regulating HAC1 mRNA Translocation, Splicing, and Translation. *Mol. Cell. Biol.* **35**, 199–210 (2015).
 138. Aragón, T. *et al.* Messenger RNA targeting to endoplasmic reticulum stress signalling sites. *Nature* **457**, 736–40 (2009).
 139. Klaips, C. L., Jayaraj, G. G. & Hartl, F. U. Pathways of cellular proteostasis in aging and disease. *J. Cell Biol.* **217**, 51–63 (2018).
 140. Scheper, G. C., Van Der Knaap, M. S. & Proud, C. G. Translation matters: Protein synthesis defects in inherited disease. *Nat. Rev. Genet.* **8**, 711–723 (2007).
 141. Pickering, B. M. & Willis, A. E. The implications of structured 5' untranslated regions on translation and disease. *Semin. Cell Dev. Biol.* **16**, 39–47 (2005).
 142. Liu, L. *et al.* Mutation of the CDKN2A 5' UTR creates an aberrant initiation codon and predisposes to melanoma. *Nat. Genet.* **21**, 128–132 (1999).
 143. Zhang, P. *et al.* The PERK Eukaryotic Initiation Factor 2 Kinase Is Required for the Development of the Skeletal System, Postnatal Growth, and the Function and Viability of the Pancreas. *Mol. Cell. Biol.* **22**, 3864–3874 (2002).
 144. Draptchinskaia, N. *et al.* The gene encoding ribosomal protein S19 is mutated in Diamond-Blackfan anaemia. *Nat. Genet.* **21**, 169–175 (1999).
 145. Antonellis, A. *et al.* Glycyl tRNA synthetase mutations in Charcot-Marie-Tooth disease type 2D and distal spinal muscular atrophy type V. *Am. J. Hum. Genet.* **72**, 1293–1299 (2003).
 146. Hipp, M. S., Kasturi, P. & Hartl, F. U. The proteostasis network and its decline in ageing. *Nat. Rev. Mol. Cell Biol.* (2019). doi:10.1038/s41580-019-0101-y
 147. Lang, L., Kurnik, M., Danielsson, J. & Oliveberg, M. Fibrillation precursor of superoxide dismutase 1 revealed by gradual tuning of the protein-folding equilibrium. *Proc. Natl. Acad. Sci. U. S. A.* **109**, 17868–17873 (2012).
 148. Ward, C. L. & Kopito, R. R. Intracellular turnover of cystic fibrosis transmembrane

- conductance regulator. Inefficient processing and rapid degradation of wild-type and mutant proteins. *J. Biol. Chem.* **269**, 25710–25718 (1994).
149. Cohen, P. The role of protein phosphorylation in human health and disease. *Eur. J. Biochem.* **268**, 5001–5010 (2001).
 150. Lahiry, P., Torkamani, A., Schork, N. J. & Hegele, R. A. Kinase mutations in human disease: interpreting genotype–phenotype relationships. *Nat. Rev. Genet.* **11**, (2010).
 151. Gu, G. J. *et al.* Role of individual MARK isoforms in phosphorylation of tau at Ser 262 in Alzheimer’s disease. *NeuroMolecular Med.* **15**, 458–469 (2013).
 152. Li, J. Q., Tan, L. & Yu, J. T. The role of the LRRK2 gene in Parkinsonism. *Mol. Neurodegener.* **9**, 47 (2014).
 153. Bando, Y. *et al.* Double-strand RNA dependent protein kinase (PKR) is involved in the extrastriatal degeneration in Parkinson’s disease and Huntington’s disease. *Neurochem. Int.* **46**, 11–18 (2005).
 154. Lu, Z. & Hunter, T. Metabolic Kinases Moonlighting as Protein Kinases. *Trends Biochem. Sci.* **43**, 301–310 (2018).
 155. George, S. *et al.* A family with severe insulin resistance and diabetes due to a mutation in AKT2. *Science (80-.)*. **304**, 1325–1328 (2004).
 156. Farese, R. V., Sajan, M. P. & Standaert, M. L. Insulin-sensitive protein kinases (atypical protein kinase C and protein kinase B/Akt): Actions and defects in obesity and type II diabetes. *Exp. Biol. Med.* **230**, 593–605 (2005).
 157. Pombo, C. M., Iglesias, C., Sartages, M. & Zalvide, J. B. MST Kinases and Metabolism. *Endocrinology* **160**, 1111–1118 (2019).
 158. Weikel, K. A., Ruderman, N. B. & Cacicedo, J. M. Unraveling the actions of AMP-activated protein kinase in metabolic diseases: Systemic to molecular insights. *Metabolism.* **65**, 634–645 (2016).
 159. Bhullar, K. S. *et al.* Kinase-targeted cancer therapies: Progress, challenges and future directions. *Mol. Cancer* **17**, 1–20 (2018).
 160. Siegel, R. L., Miller, K. D. & Jemal, A. Cancer statistics, 2015. *CA. Cancer J. Clin.* **65**, 5–29 (2015).
 161. Ben-neriah, Y., Daley, G., Mes-masson, A., Witte, O. & Baltimore, D. The Chronic Myelogenous Leukemia-specific P210 Protein Is the Product of the *ber/abl* Hybrid Gene. *Science (80-.)*. **233**, 212–214 (1985).
 162. Melo, J. V. & Deininger, M. W. N. Biology of chronic myelogenous leukemia - Signaling pathways of initiation and transformation. *Hematol. Oncol. Clin. North Am.* **18**, 545–568 (2004).
 163. Marcucci, G., Perrotti, D. & Caligiuri, M. A. Understanding the molecular basis of imatinib mesylate therapy in chronic myelogenous leukemia and the related mechanisms of resistance. *Clin. Cancer Res.* **9**, 1248–1252 (2003).

164. Shigematsu, H. *et al.* Clinical and biological features associated with epidermal growth factor receptor gene mutations in lung cancers. *J. Natl. Cancer Inst.* **97**, 339–346 (2005).
165. da Cunha Santos, G., Shepherd, F. A. & Tsao, M. S. EGFR Mutations and Lung Cancer. *Annu. Rev. Pathol. Mech. Dis.* **6**, 49–69 (2011).
166. Harari, D. & Yarden, Y. Molecular mechanisms underlying ErbB2/HER2 action in breast cancer. *Oncogene* **19**, 6102–6114 (2000).
167. Levin, D. E., Hammond, C. I., Ralston, R. O. & Bishop, J. M. Two yeast genes that encode unusual protein kinases. *Proc. Natl. Acad. Sci. U. S. A.* **84**, 6035–6039 (1987).
168. Donovan, M., Romano, P., Tibbetts, M. & Hammond, C. I. Characterization of the KIN2 gene product in *Saccharomyces cerevisiae* and comparison between the kinase activities of p145KIN1 and p145KIN2. *Yeast* **10**, 113–124 (1994).
169. Campanale, J. P., Sun, T. Y. & Montell, D. J. Development and dynamics of cell polarity at a glance. *J. Cell Sci.* **130**, 1201–1207 (2017).
170. Lehrman, M. A. Biosynthesis of N-acetylglucosamine-P-P-dolichol, the committed step of asparagine-linked oligosaccharide assembly. *Glycobiology* **1**, 553–562 (1991).
171. Walinda, E. *et al.* Solution structure of the ubiquitin-associated (UBA) domain of human autophagy receptor NBR1 and its interaction with ubiquitin and polyubiquitin. *J. Biol. Chem.* **289**, 13890–13902 (2014).
172. Goldberg, J., Nairn, A. C. & Kuriyan, J. Structural basis for the autoinhibition of calcium/calmodulin-dependent protein kinase I. *Cell* **84**, 875–887 (1996).
173. Shvartsman, D. E. *et al.* Src kinase activity and SH2 domain regulate the dynamics of Src association with lipid and protein targets. *J. Cell Biol.* **178**, 675–686 (2007).
174. Tibbetts, M., Donovan, M., Roe, S., Stiltner, A. M. & Hammond, C. I. KIN 1 and KIN 2 protein kinases localize to the cytoplasmic face of the yeast plasma membrane. *Experimental Cell Research* **213**, 93–99 (1994).
175. Yuan, S. M., Nie, W. C., He, F., Jia, Z. W. & Gao, X. D. Kin2, the budding yeast ortholog of animal MARK/PAR-1 kinases, localizes to the sites of polarized growth and may regulate septin organization and the cell wall. *PLoS One* **11**, 1–20 (2016).
176. Stoneman, M. R. *et al.* Quaternary structure of the yeast pheromone receptor Ste2 in living cells. *Biochim. Biophys. Acta - Biomembr.* **1859**, 1456–1464 (2017).
177. Moravcevic, K. *et al.* Kinase associated-1 domains drive MARK/PAR1 kinases to membrane targets by binding acidic phospholipids. *Cell* **143**, 966–977 (2010).
178. Beenstock, J., Mooshayef, N. & Engelberg, D. How Do Protein Kinases Take a Selfie (Autophosphorylate)? *Trends Biochem. Sci.* **41**, 938–953 (2016).
179. Cheng, X., Ma, Y., Moore, M., Hemmings, B. A. & Taylor, S. S. Phosphorylation and activation of cAMP-dependent protein kinase by phosphoinositide-dependent protein kinase. *Proc. Natl. Acad. Sci. U. S. A.* **95**, 9849–9854 (1998).

180. Cameron, A. J. M., Escribano, C., Saurin, A. T., Kostelecky, B. & Parker, P. J. PKC maturation is promoted by nucleotide pocket occupation independently of intrinsic kinase activity. *Nat. Struct. Mol. Biol.* **16**, 624–630 (2009).
181. Ruegsegger, U., Leber, J. H. & Walter, P. Block of HAC1 mRNA Translation by Long-Range Base Pairing Is Released by Cytoplasmic Splicing upon Induction of the Unfolded Protein Response. *October* **107**, 103–114 (2001).
182. Sathe, L., Bolinger, C., Amin-Ul Mannan, M., Dever, T. E. & Dey, M. Evidence that base-pairing interaction between intron and mRNA leader sequences inhibits initiation of HAC1 mRNA translation in yeast. *J. Biol. Chem.* **290**, 21821–21832 (2015).
183. Vasudevan, S. & Steitz, J. A. AU-Rich-Element-Mediated Upregulation of Translation by FXR1 and Argonaute 2. *Cell* **128**, 1105–1118 (2007).
184. Castello, A. *et al.* Insights into RNA Biology from an Atlas of Mammalian mRNA-Binding Proteins. *Cell* **149**, 1393–1406 (2012).
185. Tsvetanova, N. G., Riordan, D. P. & Brown, P. O. The yeast rab GTPase Ypt1 modulates unfolded protein response dynamics by regulating the stability of HAC1 RNA. *PLoS Genet.* **8**, (2012).
186. Carroll, S. Y. *et al.* Analysis of yeast endocytic site formation and maturation through a regulatory transition point. *Mol. Biol. Cell* **23**, 657–668 (2012).
187. Lee, K. P. K. *et al.* Structure of the dual enzyme Ire1 reveals the basis for catalysis and regulation in nonconventional RNA splicing. *Cell* **132**, 89–100 (2008).
188. Normington, K., Kohno, K., Kozutsumi, Y., Gething, M. J. & Sambrook, J. S. *cerevisiae* encodes an essential protein homologous in sequence and function to mammalian BiP. *Cell* **57**, 1223–1236 (1989).
189. Hinnebusch, A. G. Molecular Mechanism of Scanning and Start Codon Selection in Eukaryotes. *Microbiol. Mol. Biol. Rev.* **75**, 434–467 (2011).
190. Lee, M. E., Rusin, S. F., Jenkins, N., Kettenbach, A. N. & Moseley, J. B. Mechanisms connecting the conserved protein kinases Ssp1, Kin1, and Pom1 in fission yeast cell polarity and division. *Curr. Biol.* **28**, 84–92 (2018).
191. Nishi, Y., Rogers, E., Robertson, S. M. & Lin, R. Polo kinases regulate *C. elegans* embryonic polarity via binding to DYRK2-primed MEX-5 and MEX-6. *Development* **135**, 687–697 (2008).
192. Drewes, G. *et al.* Microtubule-associated protein/microtubule affinity-regulating kinase (p110 mark). A novel protein kinase that regulates tau-microtubule interactions and dynamic instability by phosphorylation at the Alzheimer-specific site serine 262. *J. Biol. Chem.* **270**, 7679–7688 (1995).
193. Gelperin, D. M. *et al.* Biochemical and genetic analysis of the yeast proteome with a movable ORF collection. *Genes Dev.* **19**, 2816–2826 (2005).
194. Dey, M. *et al.* Mechanistic link between PKR dimerization, autophosphorylation, and eIF2 α

- substrate recognition. *Cell* **122**, 901–913 (2005).
195. Swaney, D. L. *et al.* Global analysis of phosphorylation and ubiquitylation cross-talk in protein degradation. *Nat. Methods* **10**, 676–682 (2013).
 196. Ghosh, C., Sathe, L., Paprocki, J. D., Raicu, V. & Dey, M. Adaptation to Endoplasmic Reticulum Stress Requires Transphosphorylation within the Activation Loop of Protein Kinases Kin1 and Kin2, Orthologs of Human Microtubule Affinity-Regulating Kinase. *Mol. Cell. Biol.* **38**, 1–23 (2018).
 197. Moorthy, B. T., Sharma, A., Boettner, D. R., Wilson, T. E. & Lemmon, S. K. Identification of suppressor of Clathrin deficiency-1 (SCD1) and its connection to Clathrin-mediated endocytosis in *Saccharomyces cerevisiae*. *G3 Genes, Genomes, Genet.* **9**, 867–877 (2019).
 198. Wiley, J. C., Wailes, L. A., Idzerda, R. L. & McKnight, G. S. Role of regulatory subunits and protein kinase inhibitor (PKI) in determining nuclear localization and activity of the catalytic subunit of protein kinase A. *J. Biol. Chem.* **274**, 6381–6387 (1999).
 199. Hong, S. P., Leiper, F. C., Woods, A., Carling, D. & Carlson, M. Activation of yeast Snf1 and mammalian AMP-activated protein kinase by upstream kinases. *Proc. Natl. Acad. Sci. U. S. A.* **100**, 8839–8843 (2003).
 200. Lizcano, J. M. *et al.* LKB1 is a master kinase that activates 13 kinases of the AMPK subfamily, including MARK/PAR-1. *EMBO J.* **23**, 833–843 (2004).
 201. Andreassi, C. & Riccio, A. To localize or not to localize: mRNA fate is in 3'UTR ends. *Trends Cell Biol.* **19**, 465–474 (2009).
 202. Ge, W., Chew, T. G., Wachtler, V., Naqvi, S. N. & Balasubramanian, M. K. The Novel Fission Yeast Protein Pallp Interacts with Hip1-related Sla2p/End4p and Is Involved in Cellular Morphogenesis. *Mol. Biol. Cell* **16**, 4124–4138 (2005).
 203. Mok, J. *et al.* Deciphering protein kinase specificity through large-scale analysis of yeast phosphorylation site motifs. *Sci. Signal.* **3**, (2010).
 204. Martin, K. C. & Ephrussi, A. mRNA Localization: Gene Expression in the Spatial Dimension. *Cell* **136**, 719–730 (2009).
 205. Korennykh, A. V *et al.* The unfolded protein response signals through high-order assembly of Ire1-supplemental data. *Nature* **457**, 687–93 (2009).
 206. Micsonai, A. *et al.* BeStSel: A web server for accurate protein secondary structure prediction and fold recognition from the circular dichroism spectra. *Nucleic Acids Res.* **46**, W315–W322 (2018).
 207. Biener, G. *et al.* Development and experimental testing of an optical micro-spectroscopic technique incorporating true line-scan excitation. *Int. J. Mol. Sci.* **15**, 261–276 (2013).
 208. Patowary, S. *et al.* Experimental verification of the kinetic theory of FRET using optical microspectroscopy and obligate oligomers. *Biophys. J.* **108**, 1613–1622 (2015).

CURRICULUM VITAE

CHANDRIMA GHOSH

Lapham Hall S181, 3209 N Maryland Avenue, Milwaukee, Wisconsin 53211

chandrima.ghosh09@gmail.com

Education

- Fall 2013-Present PhD student, Department of Biological Sciences,
University of Wisconsin- Milwaukee, WI, USA.
- Fall 2008-Spring 2012 Bachelors of Technology, Department of Bio-Technology,
West Bengal University of Technology, Kolkata, India.

Research Experiences

- PhD project Understanding the mechanism of activation of yeast protein kinase Kin2, an
ortholog of human MARK and worm Par-1. Graduate advisor- Dr.
Madhusudan Dey, Biological Sciences, University of Wisconsin-
Milwaukee, WI, USA.
- Undergraduate
project Cytotoxicity of Methotrexate and Cyclophosphamide in Swiss Albino
Mice (*Mus musculus*). Undergraduate advisor- Dr. Riddhi Goswami,
Biotechnology, West Bengal University of Technology, India.
- Summer research
2011 Molecular Detection and Characterization of Etiological Agents of Viral
Diarrhea with special reference to Rotaviruses. Supervisor- Dr. Triveni
Krishnan, Department of Virology, National Institute of Cholera and
Enteric Diseases (Indian Council of Medical Research), WHO
Collaborating Centre for Diarrheal Diseases Research and Training, India.
- Fall research
2010 Status of soil enzymes in different parts of a metropolitan city: A case study
in Kolkata
Supervisor- Dr. Srabanti Basu, Department of Biotechnology,
West Bengal University of Technology, India.
- Industrial Training
2010 Supervisor- Dr. Amitabha Kundu, Department of Quality Control,
East India Pharmaceutical Works Limited, India.
- Research Project
2012 Studies on Mental Retardation and Chromosomal Anomaly
Supervisor- Dr. Ajanta Haldar, Department of Cytogenetics, Vivekananda
Institute of Medical Sciences, Kolkata, India.

Publications

- **Chandrima Ghosh**, Leena Sathe, Joel David Paprocki, Valerica Raicu, Madhusudan Dey (2018). Adaptation to Endoplasmic Reticulum Stress Requires Transphosphorylation within the Activation Loop of Protein Kinases Kin1 and Kin2, Orthologs of Human Microtubule Affinity-Regulating Kinase. *Molecular and Cellular Biology*, Volume 38, Issue 23. DOI: 10.1128/MCB.00266-18.
- Jagadeesh Kumar Uppala, **Chandrima Ghosh***, Leena Sathe, Madhusudan Dey (2018). Phosphorylation of translation initiation factor eIF2 α at Ser51 depends on site- and context-specific information. *FEBS letters*, Volume 592, Issue 18. <https://doi.org/10.1002/1873-3468.13214>. *Equally contributed.
- **Ghosh, C.**, Sathe, L., Uppala, J., Pokkuluri, P., Hammond, C., Anshu, A., Turk, B., Dey, M. Phosphorylation of Pal2 by the Kin Kinases Modulates HAC1 mRNA splicing in the *Saccharomyces cerevisiae* Unfolded Protein Response (Under Revision)
- George, J., Li, Y., Parashar, D., Tsaih, S., Gupta, P., Geethadevi, A., Kadembari, I., **Ghosh, C.**, Sun, Y., Allister, D., Dwinell, M., Rader, J., Rui, H., Dey, M., Pradeep, S., and Chaluvally-Raghavan, P. FXR1-mediated oncogenic adaptations in ovarian cancer via post transcriptional regulations of cMYC (Manuscript under preparation)

Laboratory skills

Microbiology: yeast/ bacteria growth curves, yeast genetic screens.

Molecular Biology: cloning, site-directed mutagenesis, RT-PCR, *in vitro* transcription, CRISPR-Cas9 gene editing.

Protein Biochemistry: protein expression and purification from yeast and bacteria, SDS-PAGE, Phos-Tag gel electrophoresis, beta-galactosidase assay, TLC, LPLC, *in vitro* radiolabeled kinase assay, gel-mobility shift assay, Western blotting.

Microscopy: confocal microscopy, fluorescence microscopy.

Mammalian Cell culture: cell culture maintenance, transfection.

Computer skills

Snagene, MacVector, Pymol, SPSS, Microsoft Office, Adobe Photoshop, GraphPad Prism, Image J, Swiss-Model, Programming in C.

Teaching Experiences

As a graduate Teaching Assistant, implemented the semester curriculum for undergraduate students for the laboratory sections of the courses Anatomy and Physiology, and Foundations of Biology I.

Worked with groups of 50 students each semester, helping them to learn to conduct experiments and analyze data. Conducted semester examinations and grading.

Courses taught	Human Anatomy and Physiology I (BioSci 202) Foundations of Biology I (BioSci 150)
Teaching lab coordinator	Foundation of Biological Sciences (Bio 150)

Undergraduate students trained

Anthony Pulvino, Jenny Southaphan, Noelle Klitzke, Hamzah Hamdan, Theresa Herrick, Chelsea Moore.

Awards and Honors

- **Distinguished Dissertation Fellowship**, University of Wisconsin-Milwaukee, USA (2019).
- **Best talk award**: Microbiology talk on “Novels Substrates for Budding Yeast Kinases Kin1 and Kin2, the Orthologs of the Human Microtubule Affinity-Regulating Kinase”, Research Symposium, Department of Biological Sciences, University of Wisconsin-Milwaukee, USA (2019).
- **3rd place in Three Minute Thesis Competition**, University of Wisconsin-Milwaukee, USA (2019).
- **Travel Award** to present in the annual meeting of American Society of Biochemistry and Molecular Biology: “Trans-phosphorylation Activates the Yeast Protein Kinase Kin2, An Ortholog Of Human Microtubule Affinity Regulating Kinase” (2018).
- **Graduate Ruth I. Walker Grants-in-Aid Award**, Department of Biological Sciences, Biological Sciences, University of Wisconsin-Milwaukee, USA (2018).
- **Graduate Ruth I. Walker Grants-in-Aid Award**, Department of Biological Sciences, Biological Sciences, University of Wisconsin-Milwaukee, USA (2017).
- **1st position**: Poster on “Understanding the Kin Signaling Pathway in Yeast” Biological Sciences Research Symposium, UWM (2015).
- **3rd position**: Poster on “Studies on Cytotoxicity of Methotrexate and Cyclophosphamide” at the 7th Annual Session of Students’ Chemical Engineering Congress, Heritage Institute of Technology, India (2012).
- **2nd position**: Poster on “Impact of Methotrexate and Cyclophosphamide on Swiss Albino Mice” at the Indian Institute of Science Education and Research, India (2011).

Posters and Abstracts Published

- **Chandrima Ghosh**, Madhusudan Dey. “Understanding the Kin kinase signaling pathway in the budding yeast *Saccharomyces cerevisiae*”. University of Wisconsin-Milwaukee, School of Fresh Water Sciences. (Invited Talk) (2019)
- **Chandrima Ghosh**, Leena Sathe, Madhusudan Dey. “The Budding Yeast Kinases Kin1 and Kin2, the Orthologs of the Human Microtubule Affinity-Regulating Kinase (MARK) Phosphorylate a Novel Substrate Pal2 to Regulate Cellular Endocytosis”. The Protein

- Kinases and Protein Phosphorylation Conference: Mechanisms to Therapeutics FASEB Science Research Conference, Palm Springs, USA. (2 min Flash Talk and Poster) (2019)
- Jagadeesh Uppala, **Chandrima Ghosh**, Leena Sathe, Faiz Ahmad, Madhusudan Dey. Novel Modulators in the Unfolding Protein Response Signaling Pathway. The Endoplasmic Reticulum (ER) Conference: From Unfolded Proteins to Disease FASEB Science Research Conference, Snowmass Village, USA. (Poster) (2019)
 - **Chandrima Ghosh**, Leena Sathe, Madhusudan Dey. “Novels Substrates for Budding Yeast Kinases Kin1 and Kin2, the Orthologs of the Human Microtubule Affinity-Regulating Kinase”, Research Symposium, Department of Biological Sciences, University of Wisconsin-Milwaukee, USA. (Talk) (2019)
 - Leena Sathe, Abhijit Chakrabarty, **Chandrima Ghosh**, Jagadeesh K Uppala, Hamzah Hamdan, Anthony Pulvino and Madhusudan Dey “Adaptation to Endoplasmic Reticulum Stress Through Distinct Isoform-specific Expression of HAC1 mRNA” Research Symposium, Department of Biological Sciences, University of Wisconsin-Milwaukee. (2019)
 - Leena Sathe, **Chandrima Ghosh**, Madhusudan Dey. “Mechanistic insights into translational silencing of HAC1 mRNA” Cold Spring Harbor Laboratory meeting. Translational Control. (2018)
 - **Chandrima Ghosh**, Leena Sathe, Madhusudan Dey. “Trans-phosphorylation Activates the Yeast Protein Kinase Kin2, An Ortholog Of Human Microtubule Affinity Regulating Kinase, annual meeting of American Society of Biochemistry and Molecular Biology, San Diego, USA. (Poster) (2018)
 - **Chandrima Ghosh**, Leena Sathe, Madhusudan Dey “Understanding a Novel Kin-Kinase Signaling Pathway in Protein Homeostasis” Research Symposium, Department of Biological Sciences, University of Wisconsin-Milwaukee, USA. (Poster) (2018)
 - Leena Sathe, **Chandrima Ghosh**, Madhusudan Dey. “An RNA Duplex Inhibits Initiation of HAC1 Translation by Precluding Pre-initiation Complex Formation” Research Symposium. Department of Biological Sciences, University of Wisconsin Milwaukee. (2018)
 - **Chandrima Ghosh**, Leena Sathe, Madhusudan Dey “Threonine-281 Phosphorylation Activates the Yeast Protein Kinase Kin2, an Ortholog of the Human Affinity Regulating Kinase” Research Symposium, Department of Biological Sciences, University of Wisconsin-Milwaukee, USA. (Talk) (2017)
 - **Chandrima Ghosh**, Madhusudan Dey. Transphosphorylation Activates the Yeast Protein kinase Kin2, an Ortholog of Human MARK and Worm Par1 kinases, Graduate Student Research Symposium, UW-Milwaukee, USA. (Poster) (2016)
 - **Chandrima Ghosh**, Madhusudan Dey. *HAC1* mRNA: A Model mRNA to Decipher Mechanisms of mRNA Relocation and Translation, 20th Annual Meeting of the RNA Society, Madison, USA. (Poster) (2015)
 - **Chandrima Ghosh**, Neh Nupur, Sayandeep Bhuiyan, Sayantan Bhattacharya, Bahnisikha Das, Khushboo Agarwal, Riddhi Goswami. Cytotoxicity assay of Methotrexate and Cyclophosphamide on albino mice, Proceedings of the National Seminar on Biotechnology for Sustainable Development (BSD-2012), 1, Kolkata, India. (Poster) (2012)
 - **Chandrima Ghosh**, Neh Nupur, Sayandeep Bhuiyan, Sayantan Bhattacharya, Bahnisikha Das, Khushboo Agarwal, Riddhi Goswami. Studies on Cytotoxicity of Methotrexate and

Cyclophosphamide, 7th Annual Session of Students' Chemical Engineering Congress (SCHEMCON 2012), Kolkata, India. (Poster) (2012)

- **Chandrima Ghosh**, Shreyosi Dutta, Monideepa Sengupta, Srabanti Basu. Status of Soil Enzymes in Different parts of a Metropolitan City: A Case Study in Kolkata, Proceedings of the Ninety Eighth Session of the Indian Science Congress, Environmental Sciences, 136, Chennai, India. (Poster) (2011)
- Monideepa Sengupta, **Chandrima Ghosh**, Shreyosi Dutta. Engineered plant to tolerate Mercury. Vol 14, Issue- 1, Apr-Jun 2011, Environews- The Newsletter for Students and Researchers in Environmental Sciences by National Environmental Science Academy, West Bengal chapter, India. (2011)
- **Chandrima Ghosh** (July-September 2010), Fast Detection of E. coli, Journal of Biochemistry News, Volume-17, Issue no.2, Kolkata, India. (2010)

Extracurricular activities

Active member of the Graduate Organization of Biological Sciences. Organized the Annual Biological Sciences Research Symposium (department conference attended by about 100 participants) at UWM (2018). Mentored incoming graduate students in the department with coursework and teaching duties.